Bioactive Materials 28 (2023) 284–310

Contents lists available at ScienceDirect

Bioactive Materials

journal homepage: www.keaipublishing.com/en/journals/bioactive-materials

Review article

Unraveling the potential of 3D bioprinted immunomodulatory materials for regulating macrophage polarization: State-of-the-art in bone and associated tissue regeneration

Sayan Deb Dutta [a,b], Keya Ganguly [a], Tejal V. Patil [a,c], Aayushi Randhawa [a,c], Ki-Taek Lim [a,b,c,*]

[a] Department of Biosystems Engineering, Kangwon National University, Chuncheon, 24341, Republic of Korea
[b] Institute of Forest Science, Kangwon National University, Chuncheon, 24341, Republic of Korea
[c] Interdisciplinary Program in Smart Agriculture, Kangwon National University, Chuncheon, 24341, Republic of Korea

ARTICLE INFO

Keywords:
Macrophage
Immunomodulation
Biomaterials
3D bioprinting
Tissue engineering

ABSTRACT

Macrophage-assisted immunomodulation is an alternative strategy in tissue engineering, wherein the interplay between pro-inflammatory and anti-inflammatory macrophage cells and body cells determines the fate of healing or inflammation. Although several reports have demonstrated that tissue regeneration depends on spatial and temporal regulation of the biophysical or biochemical microenvironment of the biomaterial, the underlying molecular mechanism behind immunomodulation is still under consideration for developing immunomodulatory scaffolds. Currently, most fabricated immunomodulatory platforms reported in the literature show regenerative capabilities of a particular tissue, for example, endogenous tissue (*e.g.*, bone, muscle, heart, kidney, and lungs) or exogenous tissue (*e.g.*, skin and eye). In this review, we briefly introduced the necessity of the 3D immunomodulatory scaffolds and nanomaterials, focusing on material properties and their interaction with macrophages for general readers. This review also provides a comprehensive summary of macrophage origin and taxonomy, their diverse functions, and various signal transduction pathways during biomaterial-macrophage interaction, which is particularly helpful for material scientists and clinicians for developing next-generation immunomodulatory scaffolds. From a clinical standpoint, we briefly discussed the role of 3D biomaterial scaffolds and/or nanomaterial composites for macrophage-assisted tissue engineering with a special focus on bone and associated tissues. Finally, a summary with expert opinion is presented to address the challenges and future necessity of 3D bioprinted immunomodulatory materials for tissue engineering.

1. Introduction

The human immune system plays an essential role in tissue regeneration and disease progression. Macrophages were the first phagocytes discovered by Mechnikov and Herlich in 1908 (Nobel Prize in Physiology or Medicine) [1,2]. Macrophages are associated with the host immune response through various internal or external stimuli and act as effectors for other immune cells. Macrophages are also crucial mediators of various physiological and pathological conditions, such as inflammation, acute infection, and tumors [3]. In recent years, significant efforts have been devoted to the fabrication of various immunomodulatory biomaterials for tissue regeneration. Immunomodulatory biomaterials not only interact with macrophage cells but also elicit host-specific immunity (implant-mediated immune response) and regulating the fate of macrophages [4]. The surface topology (stiff or soft matrix) [5–9], chemical composition [10–12], particle size [10,13,14], porosity [15,16], self-assembly [17,18], wettability [19–22], and roughness [23,24] of the biomaterial promote the specific immune response. Moreover, the degradation products of biomaterials may exhibit various immunomodulatory effects on immune cells, which can initiate a local immune response at the implantation site [4]. After the implantation of a biomaterial scaffold, innate immunocytes (undifferentiated monocytes or M0 macrophages) arrive at the scaffold surface. Based on the scaffold wettability, various proteins, such as collagen, fibronectin, fibrinogen, and vitronectin, accumulate on the scaffold surface and initiate the blood coagulation process through a series of

Peer review under responsibility of KeAi Communications Co., Ltd.
* Corresponding author. Department of Biosystems Engineering, Kangwon National University, Chuncheon, 24341, Republic of Korea.
E-mail address: ktlim@kangwon.ac.kr (K.-T. Lim).

https://doi.org/10.1016/j.bioactmat.2023.05.014
Received 17 November 2022; Received in revised form 29 April 2023; Accepted 20 May 2023
2452-199X/© 2023 The Authors. Publishing services by Elsevier B.V. on behalf of KeAi Communications Co. Ltd. This is an open access article under the CC BY-NC-ND license (http://creativecommons.org/licenses/by-nc-nd/4.0/).

signaling pathways. The characteristics of implanted biomaterials may influence the onset, intensity, and outcome of acute or chronic inflammatory responses [25]. For more information about the inflammatory response of biomedical implants, a reader is encouraged to study the most cited paper, 'Inflammatory response to implants' [26]. In the event of unrestrained or prolonged inflammation or the absence of bioactive cues, foreign body reaction/response (FBR) can result in fibrous encapsulation of implants, a sequence involving monocyte recruitment, macrophage activation, polarization, and integration into giant cells, to separate them from their surroundings and inhibit their direct interactions. Adaptable/suitable material properties, mechanical characteristics, physical cues, chemical functions, and biological activities play a crucial role in providing regulatory signals to guide the destiny of macrophages in response to biopolymers [27–29]. However, integrating all physical and chemical properties into a single platform for boosting immunity remains challenging owing to the low availability of biocompatible polymers. Duan et al. showed that prolonged exposure of titania nanoparticles may decrease the activity of T-lymphocytes ($CD3^+$, $CD4^+$, and $CD8^+$), NK cells, B-lymphocytes, and decreased the level of IL-2 in serum, indicating the anti-inflammatory activity [30]. Therefore, an ideal biomedical implant must have high immunomodulatory efficacy with extremely low site-specific or systemic toxicity *in vivo*.

Besides scaffold chemistry, micro/nano-fabricated scaffolds have gained significant attention for developing immunomodulatory platforms. One of the exciting biofabrication strategy is 'Additive manufacturing (AM)' or 'three-dimensional (3D) printing' or 'rapid prototyping'. 3D printing combines versatile materials (e.g., polymers, ceramics, powders, metals, and composites) into a single platform to create various biomimetic structures for industrial applications [31–33]. 3D bioprinting can be applied to tissue engineering and regenerative medicine to address the need for biomimicking the structures of native tissues by cell-laden culture and allowing us to study immunomodulation dynamically. However, the major question arise in 3D printing/-bioprinting is – 'are the 3D structures safe for implantation or capable of generating host-specific immunity?' Various 3D immunomodulatory platforms have been reported for soft (*e.g.*, skin, muscle, heart, lung, and meniscus) and complex (*e.g.*, bone and cartilage) tissue engineering. Metal/ceramic-based composites are only suitable for bone tissue regeneration and cannot be used for soft tissue engineering. Furthermore, most commercial or clinically approved biomedical implants are titania or hydroxyapatite (HAp)-based in the case of bone, and alginate, collagen, or decellularized extracellular matrix (dECM)-based in the case of soft tissues [34,35]. Importantly, the existing 3D scaffolds or bioprinted hydrogels fail to demonstrate the immune-triggering effect due to poor biodegradability, a higher chance of foreign body response (FBR), and inflammatory cells production *in vivo* [36].

To our knowledge, most 3D micro/nano-fabricated scaffolds that exhibited excellent tissue regenerative capabilities are ill-explored towards *in vitro* and *in vivo* immune response. The existing literature mainly reported using various micro/nano-fabricated scaffolds with immunomodulatory properties *via* culturing either mouse or human cells without proper demonstration of *in vivo* immunomodulation. Furthermore, the underlying signaling pathway is ill-explored and limited to titania-based implants. Anderson et al. previously demonstrated an insightful review in 2008 regarding the use of synthetic biomaterials and their effect on macrophage-mediated immune response [29]. This work overviews new concepts and understandings regarding host immune response to various biomaterials.

Similarly, Li et al. [37] recently demonstrated the biomaterial design strategies, mainly the biomaterial properties on macrophage polarization, adhesion, migration, and tissue regeneration. This review provides an overview of only biomaterial properties but not focusing on any particular fabrication technology-based macrophage polarization strategies. Moreover, Whitaker et al. also reported using various immunomodulatory biomaterials for tissue repair with a particular focus on wound healing only. None of the previously published articles illustrated macrophage immunomodulation's underlying molecular mechanism (signaling pathways involved in macrophage polarization) during complex tissue regeneration. This review summarized the use of various implantable biomaterials and their physicochemical properties for macrophage polarization. Fig. 1 briefly illustrates an overview of the design strategy of different immunomodulatory biomaterials and their impact on macrophage immunomodulation. Not only that, this review also focuses on demonstrating the signaling pathways associated with biomaterial-macrophage interaction for understanding both material scientists and clinicians for developing next-generation innovative and stimuli-assisted immunomodulatory platforms. Lastly, this review illustrates the recent progress in 3D printed immunomodulatory scaffolds for tissue engineering, focusing on bone regeneration, followed by an insightful summary and future direction.

2. Macrophage heterogeneity - tissue healing or disease progression?

2.1. Origin of macrophages – tissue residents and immigrants

Classically, macrophages are specialized phagocytes mainly involved in wound repair and regeneration. Macrophages travel through the bloodstream for immune surveillance and can be divided based on tissue specificity: skin (skin-resident macrophages, Langerhans cells), bone (bone marrow macrophages and dendritic cells), heart (cardiac macrophages), lung (alveolar macrophages), kidney (medullary macrophages), liver (Kupffer cells), intestine (intestinal macrophages), lymph (lymphatic macrophages), peritoneum (peritoneal macrophages), brain (glial macrophages), and eye (intraocular macrophages) [38]. These tissue-resident macrophages are originally derived from the ectoderm or fetal liver. Macrophages originate from monocytes derived from the adult and neonatal bone marrow. During late embryogenesis, macrophages colonize various tissues. Owing to the remarkable self-renewal (self-proliferation and differentiation capability) properties of macrophages, they are mostly retained in adult tissues [39–41]. The microglial cells of the central nervous system (CNS) and Langerhans cells of the epidermis are recognized as true '*tissue resident macrophages*' (Fig. 2a). However, there is a debate about if and to what extent the true tissue-resident macrophages are still present in adult tissues. In mice, around 2–4% of the total circulating leukocytes are recruited in most tissues to replenish the resident macrophages during healthy conditions or acute inflammation. Murine monocytes are differentiated from specialized cells called lymphocyte antigen 6 (LyC). During normal conditions, the LyC^- monocytes from bone marrow, liver, and spleen travel in the blood stream for immune surveillance. During pathogen invasion, the LyC^- cells differentiated into LyC^+ monocytes and induced the secretion of CCL2 chemokines (Fig. 2b). Without inflammation or pathogens, the LyC- cells replenish in gut, liver, spleen, skin, and lung or return to bone marrow or die after 2–3 days.

2.2. Macrophage polarization

Macrophage phenotypic plasticity is profoundly affected by stimuli from the internal or external environment. Macrophages switch to various phases during tissue healing and regeneration, thus considered primary therapeutic targets for multiple diseases [38]. During inflammation, macrophages migrate to wounded tissue and differentiate (polarize) to repair inflammation [42]. Macrophages are divided into two categories based on their nature and function: M1 (pro-inflammatory) and M2 (anti-inflammatory) macrophages (Fig. 1c). M1 macrophages are usually activated through various pro-inflammatory signals, such as tumor necrosis factor-α (TNF-α), interferon-gamma (IFN-γ), and lipopolysaccharide (LPS), leading to the secretion of various pro-inflammatory cytokines. Proinflammatory cytokines and chemokines trigger immunity against pathogenic attacks or malignancies by augmenting reactive oxygen species (ROS) and nitric oxide

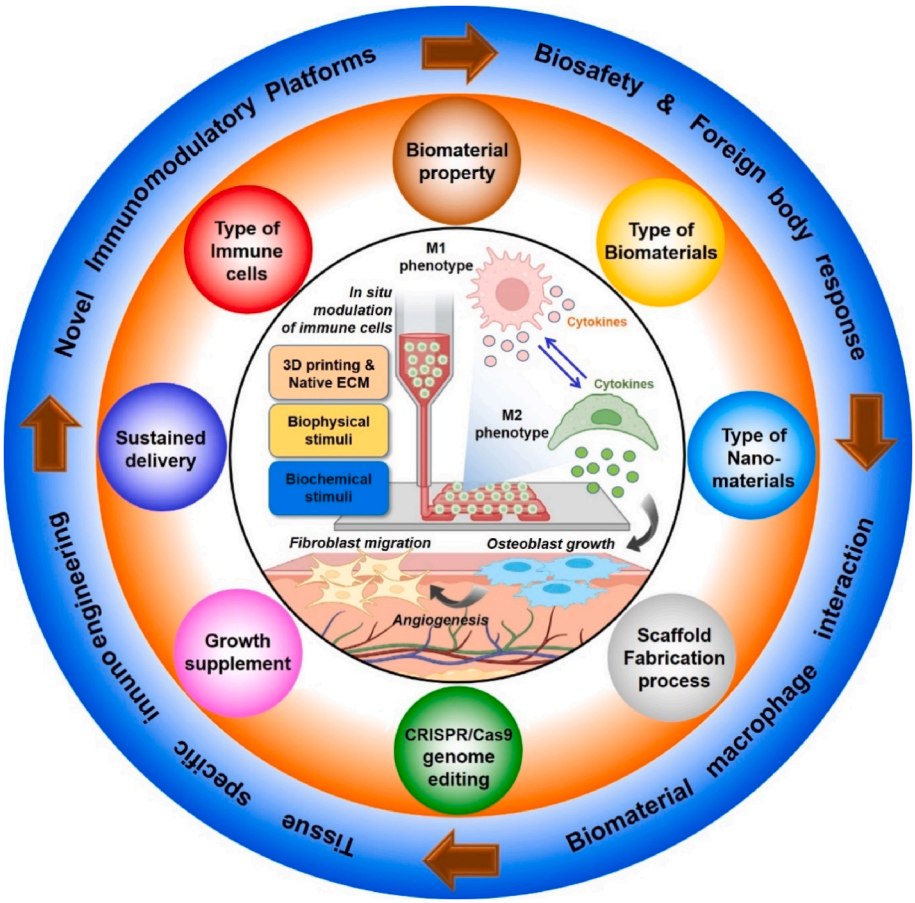

Fig. 1. Schematic illustration of the immunomodulation strategies for tissue engineering. The interaction of immune cells (e.g., macrophages) and their dynamic polarization in respond to micro/nano biomaterials. Future research must focus on the development of novel immunomodulatory biomaterials with tissue specificity and integrating advanced biofabrication tools (*e.g.*, 3D printing and bioprinting) and genome editing tools (*e.g.*, CRISPR/Cas9) for precision immunoengineering.

(NO). Natural killer (NK) and helper T-1 (Th1) cells regulate the phenotypic plasticity of M1 macrophages through TNF-α secretion [43–46]. NK cells transiently secrete TNF-α, whereas Th1 cells secrete TNF-α sustainably during a steady-state immune response against microbial pathogens. The remarkable immunity-boosting efficacy of M1 macrophages makes designing various therapeutic platforms easy [38]. For example, Gill et al. used genetically modified M1 macrophages with chimeric antigen receptors (CAR) to enhance the phagocytic function against cancer cells [47]. CAR macrophages express higher levels of pro-inflammatory cytokines and chemokines than primary dendritic macrophages. Furthermore, in addition to killing tumor cells, CAR macrophages can sense and kill healthy tissues. Moreover, many therapeutic biomaterials may trigger local inflammation upon transplantation; therefore, balancing CAR-macrophage and primary macrophages in the human body is crucial for regulating the immune response [47]. Anti-inflammatory macrophages (M2 macrophages), on the other hand, are activated by Th2 cytokines, such as IL-4 and IL-13 (secreted mainly by mast cells, T-lymphocytes, eosinophils, basophils, and neutrophils), which is entirely different from the Th1 activation axis [48–51]. M2 macrophages are primarily associated with wound healing (epithelial macrophages) and tissue regeneration (regulatory macrophages). M2 macrophages have various subtypes: M2a, M2b, and M2c [52]. Table 1 and Table 2 depict an overview of various macrophage phenotypes *in vitro* and *in vivo* systems with their activation modes and functions in tissue regeneration and therapy.

2.3. Macrophages polarization and soft tissue regeneration

Skin is one of the versatile tissue in our body. Skin wound healing is a complex biological process that comprises a series of signaling mechanisms and the activity of various skin cells. Previous research indicates that epidermal macrophages promote skin regeneration through the rapid proliferation of dermal fibroblasts and maximize protection against ROS. Macrophages eat up old or damaged cells through phagocytosis, killing the skin-tissue-embedded pathogens, and clearing the apoptotic tissues from the injury site [59,60]. M2-polarized macrophages secrete matrix metalloproteinases (MMPs) at the inflammation site [61]. Duffield et al. showed that the reduction of epidermal macrophages at the wound site delayed wound healing, leading to inefficient wound repair [62]. In contrast, M2 macrophages overexpressing the colony-stimulating factor (CSF), platelet-derived growth factor (PDGF), transforming growth factor-β (TGF-β), insulin-like growth factor-1 (IGF-1), and vascular endothelial growth factor-α (VEGF-α) have been shown to promote robust wound healing via neo-angiogenesis and skin re-epithelialization. Moreover, adjacent parenchymal and stromal cells crosstalk with macrophages during wound healing. Furthermore, M2 macrophages promote the proliferation and differentiation of other stem cells and local progenitor cells, which indirectly regulates the macrophage phenotype [63–69] (Fig. 3a). In addition, M1 macrophages protect against pathogenic attack in the wound bed and are differentiated at the early stage of wound healing. However, hyperactivation of M1 macrophages may induce a fibrotic response and delay wound healing [70]. Therefore, a balance between the M1 and M2 phenotypes is critical for vascularized wound healing.

2.4. Macrophages polarization and complex tissue regeneration

Among the hard tissues, bone is one of our body's most complex and

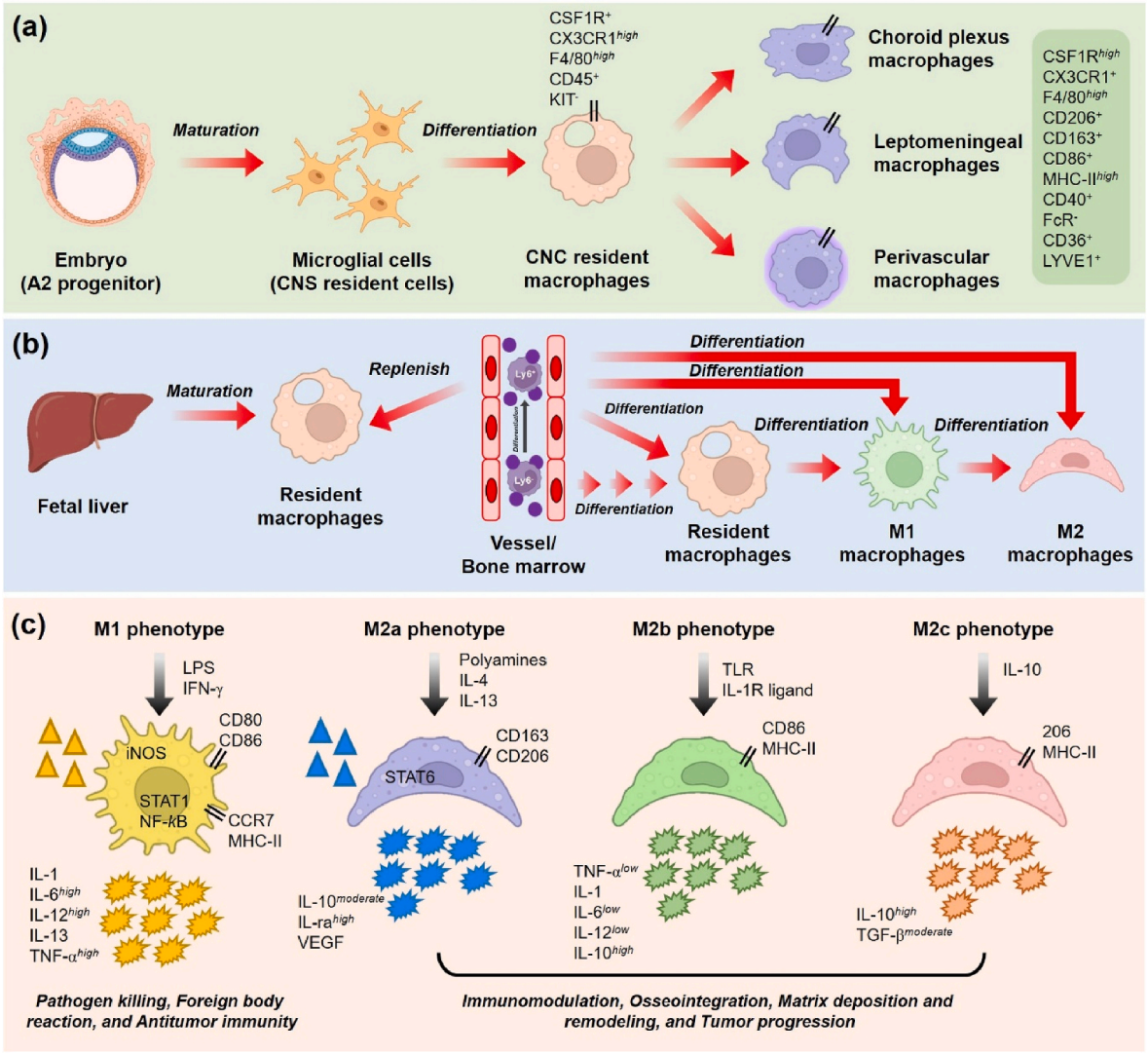

Fig. 2. Origin and classification of macrophages. **(a)** Monocytes derived from embryonic tissue differentiated into microglial cells (CNS resident cells) and Langerhans cells and later transformation into CNS resident macrophages. The resident macrophages later polarized into choroid plexus, leptomeningeal, and perivascular macrophages. **(b)** Macrophages are also derived from Kupffer cells of the fetal liver and subsequently differentiated into M1 (pro-inflammatory) or M2 (anti-inflammatory) macrophages and have self-renewal properties. **(c)** Macrophage polarization and its various sub-types. Classically activated macrophages (M1) are involved in pathogen killing, foreign body reaction, Th1 effector production, and tumor inhibition. Alternatively, activated macrophages (M2a, M2b, and M2c) are involved in immunomodulation, osteogenesis, matrix deposition, Th2 effector production, and tumor progression.

largest tissues. The bone is a highly complex and dynamic tissue that harbors various hematopoietic and mesenchymal progenitor cells. Bone remodeling is a dynamic process involving bone resorption governed by osteoclasts—a later stage of osteoblasts. Osteoblasts are mainly involved in matrix mineralization (osteoid) and are later re-organized toward osteocytes, which act as mechano-transducers for controlling the calcium-phosphate turnover in the bone. Osteoid helps the mineralization process by incorporating calcium and phosphate, forming organic moieties, and producing characteristic hydroxyapatite crystals [72–74]. It is well known that bone cells are tightly connected with immune cells (bone marrow-derived dendritic cells, BMDCs), which play a significant role in osteoimmunity. Resident macrophages commonly associated with osteoclasts promote osteogenesis by inducing mineralization [75]. Bone marrow-derived macrophages (BMDMs) play a critical role in intramembranous and endochondral bone regeneration through the receptor activator of nuclear factor kappa-B/osteoprotegerin (RANKL/OPG) signaling axis. Mesenchymal stem cells (MSCs) secrete various cytokines and growth factors, such as VEGF, TGF-β, and IGF-1, which trigger resident macrophages to polarize toward the M1 or M2 axis. During the early stage of bone fracture healing, the neutrophils are recruited at the fracture site and induce the M1 polarization of macrophages (Fig. 3b). The M1 macrophages play a protective role in this phase against pathogenic attack [71]. In the late stage of bone regeneration, the M2-polarized macrophages induce the secretion of TGF-β and IL-10, thereby inducing angiogenesis and osteogenesis [76–79]. Moreover, MSCs secrete IL-6, which triggers the sustained release of bone morphogenic protein-2 (BMP-2) and promotes the phosphorylation of suppressor of mothers against decapentaplegic (SMAD) via the TGF-β or MAPK signaling pathway in osteoblasts [80]. Therefore, the interplay between MSC immunomodulation and macrophage polarization regulates osteoblast maturation and bone mineralization.

3. Effect of biomaterial properties on macrophage polarization

3.1. Effect of biophysical properties on macrophage fate

3.1.1. Surface stiffness

Mechanical properties, such as surface stiffness and viscoelasticity

Table 1
A summary of various *in vitro* macrophage phenotypes, their activation modes, and major secretory products reported in the literature [37,45,48,53–57].

Phenotypes	Modulator/Inducer	Surface markers	Intracellular markers	Cytokines	Chemokines
M1[a]	TNF-α LPS IFN-γ	$CD86^{High}$ $MHC\text{-}II^{High}$ $IL\text{-}2Ra^{High}$ $IL\text{-}7R^{High}$	$iNOS^{High}$ $PTGS2^{High}$	$IL\text{-}6^{high}$ $IL\text{-}1^{high}$ $IL\text{-}10^{low}$ $IL\text{-}12^{high}$ $IL\text{-}15^{moderate}$ $TNF\text{-}\alpha^{high}$	$CCL8^{high}$ $CCL15^{moderate}$ $CCL20^{high}$ $CXCL9^{high}$ $CXCL10^{Low}$ $CXCL13^{Low}$
M2a[b]	IL-4 IL-13	$MHC\text{-}II^{High}$ $DCL\text{-}1^{High}$	$Arg\text{-}1^{High}$ $PTGS1^{High}$	$IL\text{-}10^{moderate}$ $IGF\text{-}1^{high}$ $TGF\text{-}\beta^{high}$ $FN1^{moderate}$ $IL\text{-}1ra^{high}$ $IL\text{-}6^{low}$	$CCL13^{High}$ $CCL14^{High}$ $CCL17^{Moderate}$ $CCL18^{High}$ $CCL23^{High}$ $CCL26^{High}$
M2b[c]	IL-1β TLR LPS IL-1R	$MHC\text{-}II^{High}$ $CD86^{Low}$	$SPHK1^{High}$	$IL\text{-}1^{low}$ $IL\text{-}4^{moderate}$ $IL\text{-}6^{low}$ $IL\text{-}10^{high}$ $IL\text{-}12^{low}$ $TNF\text{-}\alpha^{low}$	$CCL1^{Moderate}$ $CCL20^{High}$ $CXCL1^{High}$ $CXCL2^{Moderate}$ $CXCL3^{Low}$
M2c[d]	IL-10 TGF-β various glucocorticoids	$CD163^{High}$ $TLR\text{-}1^{Low}$ $TLR\text{-}8^{High}$ $CD206^{High}$	$SLAM^{High}$ MR^{High}	$IL\text{-}10^{high}$ $TGF\text{-}\beta^{moderate}$	$CCL18^{High}$ $PTX3^{Low}$

[a] Th1 activation, pro-inflammatory function (Type-I immune response), phagocytic, pathogenesis, and tumor clearance.
[b] Th2 activation, anti-inflammatory (Type-II immune response), anti-parasitic, host-specific immunity.
[c] Th2 activation, anti-inflammatory (Type-III immune response), help in antibody production via immune cross-talk with B lymphocytes), tissue healing through immunomodulation.
[d] Th2 activation, anti-inflammatory (Type-III immune response), tissue healing and regeneration, matrix mineralization, inhibition of acute inflammation.

Table 2
Summary of various *in vivo* macrophage phenotypes and their identification markers reported in the literature [58].

Phenotypes	Effector molecule	Identification markers
Primary monocytes	$F8/80^{+}$, $MHC\text{-}II^{+}$, $CSF\text{-}1R^{+}$	$CD11b^{+}$, $CD115^{+}$
Inflammatory/ circulating monocytes	$CX3CR1^{Low}$, $CD62L^{-}$, $CD43^{+}$, $Cd11c^{-}$	$Ly6C^{+}$, $CCR2^{High}$
FBR[a] macrophages	$CD64^{Moderate}$, $MHC\text{-}II^{+}$	$CD6^{High}$, $F4/80^{High}$
M1 macrophages	pSTAT1, pSTAT5, $iNOS^{High}$, IL-1R1, TLR2, TLR4, IRF-5, $IL\text{-}12^{High}$, $IL\text{-}23^{High}$, $TNF\text{-}\alpha^{High}$, $IL\text{-}1\beta^{High}$, $IL\text{-}6^{Moderate}$, CCL (2,3,4,5,8,9,10,11), CXCL9, CXCL10, CXCL11	$CD80^{+}$, $CD86^{+}$, $CCR7^{High}$, SOCS3
M2a macrophages	CD200R?, Stabilin-1, CD301, Dectin-1, SR, IL-1R, Polyamine, CCL17, CCL22, CCL24, $TGF\text{-}\beta^{Moderate}$	$IL\text{-}10^{High}$, $CD163^{High}$, SOCS1/2, $Arg1^{High}$, $CD206^{High}$, THM2, $Fizz1^{Moderate}$, Ym1/2, pSTAT6
M2b macrophages	MHC-II, IL-1, IL-6, CCL1, TNF-α	$CD86^{+}$
M2c macrophages	CD163, $TGF\text{-}\beta^{High}$	MERTK, pSTAT3, $CD206^{High}$
M2d macrophages	$IL\text{-}10^{Moderate}$, IL-12, TNF-α, and TGF-β	VEGF-A
FBGC[b]	CD11c, CD44, CD98, CD206, E-cadherin, DC-STAMP, DC-SIGN, HLA-DR, B7-H1	CD86, MMP9
Anti-fibrotic macrophages	$Arg\text{-}1^{-}$, CD206, FIZZ1, MERTK, CD74, CXCR2, CXCR4, MFGE8, MMP(3,8,9,12,13,14)	$Arg\text{-}1^{+}$, $CD280^{High}$, PPARγ

[a] FBR, foreign body response.
[b] FBGC, foreign body giant cell.

are important parameters for the primary immune response [81–86]. The stiffness of human tissues varies with age and the nature of the tissue at the time of healing, fracture, or disease. In this context, hydrogels with mechanically stiff matrices (~600–850 kPa) have been shown to promote both pro-inflammatory and anti-inflammatory activation of macrophages, while the soft matrix (~120 kPa; low stiffness) promotes only pro-inflammatory activation of macrophages *in vivo* [87]. Gloffin et al. reported that the elastic modulus of rat wound tissue increased from 18.5 kPa to 50 kPa after 12 days of wound closure through the activation of M2 polarized macrophages [88]. This study also highlighted that focal adhesion kinase-mediated α-smooth muscle actin (α-SMA) orientation in dermal macrophages is a key regulator of M2 polarization and subsequent wound healing. Moreover, activation of cell migration, gene expression, protein secretion, higher glucose metabolism, and cytokine secretion are higher in the presence of a stiff matrix than in the presence of a soft matrix in T cells [84]. The activation of mechanoreceptors (e.g., YAP, TAZ, RAC, and Rho GTPases) plays a pivotal role in macrophage immunopolarization [89–94]. Therefore, by controlling biomaterial stiffness, macrophage fate can be easily manipulated toward tissue regeneration or disease progression.

3.1.2. Surface charge

Electrophoretic light scattering analysis revealed that the human cell membrane is negatively charged, with a potential ranging from −10 to −90 mV [95]. Positively charged biomaterials significantly affect the adhesion and proliferation of macrophages onto the surface and, therefore, affect protein adsorption and release. Generally, positively charged biomaterials (cationic) elicit anti-inflammatory responses (M2 polarization) in macrophages compared with negatively charged biomaterials (anionic). Negatively charged biomaterials usually trigger both pro-inflammatory and anti-inflammatory responses, and a switch from M2 to M1 occurs in the presence of a negatively charged surface [96–98]. Cationic scaffolds made from dextran, polylysine, polyethyleneimine (PEI), and gelatin trigger M1 polarization of RAW 264.7 cells via TLR-4 signaling and induce the secretion of IL-12, thereby inhibiting the growth of M2-like tumor-associated macrophages (TAMs) toward antitumor immunity [99,100]. Ding et al. reported that incorporating strontium-doped HAp (Sr-HAp) into a dextran/chitosan hydrogel promotes rapid bone regeneration through M2 macrophage immunomodulation owing to the presence of $–NH_2$ groups of chitosan or by controlled release of Sr^{2+} ions from the chitosan scaffold [101]. This study also indicated that a combination of Sr and HAp is mainly responsible for the phenotypic switching of RAW 264.7 cells *in vitro*. Similarly, Fan et al. reported that toosendanin (bark extract of *Melia toosendan*)-loaded dextran sulfate discs inhibit colitis infection via M2 macrophage polarization through activation of the NLR pyrine domain

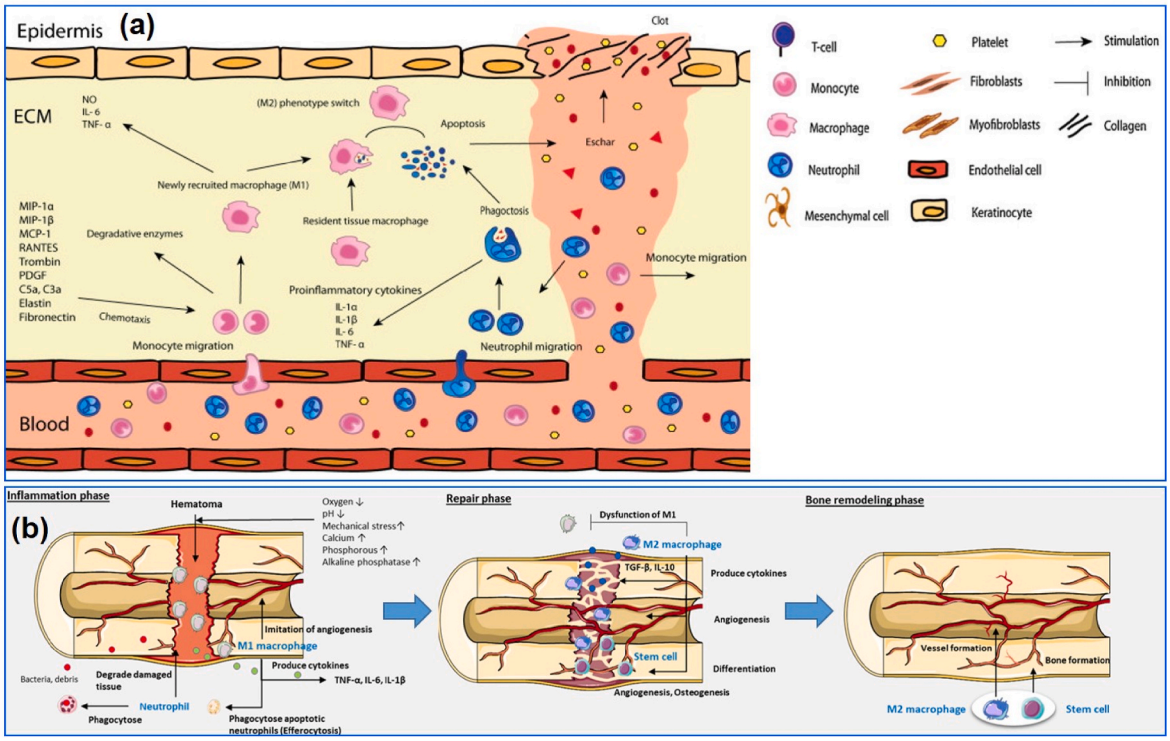

Fig. 3. Schematic illustration of macrophage-assisted skin and bone regeneration. **(a)** The various stages of the inflammatory response during the wound healing process. M1 macrophages and T cells dominate the pro-inflammatory phase of wound healing, whereas M2 macrophages primarily govern the later stage. During this time, the M2 macrophages secrete various factors that induce the differentiation of fibroblasts, keratinocytes, and myofibroblasts [69]. **(b)** Macrophages are polarized through the stress or wound signal from the fractured area and polarized into the M1 phenotype (inflammatory phase) to inhibit pathogenic attack. During bone repair and remodeling, macrophages polarize into M2 phenotype and release anti-inflammatory cytokines, such as IL-10 and TGF-β, that stimulate the osteoblast/osteoclast differentiation *via* RANKL/OPG signaling axis. The M2 macrophage also promotes angiogenesis at later fracture healing stages [71].

containing 3 (NLRP3) inflammasome and nuclear erythroid factor-2 (Nrf-2) signaling pathway [102]. 3D printed polylactic acid (PLA)/chitosan scaffolds with varying surface charges and geometries have also been shown to suppress the anti-inflammatory response in macrophages by secreting various pro-inflammatory cytokines, such as TNF-α and IL-6 [103]. The surface charge of nanocellulose can be tuned via grafting of various functional groups, such as carboxymethyl (anionic) or hydroxypropyltrimethyl ammonium (cationic) groups, to modulate the immune response [104]. Studies have shown that carboxymethyl cellulose (CMC) films induce monocytes to express the M1 phenotype, whereas hydroxypropyltrimethyl ammonium-modified films are unable to boost the inflammatory response to monocytes owing to their inert nature [105]. Cellulose nanocrystals (CNCs; anionic) have been shown to promote M1 polarization of dendritic macrophages through the activation of Th1-mediated signaling pathways [106]. Similarly, a study reported by Patel et al. showed that 3D printed CNC-modified chitosan/silk fibroin (SF) scaffolds promote osteogenic differentiation of human bone marrow mesenchymal stem cells (hBMSCs) through M2 macrophage polarization via interacting with SF protein and chitosan [107]. This study also indicated that the net surface change of the composite scaffold tended to be positive and was probably the main reason for the inhibition of M1 polarization in RAW 264.7 cells. Moreover, charged nanoparticles (NPs) have a significant impact on macrophage polarization. The M2 macrophage polarization was due to the higher availability of the positive charges onto the scaffold surface (-NH_2 from chitosan and SF) and is independent to CNCs. Table 3 summarizes different NPs with varying surface charges and their role in macrophage polarization. Collectively, surface charge plays a significant role in macrophage phenotyping and could be a potential strategy to accelerate the immune response in the human body toward tissue healing and regeneration.

Table 3
Effect of nanoparticle shape and surface charge on macrophage polarization for tissue engineering.

Type of nanoparticle	Size (nm)	Surface charge	Macrophage polarization	References
Silica NPs	10–1000	Negative	M1-type	[108]
Gold NPs	10–300	Negative	M1-type	[108]
Iron oxide NPs	30–280	Negative	M1-type	[108]
Polyurethane NPs	35–60	Negative	M1-type	[109]
NH_2-polystyrene NPs	200	Positive	M2-type	[110]
PDA-modified Fe_3O_4 MNPs	107	Positive	M2-type	[111]
Hyaluronic acid-modified PEI-pDNA NPs	120	Positive	M2-type	[112]
Paramagnetic Fe_3O_4 MNPs	15–30	Positive	M2-type	[113]
Folate-modified Ag NPs	28	Positive	M2-type	[114]
Berbarin-loaded bilirubin-IgG NPs	15	Positive	M2-type	[115]
Poly-(lactic-*co*-glycolic) acid-Dox (PLGA-Dox) NPs	76	Negative	M1-type	[116]
Silymarin-PLGA NPs	180	Negative	M2-type	[117]
Fe_3O_4@C/MnO_2 yolk-shell NPs	160	Negative	M2-type	[118]
Citrate-capped AuNPs	13–22	Negative	M2-type	[119]
Dox-loaded shMF NPs	150–160	Negative	M1-type	[120]

3.1.3. *Chirality*

Biological systems are composed of various chiral molecules, such as D-glucose, D/L-amino acids, L-phospholipids, and helical DNA, which play significant roles in the survival of an organism [121]. It has been

shown that biomaterials integrated with chiral molecules facilitate various immune responses. Sun et al. demonstrated that chiral amino acids, such as *N*-isobutyryl-L(D)-cysteine-doped gold nanoclusters, promoted M1 polarization of dendritic macrophages and effectively inhibited the invasion of human proteolytic leukemia cells [122]. The modified chiral amino acid-coated gold nanoclusters exhibited higher macrophage adhesion efficiency, followed by filopodia and pseudopodia expansion and elicited the secretion of pro-inflammatory cytokines, thereby inhibiting the growth of fatal leukemia cells. In another study, Kehr et al. reported the use of D(L)-mannose-modified periodic mesoporous organosilica (PMO-D/L-MAN) nanoparticles and their effect on the *in vitro* polarization of human macrophages [123]. This finding also revealed that MAN-modified silica had 4-fold better adhesion and proliferation properties for macrophages than pure PMO. Furthermore, this study also demonstrated that the macrophage phenotype is not dependent on surface charge or functional group, but is dependent on mannose chirality, which helps in the adhesion and spreading of individual cells. Similarly, various chiral molecules have been shown to induce CD36 and TLR-2/6 markers in RAW 264.7 cells during differentiation. Collectively, the above-mentioned features demonstrate that surface chirality has a promising role in macrophage phenotyping and could be used as a potential target for the selective activation of immune cells.

3.1.4. Surface wettability

The physical properties of the biomaterial, such as wettability (hydrophilic or hydrophobic surface), may control the immune response of macrophages via regulating the adsorption of various proteins. Hydrophilic scaffolds facilitate the absorption of albumin, which can trigger the release of anti-inflammatory cytokines in M2 macrophages. In contrast, hydrophobic surfaces inhibit the absorption of proteins and therefore restrict macrophage activity [124–126]. For example, Zheng et al. reported that hydrophilic coating on the titania surface promoted the M2 polarization of RAW 264.7 cells by secreting various anti-inflammatory factors. This study further highlighted that hydrophilic coating on the titania surface facilitated the absorption and deposition of fibronectin, which triggered the phosphoinositide-3-kinase (PI3K) and NF-*k*B signaling pathways in RAW 264.7 cells, thereby conferring the M2 phenotype expression [9]. Titania nanotube (TNT) can be modified with superhydrophilic coatings through anodic oxidation and hydrogenation for selective activation of RAW 264.7 cells [127]. The hydrogenation of TNT leads to superior proliferation and adhesion of RAW 264.7 cells and facilitates the secretion of various anti-inflammatory factors, such as IL-10, BMP-2, and TGF-β. In another study, Webster et al. used a combination of hydrophobic and hydrophilic carbon nanofibers to modulate the pro-inflammatory response in primary T-cells [128]. Thus, biomaterial wettability plays a crucial role in the immune response, and manipulation of surface wettability may confer selective activation of immune cells toward tissue regeneration.

3.1.5. Surface topography

Surface topography is another important parameter that regulates macrophage fate [129]. Surface roughness (smooth or rough) and surface geometry (2D/3D: ordered/disordered or aligned/unaligned) play equally vital roles in cellular adhesion, proliferation, and differentiation. Compared to the patterned surface, the flat surface promotes a skewed macrophage morphology. Similarly, furrowed surfaces facilitate the elongation of cytoskeletal proteins of macrophages and alter cytokine expression [9,129]. It has been shown that grooved surfaces of polycaprolactone (PCL), polydimethylsiloxane (PDMS), and poly (lactic acid) (PLA), with average spacing of 250, 2,000, and 500 nm, respectively, force M0 macrophages to elongate and polarize into M2 macrophages. It has also been reported that microcontact printing of fibronectin onto the PDMS surface skews RAW 264.7 cells toward the M2 phenotype and enhances the expression of arginase-1 (Arg-1), CD206, and bronchoalveolar larval fluid protein (Ym1) [130]. Titania-based nanocomposites are frequently used in clinics as orthopedic or dental implants. The surface properties of titania-based implants can be tuned to manipulate the macrophage phenotype and enhance osteogenesis [131]. Refai et al. reported that sandblasted and acid-treated TNT promoted M2 polarization of RAW 264.7 cells and induced osteogenesis through osteoimmunomodulation [132]. In another study, Zhu et al. reported that a honeycomb-like titania surface with a groove diameter of 3,948 ± 282 nm activated RAW 264.7 cells to polarize into the M2-phenotype via Rho family protein (RhoA, Rac1, and CDC42) signaling and facilitate the secretion of various anti-inflammatory cytokines, such as IL-4 and IL-10 [9]. This study also demonstrated that a TiO_2 nano-groove with a diameter of at least 90 nm was sufficient to stimulate filopodia development. The RAW 264.7 cells with M2 phenotype (grown on titania 3,948 nm structure) were found to stimulate BMP-2 release from MSCs by enhancing osteoimmunomodulation. Similarly, Leong et al. reported that PCL/PLA/PDMS-based micro/nanoimprinted surfaces with varying groove diameters regulate the phenotype of RAW 264.7 cells by controlling adhesion and morphology (Fig. 4). This study also found that in the control (flat 2D surface) samples, the macrophage morphology was oval-shaped and with fewer filopodia [129]. They were positive for TNF-α, a common marker of the M1 phenotype. In contrast, the RAW 264.7 cells were found to exhibit a spindle-shaped morphology with elongated filopodia in the presence of a PDMS stamp with 500 nm and 2 μm PCL/PA micro/nano patterning. They were also positive for VEGF, a common intracellular marker of the M2 phenotype. Table 4 depicts an overview of various micro/nano topology-guided macrophage polarization behaviors and possible tissue engineering applications. Therefore, surface topology greatly influences the morphological changes in macrophages and the differential secretion of cytokines due to the foreign body reaction. Apart from micro/nano topology, electrospun nanofibers have less inflammatory response and mild foreign reaction with immune cells owing to less foreign body reaction [133]. In conclusion, biomaterials with varying surface topologies have a potential influence on the polarization behavior of immune cells and could be used as ideal immunomodulatory substrates for tissue engineering. Moreover, the tissue/organ-mimicking topographical structures should be developed in the future for facilitating dynamic polarization of macrophage cells when the implantable biomaterial stays longer time in the body. Taken together, topographical cues and tissue/organ-mimicking nanostructures has potential role macrophage polarization in tissue engineering.

3.2. Effect of biochemical properties on macrophage fate

3.2.1. Material composition

Biomaterial composition is another important factor affecting the immunomodulation of macrophages. For example, biomaterials composed of silicate, silicate/phosphate, bioactive glass, bone ceramics (calcium phosphate), and metal ion-doped polymers have been designed in the form of a scaffold, printable hydrogel, thin film, coating, or fiber, which undergo time-dependent degradation and their degradation products may activate immune cells in various forms [141]. After the degradation of a biomaterial scaffold, various bioactive components, such as ions and proteins, are released in the body fluid, triggering a local immune response. Recently, various strategies have been employed to engineer bioactive scaffolds through multiple polymer grafting or surface functionalization by incorporating various functional groups. When bioengineered scaffolds are implanted at a surgical site, they effectively modulate macrophage polarization and promote the secretion of various cytokines and chemokines [28,142,143]. In a recent study, a silk fibroin/polypropylene-based scaffold showed a remarkable increase in local immune response when transplanted *in vivo*. The polypropylene effectively stimulated macrophages via foreign body reaction, and increased Th1 and cytotoxic T cells (T_C) were found to accumulate at the implantation site after 3 weeks [144]. The nature of

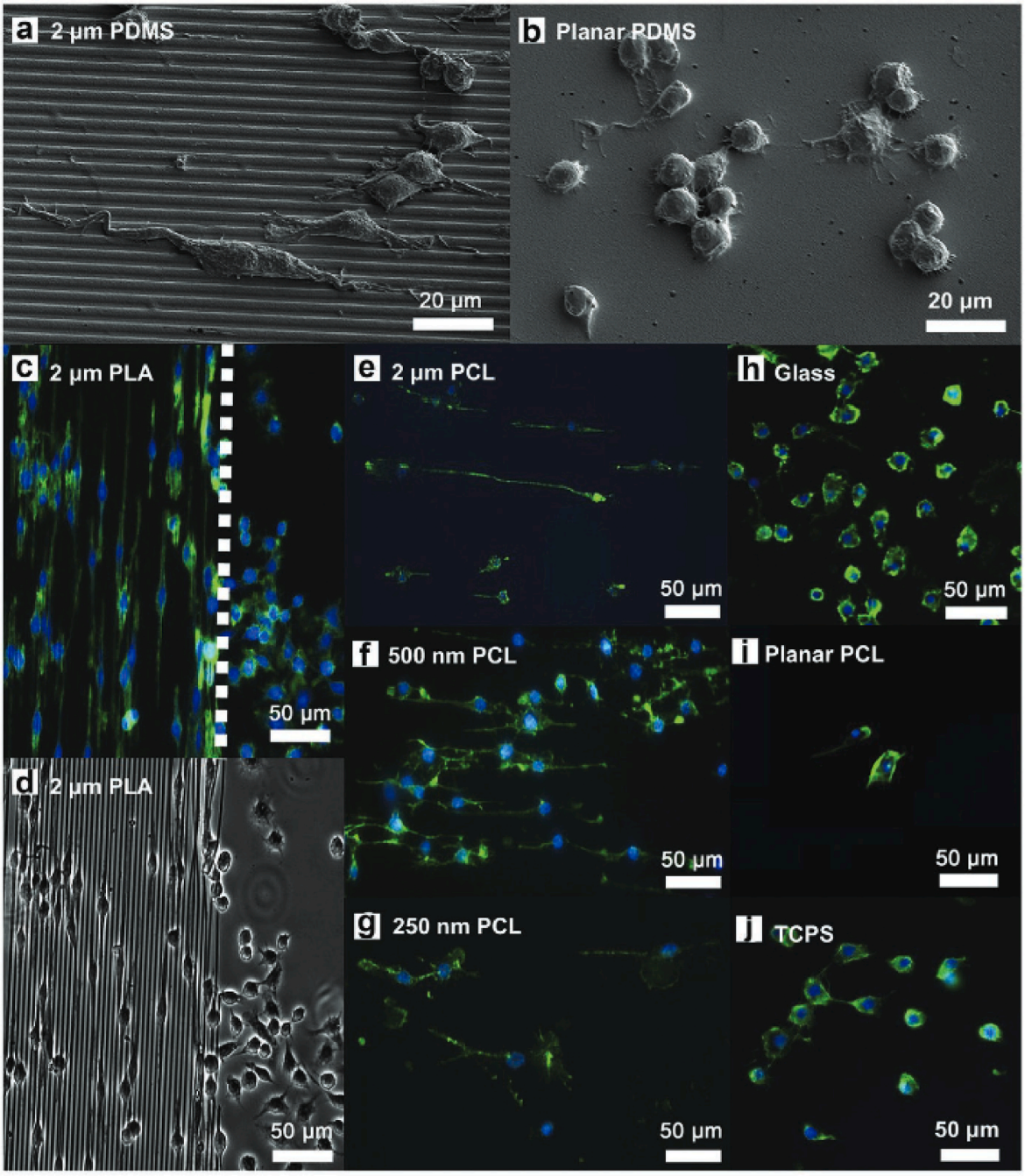

Fig. 4. Effect of micro/nano polydimethylsiloxane (PDMS) patterning on macrophage polarization. **(a & b)** Field-emission scanning electron microscopy (FE-SEM) images of RAW 264.7 cells growing on 2 μm PDMS pattern and flat PDMS surface, respectively, showing the variation in cell morphology. **(c & d)** Fluorescence (FL) and bright-field microscopy images of M2 polarized RAW 264.7 cells, showing the direction of growth in the presence of 2 μm PDMS pattern. **(e–j)** FL microscopy images of RAW 264.7 cells, showing the F-actin (green) distribution in the presence of various coated substrates. The nucleus was stained with 4′,6-diamidino-2-phenylindole (DAPI; blue). Scale bars: 20 and 50 μm [129].

biopolymers (synthetic or natural) also determines the type of immune response in the body. Synthetic or chemically derived biopolymers (e.g., polyethylene glycol) mostly interact with neutrophils and initiate a chronic inflammatory response, followed by the activation of pro-inflammatory signals. Naturally derived polymers have been found to stimulate the activation of *Arg-1*, *Chil3*, *Gata3*, and *CD163* [145]. In contrast, naturally derived polymers (e.g., gelatin, collagen, chitosan, and other bioactive components) may trigger anti-inflammatory (tissue-healing response) signals in the human body. Cha et al. showed that IL-4-loaded gelatin-methacryloyl (GelMA) and polyethylene glycol diacrylate (PEGDA) hydrogel activated M2 polarization of THP-1 cells via α2β1-integrin protein (a type of protein present in the cell membrane) signaling [146]. The authors also demonstrated that the composite hydrogel stimulated the expression of STAT6 and IL-10 and down-regulated the expression of IRF5 and IL-6. Thus, the GelMA/PEGDA hydrogel is thought to promote M2 polarization via the α2β1-integrin/STAT6 signaling axis. Table 5 depicts an overview of how material composition regulates macrophage fate during the immune response. Although several reports have demonstrated the potential role of various biomaterials in macrophage polarization, extensive research on the polarization mechanism must be conducted before actual clinical application. Furthermore, the composition of the bioceramic material is

Table 4
Examples of surface topology-guided macrophage/monocyte activation and its potential application in tissue engineering and regenerative medicine.

Topological cues	Type of immune cells	Immunomodulatory effects	Applications	References
Aligned PCL nanofiber with grooved surface	RAW 264.7	Activation of pro-inflammatory phenotype, IL-1β and TNF-α secretion	Tendon regeneration	[134]
Ti substrate with 5 μm groove	BMDM	Activation of anti-inflammatory phenotype, enhanced IL-10 secretion	Wound healing	[6]
Surface engineered Zn micro/nano pattern	THP-1	Activation of anti-inflammatory phenotype, enhanced CCR-7 and CD209 expression	Macrophage-assisted osteoinduction and enhanced osteogenic differentiation	[7]
Aligned PLCL nanofibers	RAW 264.7	Activation of pro-inflammatory phenotype	Peripheral nerve regeneration	[135]
Commercial surgical gauge	RAW 264.7	Activation of anti-inflammatory phenotype, enhanced expression of CCR7 and CD206	Myogenesis	[136]
3D printed porous titania modified with PEO	hMDM	Activation of anti-inflammatory phenotype, enhanced secretion of IL-10 and CD163	Enhancing osseointegration	[137]
Glycosaminoglycan functionalized aligned collagen fibers	Human primary monocytes	Activation of anti-inflammatory phenotype, enhanced expression of IL-10	Wound healing	[138]
PDA@TiO_2 coated with Sr^{2+} and Ag^{2+} metals	RAW 264.7	Activation of anti-inflammatory phenotype, enhanced expression of CD206 marker	Macrophage-assisted osteoinduction and enhanced osteogenic differentiation	[139]
Tanshinone-loaded aligned PCL nanofiber (1 μM Tan-PCL)	RAW 264.7	Activation of anti-inflammatory phenotype, Enhanced expression of Arg-1, Fizz-1, and Ym1	Enhancing angiogenesis	[140]

RAW 264.7 = murine macrophage cells; BMDM = human bone marrow-derived macrophages; THP-1 = human primary monocyte cells; hMDM = human monocyte-derived macrophages.

also crucial for the immune response. For example, when applying one or two metal ions or a series of various bioactive ions, it is difficult to identify which ionic gradient affects (pH or salinity) the polarization potential of macrophages. Therefore, the proper choice of bioceramic or polymer scaffold should be considered before successful implantation.

3.2.2. Material degradation

After implantation of a biomaterial scaffold, it shows time-dependent degradation owing to the activity of various enzymes present in the body fluid. The degradation of a biomaterial scaffold leads to a shift in surface topography, changes in chemical composition, and stiffness, which attracts immune cells to differentiate or polarize [141]. For example, controlled degradation of β-tricalcium phosphate (β-TCP) has shown a significant amount of Ca^{2+} release, boosting the M2 polarization of dendritic macrophages *via* signaling through the calcium-sensing receptor (CaR). CaR stimulates the production of anti-inflammatory cytokines, which enhances the production of BMP-2 in MSCs during osteogenesis [177]. In another study, a biphasic calcium phosphate scaffold was found to stimulate the M2-like phenotype of RAW 264.7, during *in vitro* immunomodulation. In contrast, non-biodegradable biomaterials (e.g., chemically crosslinked polymers or thermoplastic polymers) exhibit serious inflammatory reactions and induce the fibrotic process (delayed wound healing) owing to the recruitment of M1 pro-inflammatory macrophages [136]. Therefore, the selection of appropriate bioactive but biodegradable polymers may contribute to selective immunomodulation, which is crucial for *in vivo* tissue regeneration.

3.2.3. Soluble factors

Various soluble factors have been found to stimulate macrophage differentiation. Macrophages can be polarized into M1 or M2 macrophages *via* the direct application of soluble growth factors or cytokines. Growth factors, such as BMP-2 [178–181], VEGF [111,181–183], plasminogen activator inhibitor-1 (PAI-1) [184,185], epidermal growth factor (EGF) [186], and fibroblast growth factor (FGF) [186], and cytokines, such as IL-4 [187,188] and IL-10 [189,190], have been shown to induce inflammatory responses in human dendritic monocytes/murine macrophages. During acute burns or trauma, the skin tissue is affected by various air-borne pathogens, which initiate a local immune response known as pathogen-associated molecular patterns (PAMPs). At this stage, blood monocytes accumulate in the wounded region and secrete pro-inflammatory cytokines to combat pathogens. Approximately 2 weeks after primary wound healing, a number of anti-inflammatory cytokines (e.g., IL-4, IL-10, and IL-13) have been found to accumulate at or near the w ound bed, resulting in rapid proliferation and differentiation of fibroblast cells [191]. Biomaterial scaffolds can be used for sustained delivery of various growth factors/cytokines for tissue regeneration. Kwon et al. reported that mesoporous silica nanoparticles (MSN) loaded with IL-4 resulted in M2 macrophage polarization and upregulated the expression of *Arg-1* and *Chil3* transcription factors in BMDMs [192]. It was also demonstrated that larger pores (~180 nm) on the surface of silica are responsible for higher IL-4 loading and greater M2 polarization efficiency in BMDMs. In another study, PCL/polyvinyl alcohol (PCLPVA) nanofibers modified with BMP-2 promoted prolonged M2 polarization of macrophages and vascularized bone regeneration via immunomodulation [193]. The controlled delivery of BMP-2 from the core-shell nanofiber facilitated higher bone regeneration efficiency (~76.38 ± 4.13%) through rapid vascularization and local immune response in a calvaria defect model. Owing to the advantages of soluble factors that trigger local immunity, the optimum concentration (e.g., ng or nM or pM) or selectivity of the soluble factors (e.g., factors with one type or a combination of various factors) should also be considered. Furthermore, a thorough understanding of the soluble factors, their chemical structure, and proper immunomodulation mechanisms is highly desirable for successful clinical application.

3.2.4. Other stimuli-assisted platforms

Macrophage polarization can be tailored using various biophysical (e.g., electric, magnetic, light, and ultrasound) or biochemical (e.g., pH and gas flow) stimuli *in vivo*. Biophysical or biochemical stimuli create a dynamic microenvironment for immune cells and direct specific types of polarization based on the nature of stimulation. Bian et al. showed that non-invasive magnetic stimulation through arginine-glycyl-aspartic acid (RGD ligand)-modified superparamagnetic iron oxide nanoparticles (SPIONs) promoted RAW 264.7 cell polarization (Fig. 5a) both *in vitro* and *in vivo* [194]. Remote oscillation of SPIONs provided a dynamic environment in the mouse subcutaneous wound and promoted macrophage polarization during tissue regeneration (Fig. 5b). Magnetic fields can also alter calcium homeostasis and actin reorientation in monocytes and facilitate the polarization toward M1 or M2 phenotype (Fig. 5c). For example, Wosik et al. found that uneven magnetic field treatment caused rapid elongation of F-actin (a cytoskeletal protein) and induced polarization of macrophages (Fig. 5d) toward the M2 axis [195]. This study also revealed that RhoA protein plays a critical role in the magnetic movement of cytoskeletal proteins. Compared to control macrophages ($RhoA^{+/+}$; wild type), mutant macrophages ($RhoA^{-/-}$) exhibited early accumulation of actin stress fibers and disruption of actin fibers under

Table 5
Effect of biomaterial compositions on monocyte/macrophage polarization.

Biomaterial compositions	Components	Type of immune cells	Nature of immunomodulation	References
Inorganic materials	Ca^{2+}	Primary monocytes	Ca^{2+}/Wnt-mediated signaling and enhanced inflammatory response	[147]
	Co^{2+}	RAW 264.7	Co/TiO_2 matrix promoted M1 macrophage polarization and phagocytosis-mediated enhanced bactericidal efficacy	[148]
	Cu^{2+}	RAW 264.7	Cu-doped SPEEK material promoted rapid bacteria clearance through M1 macrophage polarization; Cu-doped mesoporous silica nanoparticle enhanced osteoclastogenesis through M2 macrophage polarization	[149,150]
	Fe^{3+}	Human primary macrophages	Concentration-dependent M1 phenotype activation of macrophages and pro-inflammatory effects	[151]
	Li^{+}	BMDMs	Li-based bone ceramics modulate *in vivo* osteoclastogenesis *via* M2 macrophage polarization	[152]
	Mg^{2+}	Human primary monocytes; RAW 264.7	Mg-based ($MgSO_4$) nanocomposite promoted anti-inflammatory phenotype and decreasing the secretion of IL-6 and TNF-α; MgSiO3-based composite exhibited better osteoclastogenic activity *via* macrophage immunomodulation; MgO NPs confers the M1 phenotypic switch of RAW 264.7 cells and induced osteogenesis	[153–155]
	Sr^{2+}	RAW 264.7	Sr-coated bioactive glass induced TRAP-medicated osteoclastogenesis	[156]
	Zn^{2+}	RAW 264.7	ZnO nanocomposite films activated M1 macrophages and induced phagocytotic bacteria killing; Zinc silicate/calcium phosphate scaffold promoted M2 macrophage polarization and immunomodulation-assisted enhanced osseointegration	[156,157]
	Se^{4+}	RAW 264.7	Se NPs coated TNTs exhibited anti-inflammatory function of RAW 264.7 cells and broad-spectrum anti-bacterial activity	[158]
	MoO_4^-	BMDMs	Sustained release of MoO_4^- from Mo-bioactive glass scaffold induced M2 macrophage polarization *via* upregulation of *Arg*, *CD206*, and *IL-4* production	[159]
Surface functional group (anionic)	Sulfonate (-SO_3H)	RAW 264.7	Nitro and sulfonic acid moieties present in poly(*N*-isopropylacrylamide-*co*-acrylic acid) hydrogel stimulated M1 polarization of macrophages, while the amide containing hydrogel induced M2 polarization	[160]
	Amine/Carboxyl (-NH_2/-COO^-)	Human primary macrophages	Stimulated the early expression of pro-inflammatory factors (M1) and later induce the anti-inflammatory factors (TGF-β and mATP) secretion in M2 polarized macrophages	[110]
	Amine (-NH_2)	RAW 264.7; BMDMs	Amine-modified bioactive glass promoted M2 polarization of macrophages and increased the production of *Arg-1* and IL-10	[161]
	Guanidinium (CH_6N^{3+})	RAW 264.7	Polarization towards M1 axis and stimulated the production of fibrotic scar at the wounded site	[162]
Surface functional group (cationic)	Polyethyleneimine (PEI)	THP-1; RAW 264.7	Cationic super paramagnetic iron oxide nanoparticles (PEI-SPIONs) induced the M1 polarization of macrophages	[163]
Membrane-derived proteins	Integrins	BMDMs	Knockout macrophage-1 antigen (Mac-1) may regulate the polarization towards M1 axis and accelerate the fibrotic scar formation	[164]
Growth factor/cytokines	IL-4	RAW 264.7; BMDMs	IL-4 incorporated biomaterials stimulated M2 polarization of macrophages for tissue regeneration; IL-4 coated/PDA incorporated TiO_2 boosted M2 polarization and facilitated soft tissue regeneration *in vivo*; sustained release of IL-4 from stiff gelatin matrix promoted M2 macrophage polarization and enhanced osteogenic differentiation	[165–167]
	IL-13	RAW 264.7	Direct application of IL-4 inhibited atherosclerotic plug clearance *via* enhancing the production of anti-inflammatory macrophages	[168]
	(IL-4 + IL-10 + TGF-β) cocktail	Human primary monocytes	Multiple application of Th2 factors may trigger the M2 polarization and enhanced anti-inflammatory factors secretion	[169]
	IFN and IL-4	Human primary macrophages	Controlled release of IFN-γ/IL-4 from d-ECM scaffold triggered the M2 macrophage polarization and enhanced the new blood vessel formation (neo-angiogenesis)	[170]
	IL-6	Murine adipose-derived macrophages	IL-6 administration boosted the activity of Th2 factors which in turn triggered the M2 polarization of macrophages during obesity	[171]
Decellularized extracellular matrices (d-ECMs)	Porcine d-ECM	RAW 264.7	d-ECM scaffold promoted M2 phenotype of murine macrophages	[172]
	Urinary bladder ECM (ub-ECM)	RAW 264.7	Initiated type-2 immune response and inhibited tumor metastasis *via* secretion of pro-inflammatory cytokines for cancer immunotherapy	[173]
	Heart-derived ECM (c-ECM)	RAW 264.7	Cardiac d-ECM scaffolds boosted the activation of M1 phenotype and induced the fibrotic scar formation	[174]
Organoids/Spheroids/ Cell sheet/enzymes	Human dermal fibroblast (hDF)-derived biomaterials	RAW 264.7	Macrophage polarization towards M2 axis and enhanced angiogenic response for wound healing application	[175]
	Lysyl-tRNA synthetase	THP-1	Induced the production of anti-inflammatory cytokines and promoted tumor metastasis (tumor associated neo-angiogenesis)	[176]

prolonged exposure to a magnetic field, which was mainly regulated by the Ca^{2+}/RhoA complex (Fig. 5e and f).

In addition, electric and magnetic fields have different effects on the macrophages. Recently, several studies have demonstrated that near-infrared light significantly manipulated macrophage migration and polarization properties both *in vitro* and *in vivo*. For example, Chen and colleagues showed that a light-responsive hyaluronic acid polymer facilitated the controlled release of RGD adhesion peptides and allowed αvβ3 integrin to bind with the polymer to modulate the immune response [196]. Thus, macrophage polarization can be augmented by various photo-responsive polymers during tissue regeneration. Human skin is electrically conductive, and its electric potential changes under varying physiological conditions, such as injury or trauma. A low voltage-frequency electric field (3 V-1 Hz, 20 min/day treatment) has been shown to promote osteogenesis [197] and allow macrophage cells to differentiate into various phenotypes [198]. Moreover, radiotherapy was found to promote pro-inflammatory activation of TAMs owing to the greater expression of inducible nitric oxide synthase (iNOS); therefore, it is ideal for cancer immunotherapy [199]. Although several biophysical or biochemical stimuli-based platforms have shown

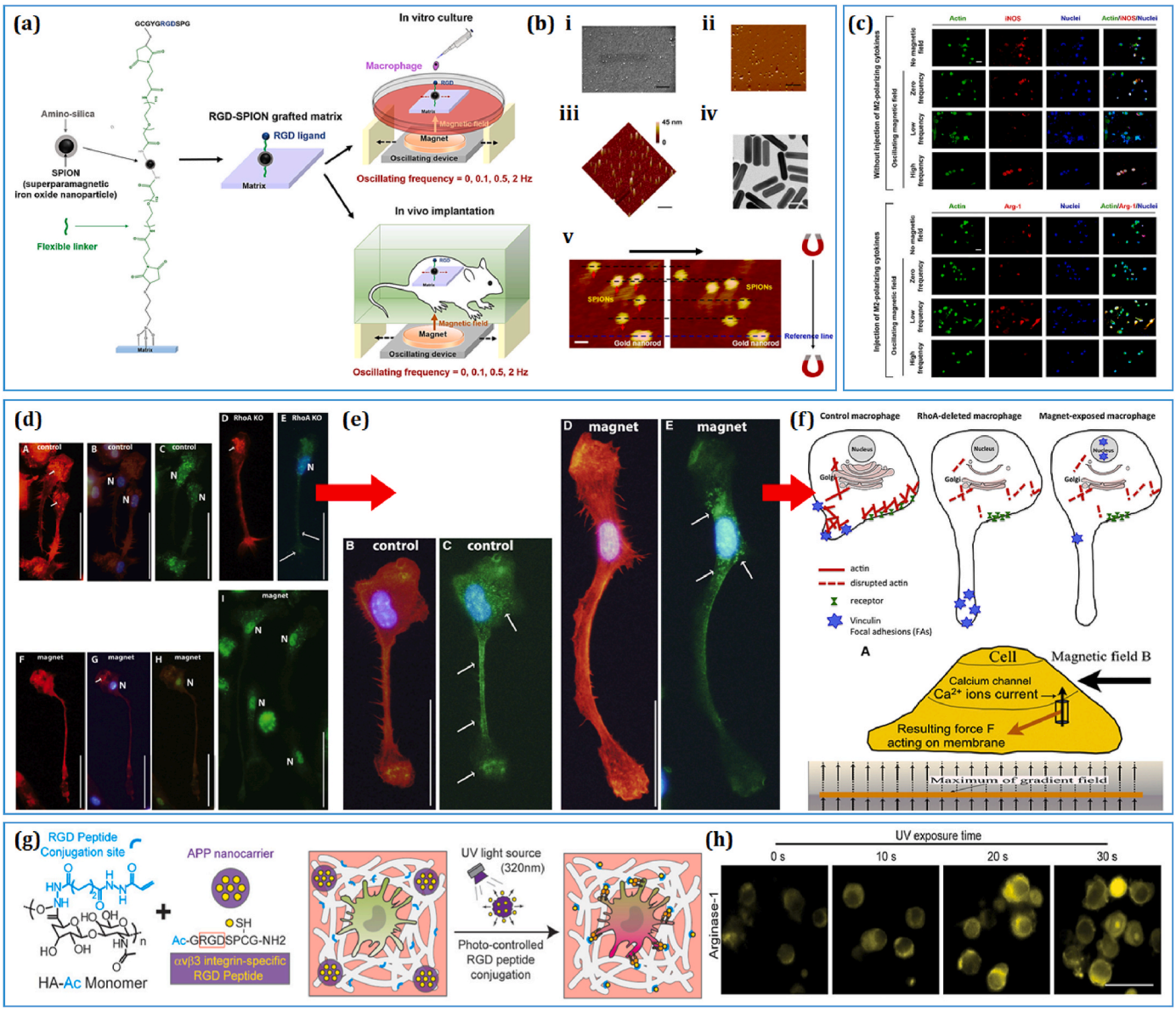

Fig. 5. Biophysical cues regulating the monocyte/macrophage fate. **(a–c)** Schematic illustration of the arginine-glycyl-aspartic acid (RGD)-modified superparamagnetic iron oxide nanoparticles (SPIONs) regulating the macrophage polarization under varying frequency range [194]. FE-SEM and atomic force microscopy images showing the morphology of the fabricated SPIONs and their magnetic field-guided oscillatory movement. The oscillatory behavior of the RGD-SPIONs promoted M1 and M2 polarization under high- and low-frequency vibrations, respectively. Scale bar: 50 nm, 1 μm, and 50 μm [194]. **(d–f)** Effect of magnetic field stimulation on the distribution of focal adhesion proteins (vinculin and RhoA). The magnetic field (1.24 T) treated macrophages exhibited an increase in podosome production. FL microscopy images of M2 polarized macrophages, showing the expression of TRMP2 protein. Schematic diagram of RhoA-dependent induction of macrophages under magnetic field stimulation. Scale bar: 50 μm [195]. **(g, h)** Schematic diagram of the light-responsive hyaluronic acid modified with RGD peptides for immunomodulation. UV light exposure significantly enhanced the expression of intracellular Arg-1 production through periodic activation of αvβ3 integrin protein. Scale bar: 30 μm [196].

promising biomedical applications, little progress has been made in understanding the molecular mechanism behind cell-stimuli interactions. Future research should be conducted using Food and Drug Administration (FDA)-approved stimulation doses and monocyte/macrophage cell lines from various sources (e.g., human, rat, and mouse), with a detailed emphasis on the molecular activation and physiological response during the immune response. Finally, extensive *in vitro* and *in vivo* studies should be conducted to validate the clinical application of physical stimuli-based platforms. Fig. 5 illustrates the use of various stimuli-responsive biomaterials for macrophage immunomodulation.

4. Molecular mechanisms of biomaterial-macrophage interaction

As discussed earlier, macrophages respond in various ways upon contact with biomaterial surfaces. The biomaterial property greatly influences the heterogenicity of immune activation in both *in vitro* and *in vivo* systems. The macrophages initiate foreign body reaction (FBR) after culturing cells in a tissue culture plate or *in vivo* system. Next, various proteins (*e.g.*, serum albumen, fibrinogen, fibronectin, vitronectin, and immunoglobulins) from the blood and intestinal fluid accumulated on the biomaterial surface, forming a thick proteinaceous coat or layer. In addition, platelets in contact with biomaterial surface release various chemoattractant signals, ensuring the migration of immune cells and

fibronectin proteins to form a primary ECM [200–202]. Long-term implantation of biomaterial may induce an acute inflammatory response in our body. The M1 macrophages secrete various pro-inflammatory factors, ROS, and degradative enzymes that influence the macrophages to fuse. After fusion, a large cell mass is generated, known as foreign body giant cells (FBGCs) (Fig. 6). At a later stage, the M2 macrophages migrate to the wound site and induce fibrotic scar formation owing to the activity of VEGF and TGF-β1 *via* cross-talk with fibroblasts. The primary ECM acts as a recognition site for recruited macrophages or resident macrophages to induce the secretion of various cytokines and chemokines [203].

Evidence also demonstrated the involvement of activation of various inflammasomes during macrophage-assisted FBR. Inflammasomes act as signal transducing for initiating a series of molecular events in macrophage cells. Inflammasomes are large cytoplasmic protein complexes having the ability to recognize pathogen-associated molecular patterns (PAMPs), danger-associated molecular patterns (DAMPs), and lifestyle-associated molecular patterns (LAMPs). To gain more insightful knowledge about inflammasomes, a reader is encouraged to study the cited literature [204–206]. The inflammasomes are primarily activated through the membrane-bound receptor proteins, known as toll-like receptors (TLRs). The signal transduction process in macrophages involving the activation of the M1 or M2 phenotype depends on the nature of the biomaterials. For example, the nanoparticles or nanocrystals with a diameter of less than 100 nm are reported to internalize by the macrophages [207], whereas the biomaterial scaffold or micro/nano-patterned surface induces the mechanobiological stimulation to macrophages during immunomodulation [9]. This section briefly summarizes the various macrophage polarization signaling mechanisms in response to multiple biomaterials and/or nanotopographical structures.

4.1. Inflammasome activation and NLPR3-mediated signaling

Various nanomaterials have been shown to promote TLR/NLPR3-mediated inflammasome activation in resident macrophages. The inflammasome activation is directly connected to the processing of IL-1β after being contacted or engulfed nanoparticles (Fig. 7a). A study conducted by Maitra et al. [208] showed that polyethylene microparticles and alkane biopolymers might induce the activation of NLPR3 inflammasome-mediated activation of pro- IL-1β and subsequent M1 polarization of macrophages. In another study, Bueter et al. [209] reported that chitosan effectively triggers the inflammasomes of macrophages by activating intracellular K^+ ions, reactive oxygen species (ROS), and lysosomal destabilization. This study used various inflammasome inhibitors, demonstrating the downregulation of different inflammasome-associated markers. Similarly, polymethyl methacrylate (PMMA) microspheres induced a higher expression of IL-1β with Caspase-1, NLPR3, or ASC when injected in a subcutaneous mice wound model [210]. This study also demonstrated that mutant mice deficient in inflammasome-mediated marker (*nrlp3*$^{-/-}$) had reduced expression of IL-1β or NLRP3 or Caspase-1, suggesting that inflammasome generation played a crucial role in M1 macrophage polarization.

4.2. MCP-1/Rac1-mediated signaling

MCP1 and Rac1-mediated signaling plays a vital role in macrophage polarization (Fig. 7b). Several studies indicated that phagocytic macrophages underwent MCP-1 and Rac1-mediated cytoskeletal remodeling with phosphatidyl serine (PtdSer) and subsequent activation of CD36. A study by Valles et al. [211] showed that THP-1 cells expressed a high level of TNF-α and MCP-1 when cultured in a 2D polystyrene scaffold up to 72 h of incubation. However, after 96 h, the expression of TNF-α and MCP-1 was downregulated in 2D culture, suggesting that the THP-1 cells were in a reduced inflammatory stage. This study also showed that 3D scaffold promoted reduced expression of TNF-α, whereas long-term incubation promoted MCP-1 dependent TNF-α expression. In another study, the MCP-1 knockout mice (*mcp*-1$^{-/-}$) exhibited reduced FBR, owing to the low secretion of TNF-α, suggesting the role of MCP-1 is involved in TNF-α mediated immune response *in vivo* [213]. Furthermore, IL-4-induced MCP1-KO mice were found to have defective macrophage fusion with normal E-cadherin (E-cad) and β-catenin expression. The reduced expression of E-cad and β-catenin were also associated with Rac1 and MMP-9 expression, which regulate a balance between MCP-1 and Rac1 expression [214].

4.3. RhoA/Rac-mediated cytoskeletal signaling

Recently, focal adhesion proteins have been found to regulate macrophage polarization in response to the 3D micro/nano topographical scaffolds (Fig. 7c). In this context, superhydrophilic titania nanosurfaces with dense nanospikes promoted M1 macrophage polarization through selective binding with focal adhesion kinases (FAK) and TLR2/4. The FAK signaling induced MACRO/SR-A mediated signaling

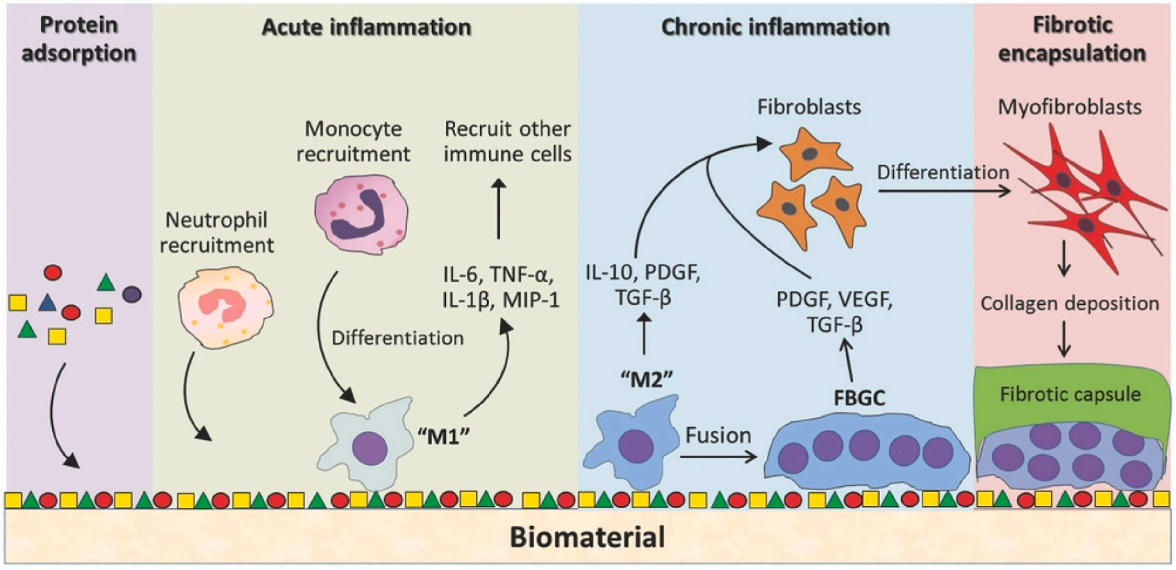

Fig. 6. Schematic illustration of the host response to biomaterials during wound healing and regeneration [203].

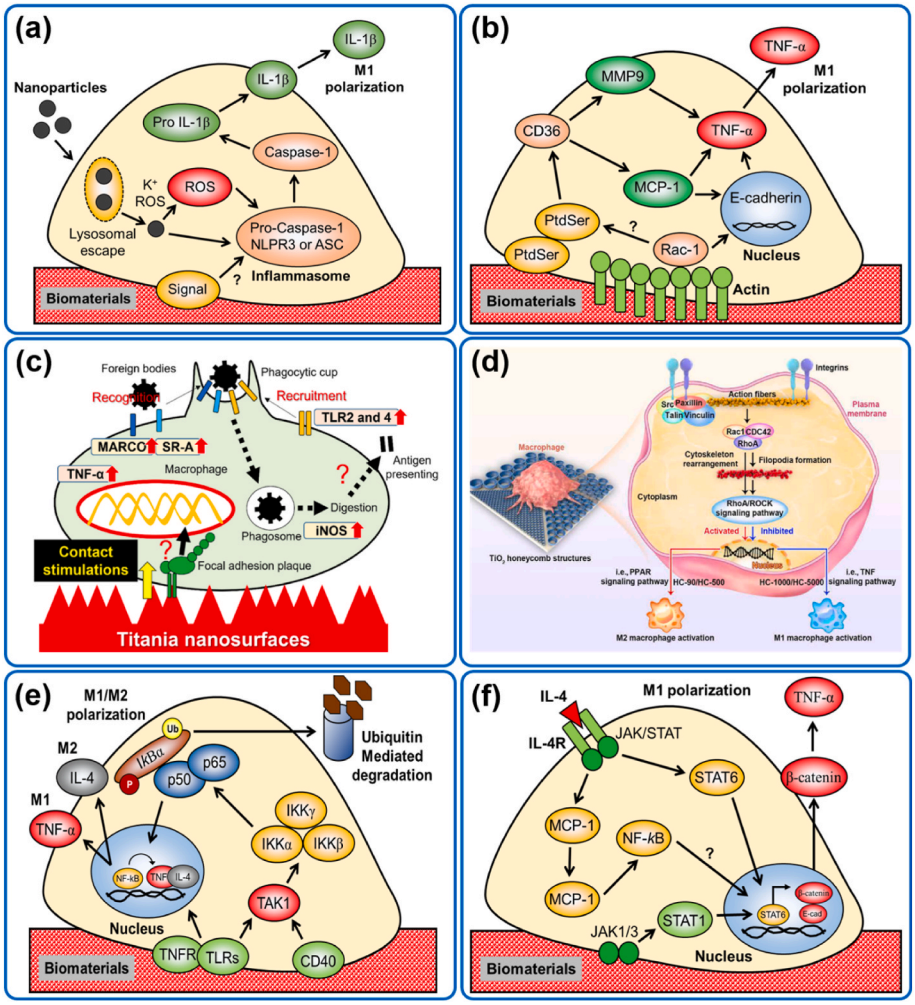

Fig. 7. Molecular mechanisms of biomaterial-macrophage interaction. **(a)** NLPR3-mediated signaling, **(b)** MCP-1/Rac1-mediated signaling, **(c, d)** RhoA/Rac-mediated cytoskeletal signaling [9,212], **(e)** TNF/NF-kB signaling, and **(f)** JAK/STAT-mediated signaling in macrophages.

cascades, resulting in the early expression of TNF-α and iNOS [212]. In another study, TiO_2 honeycomb groove with a 90 μm diameter was found to induce the *RhoA/ROCK* signaling during macrophage polarization [9]. This study also demonstrated that TiO_2 nanostructure with varying diameters facilitated the integrin-β_1 binding of macrophages and which promoted the binding of *Src/Paxillin/Vinculin* complexes (Fig. 7d). The integrin-β_1 was found to activate the *Rac1/RhoA/CDC42* complex and facilitated the filopodia or podosome formation. The study further demonstrated that filopodia formation and *RhoA/ROCK* signaling involved M1/M2 polarization. The TiO_2 structure with 90–500 μm pores induced the *RhoA/ROCK*-mediated PPAR signaling and upregulation of M2 markers, whereas, TiO_2 with 1000–5000 μm structure was found to influence the TNF-α signaling and overexpression of M1 markers in macrophages. Thus, RhoA/Rac-mediated cytoskeletal rearrangement responding to biomaterial surface is critical for macrophage polarization.

4.4. TNF/NF-kB-mediated signaling

TNF/NF-kB signaling is another important signaling pathway modulating macrophage polarization. Studies indicated that the intracellular TNF level is crucial for activating the NF-*k*B transducing element in both *in vitro* and *in vivo* models, thus conferring the development of novel immunomodulatory biomaterials [215,216]. Various topographical nanostructures have been shown to promote the M1 polarization of macrophages owing to the overexpression of TNF-α. TNFR is a potential inducer of NF-kB during FBR (Fig. 7e). In the absence of TNF-α, the p50, and p65, the canonical component of NF-*k*B remains inhibited by another element I*k*B. During FBR, the TNF-α is activated by TNFR or TLR and induces the TAK1, a cytoplasmic inducer of TNF. The activated TAK1 and TNF further promoted the aggregation of IKK hetero-dimer, which later induced the phosphorylation of I*k*B. The phosphorylated I*k*B binds with the p50/p65 and forms a trimeric complex. The trimer is later transported into the nucleus and induces the NF-kB element and pro-inflammatory gene transcription. In contrast, the non-canonical NF-kB signaling is mediated through NIK-dependent induction of IKK via phosphorylation of p100 and subsequent formation of the p52-RelB complex. The p50/p65-mediated NF-kB pathway is usually observed during *in vivo* implantation of titania and copper-based biomaterials [217]. Studies also confirmed that both the canonical and non-canonical pathways actively participate during IL-4-induced immune reaction via macrophage fusion (*in vitro* and *in vivo*) or osteoclast fusion (*in vivo*) [218,219]. Taken together, these reports confirmed that TNF/NF-*k*B signaling is essential during FBR-mediated macrophage polarization.

4.5. Wnt/β-catenin-mediated signaling

Recent studies also indicated that Wnt signaling plays a vital role in macrophage proliferation and differentiation during FBR-mediated immune response both *in vitro* and *in vivo*. Macrophage Wnt signaling initiates innate immune response, critical for tissue regeneration. Thus, inhibition or loss of Wnt function may result in fibrotic symptoms owing

to the loss of activity of MMPs in both *in vitro* and *in vivo* models [220–222]. Wnt signaling is usually connected to the bone-marrow macrophages as it plays a crucial role in osseointegration [223]. A study conducted by Abaricia et al. [224] demonstrated that biomaterial surface properties, such as roughness and hydrophilicity, induce M2 macrophage polarization *via* inducing Wnt signaling. This study also emphasized that macrophages in Wnt mutant mice ($Wnt^{-/-}$) showed reduced inflammatory properties owing to the reduced activity of IL-6, IL-12, TNF-α, and CXCL10 when implanted with titania-based biomaterials. The wild-type mice showed high expression of *Wnt* family genes (*Wnt1*, *Wnt2*, *Wnt3*, *Wnt4*, *Wnt5a*, and *Wnt5b*) in mice, with a high level of TNF-α and IL-6, indicating the role of Wnt signaling in macrophage-mediated disease progression. Thus, understanding the Wnt signaling pathway of macrophages will be beneficial for developing next-generation immunomodulatory biomaterials.

4.6. JAK/STAT-mediated signaling

Macrophage fusion is usually associated with JAK/STAT signaling pathway during FBR. It has been shown that IL-4 induction promotes macrophage fusion and activates JAK/STAT signaling cascades. The IL-4 induction triggers the JAK1/3 and STAT6 or MCP-1, leading to the upregulation of β-catenin and E-cad in M1 macrophages. Patel el al [207] recently reported that rod and spherical nanocellulose (r-CNC and s-CNC) might trigger M1 polarization of RAW 264.7 cells *via* STAT1 signaling pathway while downregulating the NF-kB signaling pathway and inducing the expression of *TNF-α*, *iNOS*, and *CD68* gene markers after 24 h of treatment *in vitro*. These results suggest that JAK/STAT signaling positively influences macrophage polarization in respond to biomaterials.

5. Host response to biomaterials *in vivo*

After the implantation of a biomaterial scaffold (foreign body), migration of both $Ly6C^{-}$ and $Ly6C^{+}$ macrophages increased at the biomaterial site. The increased mobility of $Ly6C^{+}$ monocytes enhanced the proliferation of tissue-resident macrophages. During mild inflammation, the tissue-resident macrophages proliferate rapidly [58,225]. However, the circulating monocytes were found in higher numbers during the acute inflammatory response (Fig. 8a). The circulating

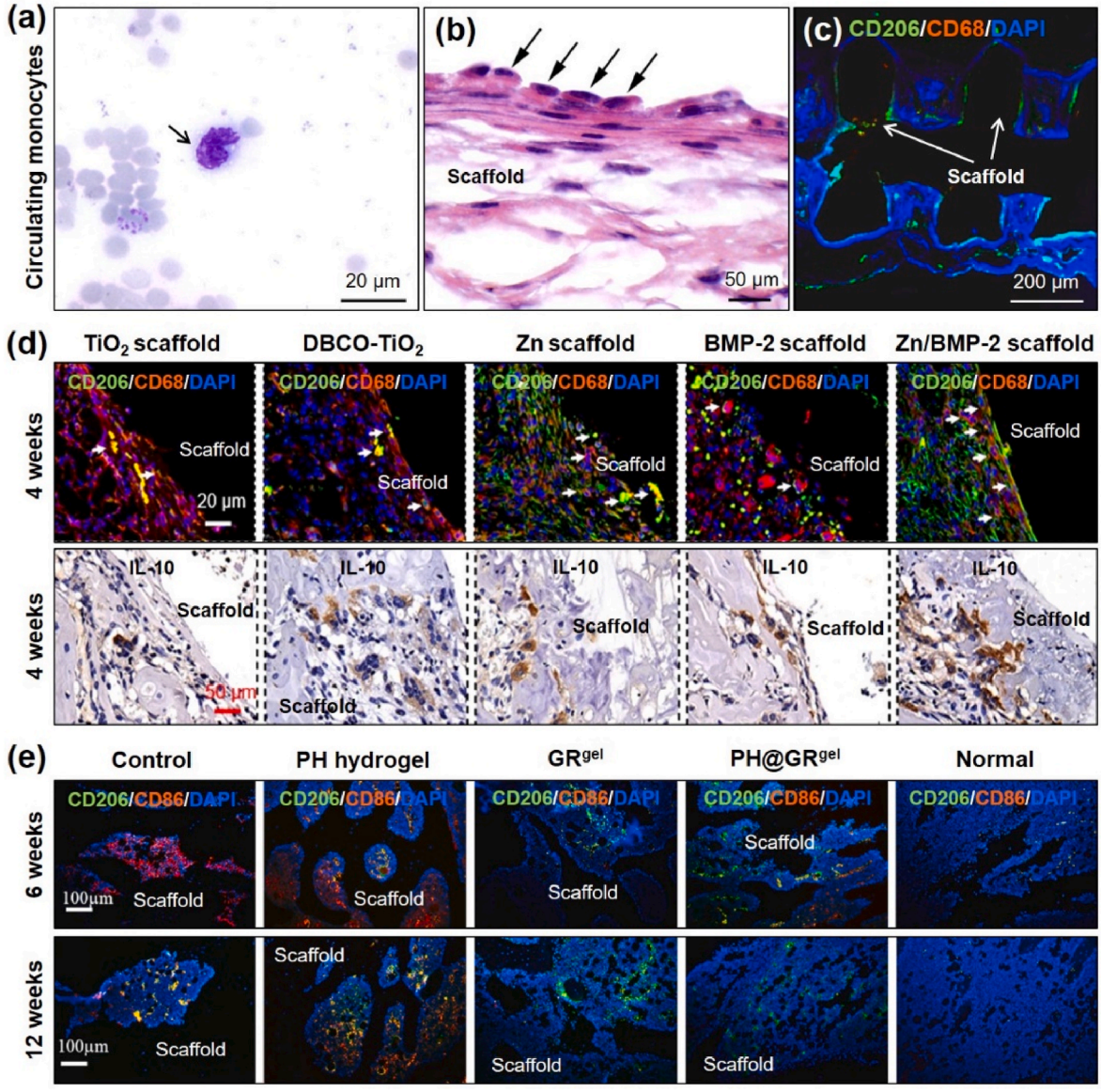

Fig. 8. (a, b) Histological identification of circulating monocyte (arrow) obtained after Pappenheim staining. Accumulation of macrophages (arrow) around the implanted biomaterial [58]. **(c–e)** Expression of M1 (CD68 and CD86) and M2 (CD206 and IL-10) macrophage markers during bone regeneration *in vivo* [226–228].

monocytes rapidly transformed into monocyte-derived macrophages and arranged themselves around the implanted biomaterial (Fig. 8b). Studies indicate that in mice, a weak *de novo* expression of CD11b, increased CD11b, and decreased CD45, CD68, CD71, CD86, and CD206 suggested a transition from monocyte to macrophage after biomaterial implantation [58]. The exact phenotype of macrophages *in vivo* is difficult to identify because both monocyte and macrophages have similar types of markers. Thus, most *in vivo* macrophage analysis is restricted to only polarization studies. A study conducted by Liu et al. reported that macrophages in response to a 3D hetero-nanostructured scaffold displayed positive for CD68 (M1 marker) and CD206 (M2 marker) after 4 weeks' post-implantation (Fig. 8c). This study also indicated that long-term scaffold implantation might promote the higher expression of CD206 than CD68, suggesting tissue healing and regeneration [226]. Similarly, Wang et al. reported that surface-functionalized TiO_2 bone implants showed variable expression of CD68 and CD206 *in vivo*. The expression of CD68 was higher in pure TiO_2 and DBCO-modified TiO_2. However, the CD68 expression was drastically decreased after incorporating Zn, BMP-2, or Zn/BMP-2 modification, suggesting that M1 polarization was only dominant in the early phase of biomaterial implantation during bone regeneration (Fig. 8d). Following that, the expression of IL-10 (anti-inflammatory cytokine) was significantly increased after 4 weeks post-implantation of Zn/BMP-2 modified titania scaffold [227]. These two studies indicate that proper modification of biomaterials with various nanomaterials or proteins may induce M1 polarization of macrophages immediately after implantation owing to FBR and M2 polarization after 2–4 weeks. 3D-printed PCL/nHAp scaffolds have long been explored as an ideal bone implant for *in vivo* bone regeneration. The glycopeptide-modified PCL/nHAp scaffold (Fig. 8e) demonstrated strong evidence of M2 macrophage polarization during *in vivo* bone regeneration by enhancing the expression of the CD206 marker [228]. It is also noticed that the higher expression of the CD206 marker positively correlates with osteogenic markers expression (*e.g.*, Runx2), further suggesting that M2 polarization plays a crucial role tissue healing and regeneration.

6. Tissue-specific biomaterials for immunoengineering

As discussed earlier, monocytes/macrophages reside in various tissues, such as skin, muscle, liver, heart, spleen, lung, kidney, eye, and bone. Based on the localization, the macrophages play essential roles in healing and regeneration of various organs. Recently, extensive research has been devoted to studying the effects of biomaterials on macrophage polarization and their positive feedback on tissue healing and regeneration. During wound healing, macrophages are polarized to the M1 phenotype to combat pathogenic attacks. However, at later stages, M2 macrophages accumulated in the wound site, promoting fibroblast maturation, blood vessel formation, and skin re-epithelialization. Based on their function and activation, cytokines that play major roles in tissue remodeling are IFN-γ, TNF-α, IL-17, MCP-1, IL-10, IL-13, IL-6, EGF, FGF, TGF-, PDGF, and VEGF. M2 macrophages promote growth factor secretion, angiogenesis, cell proliferation, and ECM assembly to accelerate tissue regeneration. Therefore, biomaterials with excellent immunomodulatory properties, low cytotoxicity, and exceptional antimicrobial properties are highly desirable for wound-healing applications. Similarly, bioceramic-based bone grafts play an important role in immunopolarization by recognizing the body's immune system and facilitating the desired immune reaction. An ideal bone graft must have desirable mechanical strength, porosity, particle size, and mineral ions to boost osteogenesis and osteoimmunity. Surface wettability and topography significantly affect bone development and trigger the production of various cytokines (IL-6 and IL-1β) and chemokines (IL-8 and RANTES), epithelial-derived neutrophil-activating peptide-78 (ENA-78, also known as CXCL5), and monocyte chemoattractant protein-1 (MCP-1) [229,230]. The porous nature of the bone implants may affect the immune response and subsequent osteoimmunomodulation [231,232]. Implants with small pores may hinder the diffusion of nutrients and oxygen from the blood and body fluids (interstitial fluid), creating a local hypoxic microenvironment [233]. Local hypoxia leads to the activation of M1 macrophages, ultimately leading to granuloma formation. Additionally, local hypoxia may trigger the bone cells to release hypoxia-inducible factor-1α (HIF-1α), which promotes angiogenesis. The induction of HIF-1α and neo-angiogenesis is beneficial for bone regeneration. Previous studies have demonstrated that biomaterial scaffolds with moderate porosity (~90–120 μm) hinder angiogenesis while triggering chondrogenesis. In addition, biomaterial scaffolds with larger pores (~220–350 μm) may induce vascularization and osteogenesis by enhancing nutrient exchange and oxygen diffusion [234–240]. Table 6 depicts an overview of the biomaterial scaffold-induced immunomodulation of macrophages for tissue healing and regeneration.

7. 3D bioprinting and immunoengineering for tissue regeneration

3D bioprinting is an emerging AM technique that surpasses the existing barriers in tissue engineering and regenerative medicine. The key principles of 3D bioprinting rely on three basic concepts: (1) biomimicry, (2) self-assembly, and (3) tissue-specific bioinks. The 3D bioprinting process usually comprises the following four steps: (1) scanning the body organs/tissue area using X-rays, computed tomography (CT) scans, or ultrasound scanners; (2) importing the medical images into editable 3D files; (3) importing the medical models and slicing to form printable files (STL files); (4) layer-by-layer printing with tissue-specific bioinks using organ-specific cells [253,254]. Bioink is generally referred to as a biocompatible hydrogel ink mixed with cells for 3D printing [255]. Owing to their attractive biomimicking properties and excellent biocompatibility, naturally derived biopolymers are among the most suitable components for bioink fabrication. Naturally derived hydrogels provide better ECM-mimicking functions than chemically synthesized hydrogels, thus facilitating greater nutrient and oxygen diffusion to printed cells [255–258]. Previous studies have shown that bioprinted constructs may sustain cell viability of up to 90%, depending on the bioink composition and nature of the cell [259–267].

Various bioprinted constructs, such as *in vitro* organ models with single or multiple cells, have been developed for testing patient-specific tumors, diseases, drug screening, and preclinical therapy to recapitulate the native tissue/organ [268–271]. In the case of precision bioprinting, patient-specific (personalized) cells are isolated from biopsies (autologous donor) to manipulate the 3D microenvironment or non-invisibly print onto the patient's body (also known as non-contact bioprinting). Therefore, patient-specific in situ bioprinting is an attractive tool to fulfill the doctor's need at an operation table with minimal surgery and lower chances of immune rejection [32,272,273]. Besides the 3D bioprinting approach, four-dimensional (4D) printing is a next-generation advanced tool that integrates the spatial and temporal transformation of 3D printed constructs. Recent studies have demonstrated that 4D printing is applicable in the industry and biomedical engineering to develop neural, cardiac, renal, and osteochondral models [274–276]. 4D bioprinting allows additional bioprinting on the 4th axis, which is impossible to obtain in conventional 3D bioprinting. Thus, 3D/4D bioprinting holds great promise for future stem cell-based regenerative medicine by biomimicking live tissues/organs to combat various diseases. In the following two subsections, we discuss the recent progress in 3D bioprinting and immunoengineering for bone tissue regeneration.

8. 3D printing/bioprinting and immunoengineering for bone regeneration

Bone is a highly mineralized tissue that provides mechanical support and protection to internal organs during locomotion [277]. According to a World Health Organization report, the increasing rate of osteoporotic

Table 6
Biomaterial scaffold-guided immunomodulation for tissue healing and regeneration.

Tissue/ organ	Biomaterial	Immunomodulatory functions	References
Bone	Cerium oxide NPs/ TiO_2 nanocomposite	Ce^{4+}/Ce^{3+} exhibited concentration dependent M2 polarization of macrophages and promoted bone regeneration	[154]
	γ-Fe_2O_3/HAp/PLA scaffold	Magnetic nanoparticles stimulated the mechanosensing responsive factors and boosted M2 polarization of macrophages, induced bone mineralization, and vascularized bone formation	[241]
	Al_2O_3 nanoporous scaffold	Al^{2+} exhibited size-dependent macrophage phenotyping and directed anti-inflammatory cytokines secretion for bone regeneration	[242]
	Alginate/Tyramine/ Sericin/GO-based injectable hydrogel	Sericin/GO induced M2 polarization *via* NF-kB and MAPK signaling pathway and induced osteogenesis in rat BMSCs; accelerated irregular bone defect in a distal femur defect model	[243]
	Silicified gelatin/ polyacrylamide nanocomposite	Promoted M2 macrophage polarization and induced vascularized bone regeneration in a calvaria defect model	[244]
	Fe_2O_3/PEG/collagen nanocomposite scaffold	Magnetically guided M2 polarization and robust bone regeneration; the scaffold induced the secretion of IL-10 and promoted differentiation of BMSCs	[245]
	Piezoresistive Ti_3C_2/ SF nanocomposite hydrogel	The Ti_3C_2 boosted M2 macrophage polarization; secreted IL-4; induced the angiogenesis and osteogenesis *via* immunomodulation; the macrophage conditioned media activated Ca^{2+}/CAM signaling in osteoblast during osteogenesis	[246]
Skin	PEG/heparin/PCL scaffold	Anti-inflammatory activation (MCP-1, MIP-1α, MIP-1β, and IL-8) of macrophages and promote wound healing in a subcutaneous wound model	[247]
	SF/HA/PCL scaffold	HA induced the M1 phenotype of macrophage, inhibited protein absorption, and promoted fibrotic scar formation	[248]
	FTY720-doped PLGA scaffold	Repaired skin injury *via* activation of M2 macrophages and boosted the wound healing process	[249]
Nerve	Cerium oxide NPs	Decreased ROS level and recovered from spinal cord injury	[250]
Muscle	ECM-derived bioscaffold	The enzymatic degradation product of bioscaffold induced M2 macrophage polarization and favored muscle tissue regeneration	[251]
Blood vessel	PCL scaffold	PCL scaffold with larger pore (~30 μm) promoted M2 polarization and enhanced the angiogenesis	[252]
Heart	Decellularized cardiac ECM scaffold	Decellularized pericardium scaffold promoted anti-inflammatory activation of immune cells and sustained the regeneration capability of cardiomyocytes	[174]

patients worldwide is estimated to be 8.9 million by 2030. Osteoporosis at a later stage becomes fatal, and its postoperative complications are huge [278–280]. Bone marrow transplantation [281] and stem cell therapy [282,283] are two leading strategies for treating osteoporosis. However, this procedure is complicated and may lead to severe threats to life. Therefore, conventional treatment strategies, such as autografts or xenografts, are usually employed to treat osteoporosis. In most cases, graft transplantation may require thousands of dollars, creating a massive socio-economic burden [284–286]. In this regard, 3D bioprinting can overcome the existing challenges in bone tissue engineering, particularly in bone-related diseases [287,288]. 3D bioprinting helps re-create bone-mimicking structures through layer-by-layer printing of bone stem cells with bone-specific bioinks [289]. For example, 3D-printed bioactive glass/β-TCP has been shown to promote bone regeneration owing to its unique microporosity and mechanical stiffness after calcination at high temperatures [290]. However, calcium phosphate (CaP)-based bioceramics have poor bioprintablity owing to their low cell-loading capacity. To address this issue, Chen et al. reported a bioprinting strategy using Li^{2+}/Ca^{2+}-reinforced silicate nanocomposites to control cell alignment and induce osteogenesis both *in vitro* and *in vivo* [291]. Hard and calcified 3D printing is usually achieved through FDM printing [292–295], wherein the 3D printed constructs require post-processing, such as high-temperature sintering or cold isotactic pressing (CIP). Thus, bioprinting is unsuitable for FDM-type 3D printing. Although several attempts have been made to create large-scale bone constructs, the clinical application of printed constructs is still under consideration owing to the availability of suitable bone bioceramics with less immunotoxicity [296–298]. Currently, various biomaterials, such as ceramics, metals, natural and chemical polymers, and polyesters, are used to fabricate bone constructs [299–302]. An ideal bone graft must have desirable mechanical properties, including superior biocompatibility, controlled biodegradability, unique porosity, and immunomodulatory properties. Rapid angiogenesis and macrophage polarization (anti-inflammatory macrophages) during bone injury are other important phenomena in vascularized bone regeneration [303] (Fig. 9a). It has been shown that early activation of VEGF during osteoblast maturation is critical for angiogenesis. MSCs cross-talk with endothelial cells during bone remodeling (Fig. 9b); thus, vascularized bone regeneration in a clinical setting remains a challenge in regenerative medicine [304]. Sun et al. reported that MSN-loaded GelMA/Gelatin/PEG-based 3D bioprinted hydrogel induced the sustained release of BMP-2, which induced M2 polarization of RAW 264.7 cells during osteogenic differentiation [305]. This study also highlighted that the MSN/BMP-2 nanocomposite mainly stimulated anti-inflammatory factors (IL-4 and IL-10), which helped in robust bone regeneration in a calvaria defect model under diabetic conditions (Fig. 9c). In another study, 3D printed monetite (a modified calcium phosphate compound, $CaHPO_4$)-coated Ti_6Al_4V composite was shown to induce osteoimmunomodulation via the activation of M2 macrophages [306]. Owing to the superior mechanical properties of Ti_6Al_4V (Young's modulus 4–8 times higher than that of human bone) and stiff matrix, the macrophages could differentiate into an anti-inflammatory phenotype and secrete IL-4, which accelerated the osteogenesis of BMSCs (Fig. 9d–f). Table 7 lists various types of 3D bioprinted scaffolds with osteoimmunomodulatory properties for bone tissue engineering applications.

Peptide-based hydrogels have been shown to promote macrophage polarization by inducing the adhesion, elongation, and activation of various signaling pathways. Previous studies have demonstrated that

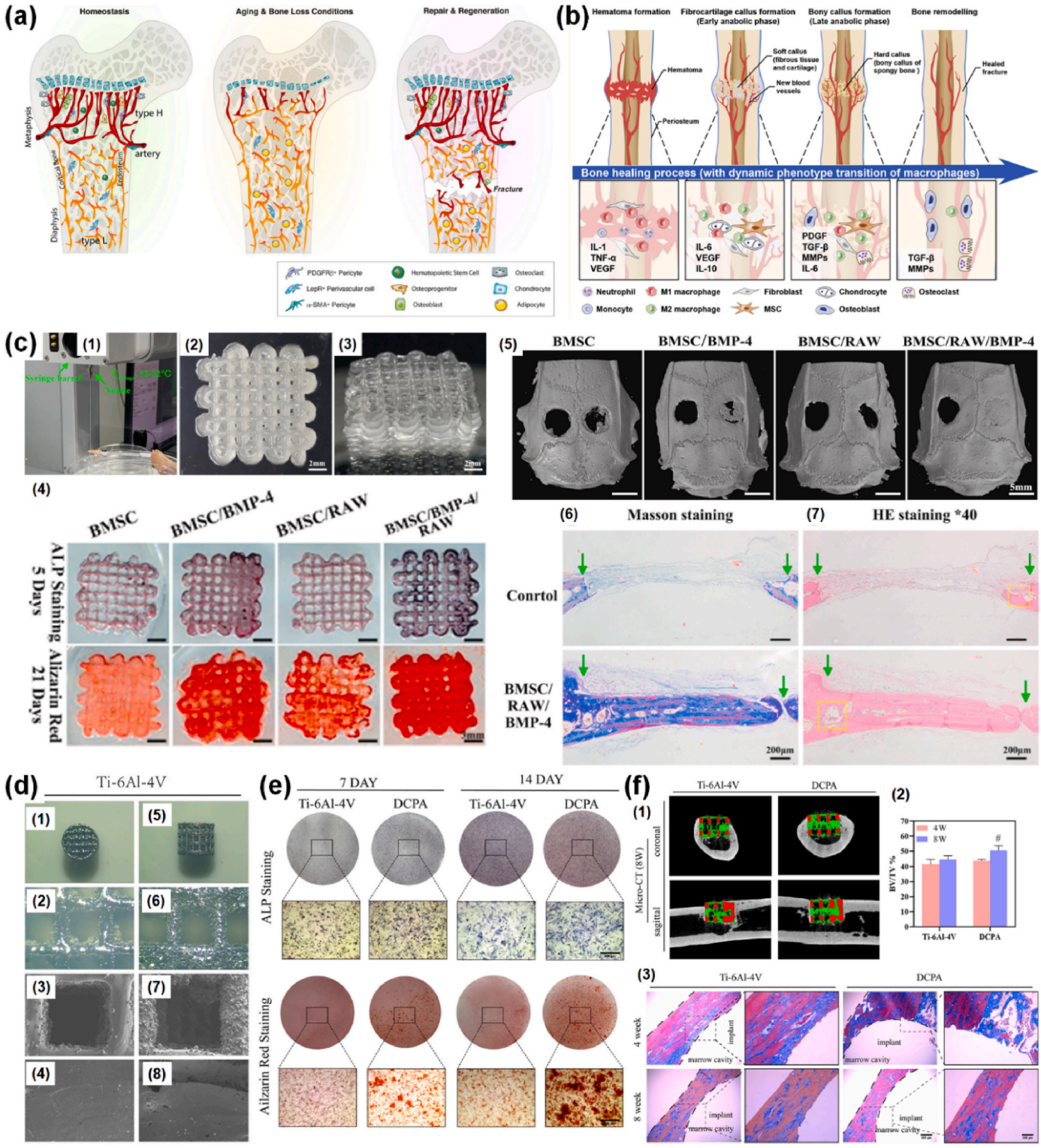

Fig. 9. **(a)** Schematic diagram showing the blood vessel organization of an adult bone marrow. Bone marrow comprises numerous H-type blood vessels in the metaphysis region with osteoprogenitor cells. The osteoprogenitor cells support the angiogenesis of the H-type vessel during bone remodeling [303]. **(b)** Schematic illustration of fracture healing in the femur, which requires a series of molecular cross-talk between bone cells, endothelial cells, and immune cells [307]. **(c)** Demonstration of 3D bioprinting of MSN-BMP-2 loaded GelMA/gelatin/PEG hydrogels with enhanced osteoimmunity and robust *in vivo* bone regeneration [305]. **(d–f)** 3D printed Ti6Al4V scaffolds promote the osteogenic differentiation of BMSCs and enhance vascularized bone regeneration via immunomodulation [306].

bioactive peptides or peptide-coated metal nanoparticles promote M2 macrophage polarization and elicit protection against xenobiotic-induced organ injury [318–321]. Wang et al. reported that 3D printed glycopeptide (RADA-16)-conjugated PCL/nano-HAp scaffold promoted bone regeneration by activating M2 macrophages *in vivo* [228]. This study also highlighted that the RADA-16 peptide induced the activation of STAT6/ERK signaling in RAW 264.7 cells and boosted the secretion of anti-inflammatory cytokines, which accelerated the osteogenesis of

Table 7
Recent advances in 3D printed/bioprinted osteoimmunomodulatory hydrogel scaffolds for bone tissue engineering.

Composition	Monocyte/ macrophage polarization	Immunomodulatory activity	References
Glycopeptide-conjugated PCL/ nHAp scaffolds	M2 phenotype	β-sheets of Glycopeptide promoted higher expression of *STAT-6*, *IL-10*, and *TGF-β* through ERK signaling pathway which induced the osteoblast differentiation	[228]
Strontium-doped nHAp/silk scaffold	M2 phenotype	Strontium induced the *HIF-1α* activity and promoted angiogenesis and chondrogenesis; the composite scaffold also boosted the secretion of anti-inflammatory factors and accelerated osteogenesis	[308]
Haversian canal mimicking bioprinting using $Ca_2MgSi_2O_7$ + BMSCs (2×10^4) + RAW 264.7 cells (2×10^4)	M2 phenotype	The co-culture of BMSC/ RAW 264.7 increased the expression of *Arg-1*, *IL-10*, and *CD163* in RAW 264.7 cells and induced the expression of *BMP-2*, *TGF-β1*, *PDGF*, and *VEGF*; enhanced osteogenic differentiation through activation of *BMP2R/Smad4* signaling	[309]
3D printed β-TCP/ Alginate/ hyaluronic acid scaffold	M2 phenotype	The soft hydrogel promoted M2 polarization *via* enhancing the expression of *Arg-1*, *IL-1ra*, *IL-10*, *TGF-β1*, and *VEGFA*; the M2 macrophage derived exosome promoted bone regeneration through activation of *Runx2*, *ALP*, *BSP*, *BMP-2*, *OCN*, and *OPN* transcription factors	[305]
3D printed PLA/ MSC-exosome	M2 phenotype	3D printed MSC-exosome loaded scaffold promoted M2 macrophage polarization and hBMSCs differentiation *via* immunomodulation; the MSC-exosome downregulated the pro-inflammatory factors, such as *IL-1β*, *IL-6*, *iNOS*, and *TNF-α*	[310]
3D bioprinted Dox-loaded MBG/ GelMA/HAMA scaffold	M1 phenotype	Enhanced activation of pro-inflammatory cytokines and anti-bacterial effect; sustained BMP-2 release boosted *in vivo* bone regeneration	[311]
3D printed hydroxypropyl chitin/PLA/ nHAp	M2 phenotype	Enhanced activation of M2 macrophages via activation of *IL-10*, *Arg-1*, *CCL22*, *VEGFFA*, *PDGFB*, and *MMP9*; robust *in vivo* bone regeneration in calvaria defect model through osteo-immunomodulation	[312]
3D/4D printing of polydopamine (PDA)-modified collagen/PGS/ PLA scaffold	M2 phenotype	PDA modification induced the M2 polarization of RAW 264.7 cells and sustained the release of anti-inflammatory cytokines for robust craniofacial regeneration	[313]
3D bioprinted AgGNRs/ dextran/GelMA scaffold	M2 phenotype	Activation of anti-inflammatory phenotype of RAW 264.7 cells; sustained the secretion of IL-4; enhanced osteoimmunomodulation of BMSCs; anti-bactericidal effect	[314]
3D printed $Ca_7Si_2P_2O_{16}$ scaffold	M2 phenotype	The multicellular patterning of MSCs and RAW 264.7 cells exhibited a neighborhood effect; enhancement of M2 markers (CD206, Arg-1, IL-10, and IL-1ra); M2 macrophage triggered the osteogenesis *via* Smad/ β-catenin/LRP5 signaling axis and promoted robust bone regeneration *in vivo*; enhancement of *in vivo* activation of IL-10 marker	[315]
QCS/GO/PDA-based 3D printed scaffold	M2 phenotype	The nanohybrid scaffold promote M2 macrophage polarization and accelerated bone and skin regeneration	[316]
Cryogenic 3D printing of Sr^{2+}/ Fe^{3+} co-substituted nHAp	M2 phenotype	The metal ions facilitated angiogenesis and osteogenesis through M2 macrophage polarization; secretion of anti-inflammatory factors (IL-10 and Arginase)	[317]

BMSCs (Fig. 10a and b). Furthermore, it was also demonstrated that RADA-16 coated PCL/nano-HAp scaffold induced higher mineralization and new bone formation (~88.3%) than the blank scaffold. In another study, MSC/RAW 264.7 cells co-cultured in a 3D printed $Ca_2MgSi_2O_7$ scaffold exhibited enhanced osteoimmunomodulation during bone regeneration [309]. The RAW 264.7 cell-secreted cytokines (bioactive proteins) promoted the proliferation and differentiation of BMSCs (Fig. 10c and d). Thus, the use of various bioactive protein/peptide coatings may help regulate macrophage activity, which is crucial for bone regeneration. Macrophage-derived secreted biomaterials, such as soluble factors, cytokines, and exosomes, can be used to prepare soft hydrogels for controllable delivery of growth factors/exosomes during osteogenesis. Sun et al. showed that β-TCP induced M2 macrophage polarization, and the secreted exosomes also displayed enhanced angiogenic and osteogenic activity in human umbilical vein endothelial cells (HUVECs) and BMSCs [322]. The M2-exosome of RAW 264.7 cells, when encapsulated in an alginate/hyaluronic acid hydrogel, exhibits controlled release after incubation in culture media and accelerates osteogenesis (Fig. 10e). The authors also demonstrated that pro-angiogenic and pro-osteogenic microRNAs (miRNAs) present in M2 macrophage-derived exosomes play a crucial role in osteo-angiogenesis. Thus, the immune response can be manipulated by controlling scaffold morphology, surface topography, chemical composition, or bioactive protein/peptide coating; this could be beneficial in developing new-generation immunomodulatory scaffolds for bone tissue regeneration.

9. Limitations of 3D bioprinting in immunoengineering

3D bioprinting is a groundbreaking AM technology that enables the manipulation of various types of cells with superior complexity and accuracy using a single bioink. Although 3D bioprinting has gained enormous attention in regenerative medicine, many challenges remain unsolved in developing immunomodulatory platforms. One of the significant challenges is the viability and proliferation of immune cells inside the bioprinted hydrogel. The bioink viscosity and modulus (*e.g.*, elastic modulus) play a crucial role in the survival and proliferation of immune cells. Soft hydrogel matrix may promote greater mobility and

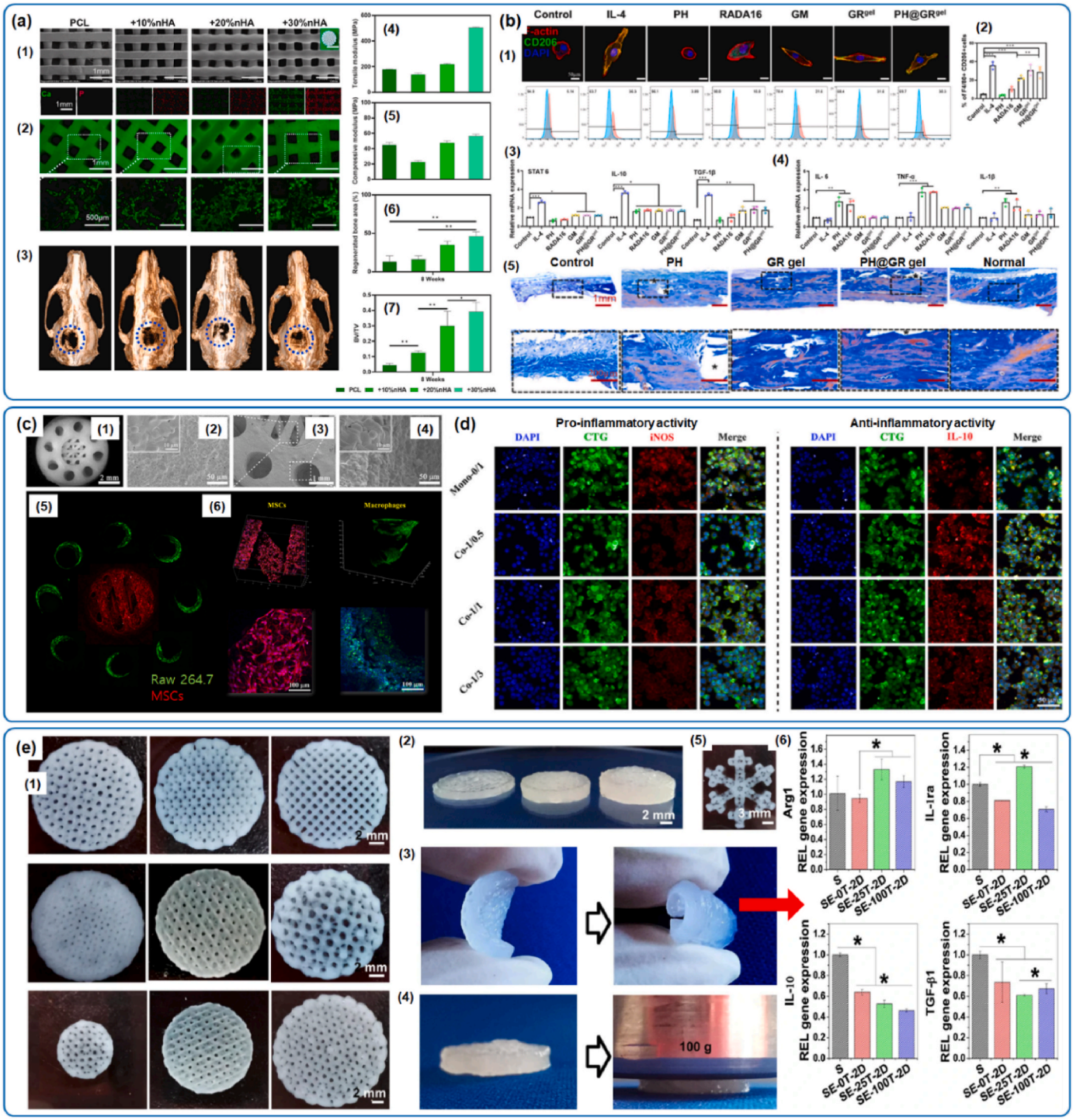

Fig. 10. Recent advances in 3D bioprinted osteoimmunomodulatory platforms for robust bone regeneration. **(a, b)** Glycopeptide-modified polycaprolactone/nano-hydroxyapatite (PCL/nHAp) scaffold (1, 2) promoted robust bone regeneration (3–7) through M2 macrophage polarization (b, 1–5). Scale bars: 50, 200, 500 μm, 1 mm, and 5 mm [228]. **(c, d)** Demonstration of 3D bioprinted Haversian canal mimicking hydrogel (1–4) for immunomodulation of MSCs and RAW 264.7 cells (5, 6). The fabricated hydrogel promoted anti-inflammatory phenotype activation of RAW 264.7 cells during MSC/RAW 264.7 co-culture. Scale bars: 50 and 100 μm [309]. **(e)** Fabrication of macrophage exosome-laden alginate hydrogel (1–5) for immunity boosting (6) and enhancing the osteogenic differentiation. Scale bars: 2 and 3 mm [322].

differentiation of immune cells; however, the stiff hydrogel will not promote cell mobility due to the less availability of nutrients and poor oxygen diffusion. Thus, most of the literature research relies on a simple 2D culture of immune cells onto the 3D printed hydrogels. Therefore, tissue-specific and soft hydrogel matrix development is desirable for enhancing macrophage/monocyte encapsulation efficiency with greater viability. Various decellularized extracellular matrix (d-ECM) bioinks have recently been proposed to tune macrophage polarization during tissue regeneration. However, using d-ECM-based hydrogels for *in vivo* applications is quite questionable. This is because the cells of the native tissue contain various surface markers and intracellular proteins, which act as a recognition site for several immunocytes. Removal of cellular

components by detergents (e.g., sodium dodecyl sulfate and Triton-X 100) more likely remove the surface markers and intracellular proteins, thereby reducing the chance of macrophage/monocyte cells to activate. Thus, the use of only d-ECM hydrogel is quite ineffective for immunomodulation. Therefore, future bioink development must focus on studying not only the d-ECM hydrogels for bioprinting but also focus on immunomodulatory effects for precision medicine. Most fabricated cell-printing platforms demonstrate excellent physiochemical properties towards macrophage culture *in vitro*; however, they fail to recapitulate the native immune environment when implanted *in vivo*. For example, the bioprinted structure and their implantation, analysis of immunological markers, FBR, long-term *in vivo* trackability, and degradation behavior must be addressed before entering human clinical trials.

10. Summary and outlook

In this review, we attempt to document the present status of the immunomodulatory biomaterials and their properties for tissue healing and regeneration. As discussed above, the phenotypic plasticity of monocyte/macrophage profoundly affected by the material property, surface topography, and porosity during interaction with biomaterials [28]. Conventional hydrogels and nanomaterials are insufficient for inducing dynamic macrophage polarization due to the lack of a suitable 3D environment, ECM function, and long-term dynamic stability. To some extent, the hydrogel scaffolds can only initiate the local immune response rather than systemic immunity. As a result, biomaterials' degradation product sometimes induces immunomodulation (adaptive immunity) and is later excised from the body *via* urine [323–325]. Similarly, nanoparticle-based immunotherapeutic have similar issues with long-term dynamic immunomodulation. Thus, a 3D hydrogel platform that can effectively encapsulate the immune cells and offers greater immunity is highly desirable for successful clinical application. 3D printing is a groundbreaking additive manufacturing tool offering a wide range of biomaterials for rapid prototyping [326]. Although 3D bioprinting and immunomodulation are the 'hot topic' in tissue engineering and regenerative medicine; before going forward, some key aspects need to be addressed for the successful application of the immunomodulatory scaffolds. Of them, the major issue is the commercialization and mass production with an eco-friendly and economic approach. Moreover, the biomaterial-assisted immunotherapy should be taken into consideration in terms of safety and body's innate immunity. Furthermore, the 3D bioprinted immunomodulatory hydrogels can also be used as a novel platform for delivering vaccines and drugs individually, known as precision medicine [327].

With the advent of modern biotechnology, various genome editing tools has gained significance attention in the therapeutics. In particular, various nucleic acid-based biopolymers and genes are mixed with other polymers for re-engineering the genetic makeup of the cells. Such genome editing tools are commonly known as 'God's scalpel,' which is a precise and efficient tool for editing the DNA or RNA of the cells [328]. One of the promising gene editing tools used in immunology and molecular biology is known as clustered, regularly interspaced, short palindromic repeat or CRISPR after being discovered by Ishino et al., 1987 [328,329]. CRISPR is usually associated with other regulatory genes known as the Cas9 gene. Engineering macrophage cells with CRISPR/Cas9 expression plasmid regulated the specific polarization and enhanced the tissue-specific immunity during inflammation or restoration [330–332]. Even though, commercially available viral or non-viral (PEG-based polymeric nanocarriers) are extensively used for delivery of CRISPR/Cas9 plasmids; however, the release of those nanocarriers from a 3D printed hydrogel is quite questionable. Several factors, such as polymer ink composition, concentration, crosslinking degree, and viscosity is related to the sustained release of various drugs, nanoparticles, and nanocarriers. Therefore, development of novel biomaterial-based nanocarriers with controlled release of CERSPR/Cas9 is highly required for dynamic macrophage immunomodulation (Fig. 11). In addition, extensive *in vitro* and *in vivo* analysis is also necessary for the successful clinical application of the CRISPR/Cas9-based 3D hydrogels. Thus, future research also focuses not only developing novel platforms but also integrating CRISPR-Cas9 based advanced tools which can cut, edit, and re-engineer the macrophages towards tissue healing and regeneration.

Macrophages interact with stem cells to secrete various growth factors and cytokines which may induce the proliferation and

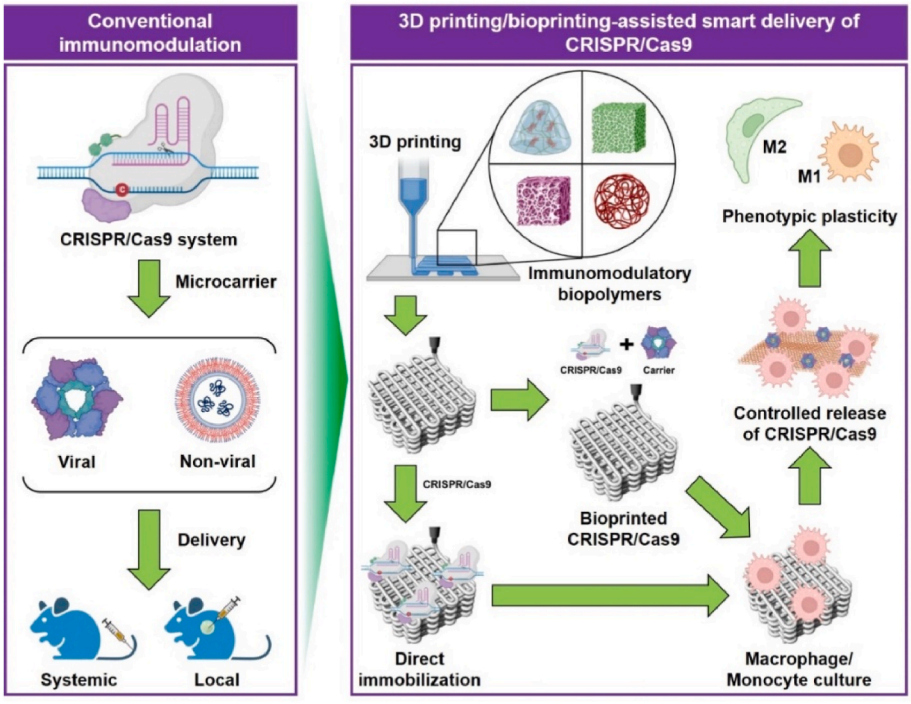

Fig. 11. Schematic illustration showing the role of CRISPRized technology with 3D printing/bioprinting technology to regulate macrophage polarization.

differentiation of other cells. In addition to biomaterials properties, including stiffness/elasticity, topography, and porosity, various biophysical simulations have also been shown to modulate cell adhesion, proliferation, and differentiation [333–336]. For instance, electric field (EF) [246,337,338], magnetic field (MF) [339], hydrostatic pressure [340], and electromagnetic field (EMF) [341] can also be used to stimulate biomaterials for dynamic immunomodulation and regeneration. Various electro active polymers (EAPs) and magneto-active polymers (MAPs) or their composites have been extensively studied in the past few years for understanding mechanobiological cues of cell adhesion and differentiation [342–344]. In this context, the development of novel and stimuli-responsive materials should be required for studying the immunomodulation of macrophages in the future for a better understanding of the effects of biophysical stimulation. Recently, the phenotypic classification of macrophage is migrated towards smart-computer-based identification techniques for better interpretation of immune cells [345–347]. Conventional identification procedures of macrophages include the use of fluorescence (FL) microscopy, quantitative real-time PCR (qRT-PCR), and western blotting (WB), which usually takes a longer time to perform the experiments [348–352]. On the other hand, morphological identification *via* digital or optical microscopy is relatively simple and effective and provides a gross overview of macrophage polarization based on surface morphology. Among various computer-based morphometric tools, artificial intelligence (AI), machine learning (ML), single-cell autofluorescence (SCF), and Raman spectroscopy (*e.g.*, surface enhanced raman spectroscopy or SARS) tools are 'hot spots' in biological research owing to the high-accuracy (~90%) of prediction and cost-effectiveness. Next-generation multi-stimulation-assisted bioprinting platforms must integrate biochemical and biophysical properties that can dynamically modulate macrophage polarization during bone healing and regeneration.

Ethics approval and consent to participate

This review article does not require any ethical approval or allied consents for publication

Declaration of competing interest

The authors declare no competing financial interests related to this article.

Acknowledgements

This work was supported by the Basic Science Research Program' through the 'National Research Foundation of Korea' funded by the 'Ministry of Education' (NRF-2018R1A16A1A03025582, NRF-2019R1D1A3A03103828, and NRF2022R1I1A3063302).

Appendix A. Supplementary data

Supplementary data to this article can be found online at https://doi.org/10.1016/j.bioactmat.2023.05.014.

References

[1] S.H. Kaufmann, Intracellular pathogens: living in an extreme environment, Immunol. Rev. 240 (2011) 5–10.
[2] T. Chtanova, M. Schaeffer, S.-J. Han, G.G. van Dooren, M. Nollmann, P. Herzmark, et al., Dynamics of neutrophil migration in lymph nodes during infection, Immunity 29 (2008) 487–496.
[3] T.A. Wynn, A. Chawla, J.W. Pollard, Macrophage biology in development, homeostasis and disease, Nature 496 (2013) 445–455.
[4] A.K. Gaharwar, I. Singh, A. Khademhosseini, Engineered biomaterials for in situ tissue regeneration, Nat. Rev. Mater. 5 (2020) 686–705.
[5] W. Liu, J. Li, M. Cheng, Q. Wang, K.W. Yeung, P.K. Chu, et al., Zinc-modified sulfonated polyetheretherketone surface with immunomodulatory function for guiding cell fate and bone regeneration, Adv. Sci. 5 (2018), 1800749.
[6] T.U. Luu, S.C. Gott, B.W. Woo, M.P. Rao, W.F. Liu, Micro-and nanopatterned topographical cues for regulating macrophage cell shape and phenotype, ACS Appl. Mater. Interfaces 7 (2015) 28665–28672.
[7] I. Cockerill, Y. Su, J.H. Lee, D. Berman, M.L. Young, Y. Zheng, et al., Micro-/nanotopography on bioresorbable zinc dictates cytocompatibility, bone cell differentiation, and macrophage polarization, Nano Lett. 20 (2020) 4594–4602.
[8] X. Zheng, L. Xin, Y. Luo, H. Yang, X. Ye, Z. Mao, et al., Near-infrared-triggered dynamic surface topography for sequential modulation of macrophage phenotypes, ACS Appl. Mater. Interfaces 11 (2019) 43689–43697.
[9] Y. Zhu, H. Liang, X. Liu, J. Wu, C. Yang, T.M. Wong, et al., Regulation of macrophage polarization through surface topography design to facilitate implant-to-bone osteointegration, Sci. Adv. 7 (2021), eabf6654.
[10] C.D. Walkey, J.B. Olsen, H. Guo, A. Emili, W.C. Chan, Nanoparticle size and surface chemistry determine serum protein adsorption and macrophage uptake, J. Am. Chem. Soc. 134 (2012) 2139–2147.
[11] Z. Zhao, A. Ukidve, V. Krishnan, S. Mitragotri, Effect of physicochemical and surface properties on in vivo fate of drug nanocarriers, Adv. Drug Deliv. Rev. 143 (2019) 3–21.
[12] J. Li, D. Zou, K. Zhang, X. Luo, P. Yang, Y. Jing, et al., Strong multi-functions based on conjugating chondroitin sulfate onto an amine-rich surface will direct the vascular cell fate for cardiovascular implanted devices, J. Mater. Chem. B 5 (2017) 8299–8313.
[13] M. Bartneck, H.A. Keul, S. Singh, K. Czaja, J. Bornemann, M. Bockstaller, et al., Rapid uptake of gold nanorods by primary human blood phagocytes and immunomodulatory effects of surface chemistry, ACS Nano 4 (2010) 3073–3086.
[14] M.M. Maciel, T.R. Correia, M. Henriques, J.F. Mano, Microparticles orchestrating cell fate in bottom-up approaches, Curr. Opin. Biotechnol. 73 (2022) 276–281.
[15] X. Bai, W. Liu, L. Xu, Q. Ye, H. Zhou, C. Berg, et al., Sequential macrophage transition facilitates endogenous bone regeneration induced by Zn-doped porous microcrystalline bioactive glass, J. Mater. Chem. B 9 (2021) 2885–2898.
[16] S. Jiang, C. Lyu, P. Zhao, W. Li, W. Kong, C. Huang, et al., Cryoprotectant enables structural control of porous scaffolds for exploration of cellular mechano-responsiveness in 3D, Nat. Commun. 10 (2019) 1–14.
[17] G. Chan, D.J. Mooney, New materials for tissue engineering: towards greater control over the biological response, Trends Biotechnol. 26 (2008) 382–392.
[18] L. Wu, Y. Xu, K. Xi, Y. Gu, J. Tang, T. Xin, et al., Regulation of macrophage subtype via injectable micro/nano-structured porous microsphere for reprogramming osteoimmune microenvironment, Chem. Eng. J. 439 (2022), 135692.
[19] D. Yang, J. Xiao, B. Wang, L. Li, X. Kong, J. Liao, The immune reaction and degradation fate of scaffold in cartilage/bone tissue engineering, Mater. Sci. Eng. C 104 (2019), 109927.
[20] M. Deng, J. Tan, C. Hu, T. Hou, W. Peng, J. Liu, et al., Modification of PLGA scaffold by MSC-derived extracellular matrix combats macrophage inflammation to initiate bone regeneration via TGF-β-induced protein, Advanced Healthcare Materials 9 (2020), 2000353.
[21] C. Best, S. Tara, M. Wiet, J. Reinhardt, V. Pepper, M. Ball, et al., Deconstructing the tissue engineered vascular graft: evaluating scaffold pre-wetting, conditioned media incubation, and determining the optimal mononuclear cell source, ACS Biomater. Sci. Eng. 3 (2017) 1972–1979.
[22] I.S. Raja, S.H. Lee, M.S. Kang, S.-H. Hyon, A.R. Selvaraj, K. Prabakar, et al., The predominant factor influencing cellular behavior on electrospun nanofibrous scaffolds: wettability or surface morphology? Mater. Des. 216 (2022), 110580.
[23] J. Li, Y.-J. Zhang, Z.-Y. Lv, K. Liu, C.-X. Meng, B. Zou, et al., The observed difference of macrophage phenotype on different surface roughness of mineralized collagen, Regenerative Biomaterials 7 (2020) 203–211.
[24] X. Li, Q. Huang, T.A. Elkhooly, Y. Liu, H. Wu, Q. Feng, et al., Effects of titanium surface roughness on the mediation of osteogenesis via modulating the immune response of macrophages, Biomed. Mater. 13 (2018), 045013.
[25] Z. Chen, T. Klein, R.Z. Murray, R. Crawford, J. Chang, C. Wu, et al., Osteoimmunomodulation for the development of advanced bone biomaterials, Mater. Today 19 (2016) 304–321.
[26] J.M. Anderson, Inflammatory response to implants, ASAIO transactions 34 (1988) 101–107.
[27] D.F. Williams, On the mechanisms of biocompatibility, Biomaterials 29 (2008) 2941–2953.
[28] A. Vishwakarma, N.S. Bhise, M.B. Evangelista, J. Rouwkema, M.R. Dokmeci, A. M. Ghaemmaghami, et al., Engineering immunomodulatory biomaterials to tune the inflammatory response, Trends Biotechnol. 34 (2016) 470–482.
[29] J.M. Anderson, A. Rodriguez, D.T. Chang, Foreign Body Reaction to Biomaterials. Seminars in Immunology, Elsevier, 2008, pp. 86–100.
[30] Y. Duan, J. Liu, L. Ma, N. Li, H. Liu, J. Wang, et al., Toxicological characteristics of nanoparticulate anatase titanium dioxide in mice, Biomaterials 31 (2010) 894–899.
[31] S.V. Murphy, A. Atala, 3D bioprinting of tissues and organs, Nat. Biotechnol. 32 (2014) 773–785.
[32] M. Albanna, K.W. Binder, S.V. Murphy, J. Kim, S.A. Qasem, W. Zhao, et al., In situ bioprinting of autologous skin cells accelerates wound healing of extensive excisional full-thickness wounds, Sci. Rep. 9 (2019) 1–15.
[33] R.I. R Ibañez, R.J. Do Amaral, R.L. Reis, A.P. Marques, C.M. Murphy, F.J. O'Brien, 3D-printed gelatin methacrylate scaffolds with controlled architecture and stiffness modulate the fibroblast phenotype towards dermal regeneration, Polymers 13 (2021) 2510.

[34] M.M. De Santis, H.N. Alsafadi, S. Tas, D.A. Bölükbas, S. Prithiviraj, I.A. Da Silva, et al., Extracellular-matrix-reinforced bioinks for 3D bioprinting human tissue, Adv. Mater. 33 (2021), 2005476.
[35] I.T. Ozbolat, W. Peng, V. Ozbolat, Application areas of 3D bioprinting, Drug Discov. Today 21 (2016) 1257–1271.
[36] Y. Wu, D.J. Ravnic, I.T. Ozbolat, Intraoperative bioprinting: repairing tissues and organs in a surgical setting, Trends Biotechnol. 38 (2020) 594–605.
[37] J. Li, X. Jiang, H. Li, M. Gelinsky, Z. Gu, Tailoring materials for modulation of macrophage fate, Adv. Mater. 33 (2021), 2004172.
[38] P.J. Murray, T.A. Wynn, Protective and pathogenic functions of macrophage subsets, Nat. Rev. Immunol. 11 (2011) 723–737.
[39] D.A. Munro, J. Hughes, The origins and functions of tissue-resident macrophages in kidney development, Front. Physiol. 8 (2017) 837.
[40] S. Yona, K.-W. Kim, Y. Wolf, A. Mildner, D. Varol, M. Breker, et al., Fate mapping reveals origins and dynamics of monocytes and tissue macrophages under homeostasis, Immunity 38 (2013) 79–91.
[41] B. Ajami, J.L. Bennett, C. Krieger, W. Tetzlaff, F. Rossi, Local self-renewal can sustain CNS microglia maintenance and function throughout adult life, Nat. Neurosci. 10 (2007) 1538–1543.
[42] D.M. Mosser, J.P. Edwards, Exploring the full spectrum of macrophage activation, Nat. Rev. Immunol. 8 (2008) 958–969.
[43] A. Sica, A. Mantovani, Macrophage plasticity and polarization: in vivo veritas, J. Clin. Investig. 122 (2012) 787–795.
[44] P.J. Murray, J.E. Allen, S.K. Biswas, E.A. Fisher, D.W. Gilroy, S. Goerdt, et al., Macrophage activation and polarization: nomenclature and experimental guidelines, Immunity 41 (2014) 14–20.
[45] F.O. Martinez, A. Sica, A. Mantovani, M. Locati, Macrophage activation and polarization, Frontiers in Bioscience-Landmark 13 (2008) 453–461.
[46] P. Wang, H. Wang, Q. Huang, C. Peng, L. Yao, H. Chen, et al., Exosomes from M1-polarized macrophages enhance paclitaxel antitumor activity by activating macrophages-mediated inflammation, Theranostics 9 (2019) 1714.
[47] M. Klichinsky, M. Ruella, O. Shestova, X.M. Lu, A. Best, M. Zeeman, et al., Human chimeric antigen receptor macrophages for cancer immunotherapy, Nat. Biotechnol. 38 (2020) 947–953.
[48] A. Mantovani, A. Sica, S. Sozzani, P. Allavena, A. Vecchi, M. Locati, The chemokine system in diverse forms of macrophage activation and polarization, Trends Immunol. 25 (2004) 677–686.
[49] T.A. Reese, H.-E. Liang, A.M. Tager, A.D. Luster, N. Van Rooijen, D. Voehringer, et al., Chitin induces accumulation in tissue of innate immune cells associated with allergy, Nature 447 (2007) 92–96.
[50] E. Brandt, G. Woerly, A.B. Younes, S. Loiseau, M. Capron, IL-4 production by human polymorphonuclear neutrophils, J. Leukoc. Biol. 68 (2000) 125–130.
[51] D.R. Neill, S.H. Wong, A. Bellosi, R.J. Flynn, M. Daly, T.K. Langford, et al., Nuocytes represent a new innate effector leukocyte that mediates type-2 immunity, Nature 464 (2010) 1367–1370.
[52] S. Gordon, Alternative activation of macrophages, Nat. Rev. Immunol. 3 (2003) 23–35.
[53] B. Liu, Y. Jia, J. Ma, S. Wu, H. Jiang, Y. Cao, et al., Tumor-associated macrophage-derived CCL20 enhances the growth and metastasis of pancreatic cancer, Acta Biochim. Biophys. Sin. (2016) 1–8.
[54] V. Pandey, A. Fleming-Martinez, L. Bastea, H.R. Doeppler, J. Eisenhauer, T. Le, et al., CXCL10/CXCR3 signaling contributes to an inflammatory microenvironment and its blockade enhances progression of murine pancreatic precancerous lesions, Elife 10 (2021), e60646.
[55] W. Zeng, L. Xiong, W. Wu, S. Li, J. Liu, L. Yang, et al., CCL18 signaling from tumor-associated macrophages activates fibroblasts to adopt a chemoresistance-inducing phenotype, Oncogene 42 (2023) 224–237.
[56] Y. Feng, R. Mu, Z. Wang, P. Xing, J. Zhang, L. Dong, et al., A toll-like receptor agonist mimicking microbial signal to generate tumor-suppressive macrophages, Nat. Commun. 10 (2019) 2272.
[57] F.O. Martinez, S. Gordon, M. Locati, A. Mantovani, Transcriptional profiling of the human monocyte-to-macrophage differentiation and polarization: new molecules and patterns of gene expression, J. Immunol. 177 (2006) 7303–7311.
[58] R. Klopfleisch, Macrophage reaction against biomaterials in the mouse model–Phenotypes, functions and markers, Acta Biomater. 43 (2016) 3–13.
[59] L. Peiser, S. Mukhopadhyay, S. Gordon, Scavenger receptors in innate immunity, Curr. Opin. Immunol. 14 (2002) 123–128.
[60] J. Mao, L. Chen, Z. Cai, S. Qian, Z. Liu, B. Zhao, et al., Advanced biomaterials for regulating polarization of macrophages in wound healing, Adv. Funct. Mater. 32 (2022), 2111003.
[61] T.A. Wynn, L. Barron, Macrophages: Master Regulators of Inflammation and Fibrosis. Seminars in Liver Disease, © Thieme Medical Publishers, 2010, pp. 245–257.
[62] J.S. Duffield, S.J. Forbes, C.M. Constandinou, S. Clay, M. Partolina, S. Vuthoori, et al., Selective depletion of macrophages reveals distinct, opposing roles during liver injury and repair, J. Clin. Investig. 115 (2005) 56–65.
[63] B. Berse, L.F. Brown, L. Van De Water, H.F. Dvorak, D.R. Senger, Vascular permeability factor (vascular endothelial growth factor) gene is expressed differentially in normal tissues, macrophages, and tumors, Mol. Biol. Cell 3 (1992) 211–220.
[64] S. Chujo, F. Shirasaki, M. Kondo-Miyazaki, Y. Ikawa, K. Takehara, Role of connective tissue growth factor and its interaction with basic fibroblast growth factor and macrophage chemoattractant protein-1 in skin fibrosis, J. Cell. Physiol. 220 (2009) 189–195.
[65] D.A. Rappolee, D. Mark, M.J. Banda, Z. Werb, Wound macrophages express TGF-α and other growth factors in vivo: analysis by mRNA phenotyping, Science 241 (1988) 708–712.
[66] K. Shimokado, E.W. Raines, D.K. Madtes, T.B. Barrett, E.P. Benditt, R. Ross, A significant part of macrophage-derived growth factor consists of at least two forms of PDGF, Cell 43 (1985) 277–286.
[67] S. Willenborg, T. Lucas, G. Van Loo, J.A. Knipper, T. Krieg, I. Haase, et al., CCR2 recruits an inflammatory macrophage subpopulation critical for angiogenesis in tissue repair. Blood, The Journal of the American Society of Hematology 120 (2012) 613–625.
[68] P. Ramachandran, J.P. Iredale, J.A. Fallowfield, Resolution of Liver Fibrosis: Basic Mechanisms and Clinical Relevance. Seminars in Liver Disease, Thieme Medical Publishers, 2015, pp. 119–131.
[69] B.M. Delavary, W.M. van der Veer, M. van Egmond, F.B. Niessen, R.H. Beelen, Macrophages in skin injury and repair, Immunobiology 216 (2011) 753–762.
[70] F. Durant, J.L. Whited, Finding solutions for fibrosis: understanding the innate mechanisms used by super-regenerator vertebrates to combat scarring, Adv. Sci. 8 (2021), 2100407.
[71] Y.-H. Kim, R.O. Oreffo, J.I. Dawson, From hurdle to springboard: the macrophage as target in biomaterial-based bone regeneration strategies, Bone (2022), 116389.
[72] C. Schlundt, H. Fischer, C.H. Bucher, C. Rendenbach, G.N. Duda, K. Schmidt-Bleek, The multifaceted roles of macrophages in bone regeneration: a story of polarization, activation and time, Acta Biomater. 133 (2021) 46–57.
[73] L.F. Bonewald, Osteocytes as dynamic multifunctional cells, Ann. N. Y. Acad. Sci. 1116 (2007) 281–290.
[74] R. Weinkamer, P. Kollmannsberger, P. Fratzl, Towards a connectomic description of the osteocyte lacunocanalicular network in bone, Curr. Osteoporos. Rep. 17 (2019) 186–194.
[75] A. Singh, A.A. Mehdi, R.N. Srivastava, N.S. Verma, Immunoregulation of bone remodelling, International journal of critical illness and injury science 2 (2012) 75.
[76] B.F. Boyce, Y. Xiu, J. Li, L. Xing, Z. Yao, NF-κB-mediated regulation of osteoclastogenesis, Endocrinology and metabolism 30 (2015) 35–44.
[77] T. Ono, T. Nakashima, Recent advances in osteoclast biology, Histochem. Cell Biol. 149 (2018) 325–341.
[78] A.-P. Trouvin, V. Goëb, Receptor activator of nuclear factor-κB ligand and osteoprotegerin: maintaining the balance to prevent bone loss, Clin. Interv. Aging 5 (2010) 345.
[79] Q-l Ma, L. Fang, N. Jiang, L. Zhang, Y. Wang, Y-m Zhang, et al., Bone mesenchymal stem cell secretion of sRANKL/OPG/M-CSF in response to macrophage-mediated inflammatory response influences osteogenesis on nanostructured Ti surfaces, Biomaterials 154 (2018) 234–247.
[80] S. Yang, N. Wang, Y. Ma, S. Guo, S. Guo, H. Sun, Immunomodulatory effects and mechanisms of distraction osteogenesis, Int. J. Oral Sci. 14 (2022) 1–11.
[81] F. Lebre, C.H. Hearnden, E.C. Lavelle, Modulation of immune responses by particulate materials, Adv. Mater. 28 (2016) 5525–5541.
[82] A. Singh, Biomaterials innovation for next generation ex vivo immune tissue engineering, Biomaterials 130 (2017) 104–110.
[83] P. Moshayedi, G. Ng, J.C. Kwok, G.S. Yeo, C.E. Bryant, J.W. Fawcett, et al., The relationship between glial cell mechanosensitivity and foreign body reactions in the central nervous system, Biomaterials 35 (2014) 3919–3925.
[84] W. Jin, F. Tamzalit, P.K. Chaudhuri, C.T. Black, M. Huse, L.C. Kam, T cell activation and immune synapse organization respond to the microscale mechanics of structured surfaces, Proc. Natl. Acad. Sci. USA 116 (2019) 19835–19840.
[85] T.D. Smith, R.R. Nagalla, E.Y. Chen, W.F. Liu, Harnessing macrophage plasticity for tissue regeneration, Adv. Drug Deliv. Rev. 114 (2017) 193–205.
[86] M.S. Wang, Y. Hu, E.E. Sanchez, X. Xie, N.H. Roy, M. de Jesus, et al., Mechanically active integrins target lytic secretion at the immune synapse to facilitate cellular cytotoxicity, Nat. Commun. 13 (2022) 1–15.
[87] A.K. Blakney, M.D. Swartzlander, S.J. Bryant, The effects of substrate stiffness on the in vitro activation of macrophages and in vivo host response to poly (ethylene glycol)-based hydrogels, J. Biomed. Mater. Res., Part A 100 (2012) 1375.
[88] J.M. Goffin, P. Pittet, G. Csucs, J.W. Lussi, J.-J. Meister, B. Hinz, Focal adhesion size controls tension-dependent recruitment of α-smooth muscle actin to stress fibers, J. Cell Biol. 172 (2006) 259–268.
[89] H. Jiang, S. Hegde, B.L. Knolhoff, Y. Zhu, J.M. Herndon, M.A. Meyer, et al., Targeting focal adhesion kinase renders pancreatic cancers responsive to checkpoint immunotherapy, Nat. Med. 22 (2016) 851–860.
[90] S.K. Mitra, D.A. Hanson, D.D. Schlaepfer, Focal adhesion kinase: in command and control of cell motility, Nat. Rev. Mol. Cell Biol. 6 (2005) 56–68.
[91] K.A. Owen, C.B. Meyer, A.H. Bouton, J.E. Casanova, Activation of focal adhesion kinase by Salmonella suppresses autophagy via an Akt/mTOR signaling pathway and promotes bacterial survival in macrophages, PLoS Pathog. 10 (2014), e1004159.
[92] M. Okigaki, C. Davis, M. Falasca, S. Harroch, D. Felsenfeld, M. Sheetz, et al., Pyk2 regulates multiple signaling events crucial for macrophage morphology and migration, Proc. Natl. Acad. Sci. USA 100 (2003) 10740–10745.
[93] M.M. Mia, D.M. Cibi, S.A.B. Abdul Ghani, W. Song, N. Tee, S. Ghosh, et al., YAP/TAZ deficiency reprograms macrophage phenotype and improves infarct healing and cardiac function after myocardial infarction, PLoS Biol. 18 (2020), e3000941.
[94] M.M. Mia, D.M. Cibi, S.A.B.A. Ghani, A. Singh, N. Tee, V. Sivakumar, et al., Loss of Yap/Taz in cardiac fibroblasts attenuates adverse remodelling and improves cardiac function, Cardiovasc. Res. 118 (2022) 1785–1804.

[95] M. Nishino, I. Matsuzaki, F.Y. Musangile, Y. Takahashi, Y. Iwahashi, K. Warigaya, et al., Measurement and visualization of cell membrane surface charge in fixed cultured cells related with cell morphology, PLoS One 15 (2020), e0236373.
[96] H. Shen, B. Xu, C. Yang, W. Xue, Z. You, X. Wu, et al., A DAMP-scavenging, IL-10-releasing hydrogel promotes neural regeneration and motor function recovery after spinal cord injury, Biomaterials 280 (2022), 121279.
[97] S.D. Kumar, J.H. Park, H.S. Kim, C.D. Seo, C. Ajish, E.Y. Kim, et al., Cationic, amphipathic small molecules based on a triazine-piperazine-triazine scaffold as a new class of antimicrobial agents, Eur. J. Med. Chem. (2022), 114747.
[98] M.A. Dobrovolskaia, S.E. McNeil, Immunological properties of engineered nanomaterials, Nat. Nanotechnol. 2 (2007) 469–478.
[99] H. Chen, P. Li, Y. Yin, X. Cai, Z. Huang, J. Chen, et al., The promotion of type 1 T helper cell responses to cationic polymers in vivo via toll-like receptor-4 mediated IL-12 secretion, Biomaterials 31 (2010) 8172–8180.
[100] F.J. Van Dalen, M.H. Van Stevendaal, F.L. Fennemann, M. Verdoes, O. Ilina, Molecular repolarisation of tumour-associated macrophages, Molecules 24 (2018) 9.
[101] X. Ding, X. Li, C. Li, M. Qi, Z. Zhang, X. Sun, et al., Chitosan/dextran hydrogel constructs containing strontium-doped hydroxyapatite with enhanced osteogenic potential in rat cranium, ACS Biomater. Sci. Eng. 5 (2019) 4574–4586.
[102] H. Fan, W. Chen, J. Zhu, J. Zhang, S. Peng, Toosendanin alleviates dextran sulfate sodium-induced colitis by inhibiting M1 macrophage polarization and regulating NLRP3 inflammasome and Nrf2/HO-1 signaling, Int. Immunopharm. 76 (2019), 105909.
[103] C.R. Almeida, T. Serra, M.I. Oliveira, J.A. Planell, M.A. Barbosa, M. Navarro, Impact of 3-D printed PLA-and chitosan-based scaffolds on human monocyte/macrophage responses: unraveling the effect of 3-D structures on inflammation, Acta Biomater. 10 (2014) 613–622.
[104] K. Hua, E. Ålander, T. Lindström, A. Mihranyan, M. Strømme, N. Ferraz, Surface chemistry of nanocellulose fibers directs monocyte/macrophage response, Biomacromolecules 16 (2015) 2787–2795.
[105] H. Okada, P. Kalinski, R. Ueda, A. Hoji, G. Kohanbash, T.E. Donegan, et al., Induction of CD8+ T-cell responses against novel glioma–associated antigen peptides and clinical activity by vaccinations with α-type 1 polarized dendritic cells and polyinosinic-polycytidylic acid stabilized by lysine and carboxymethylcellulose in patients with recurrent malignant glioma, J. Clin. Oncol. 29 (2011) 330.
[106] J.S. Erdem, M. Alswady-Hoff, T.K. Ervik, Ø. Skare, D.G. Ellingsen, S. Zienolddiny, Cellulose nanocrystals modulate alveolar macrophage phenotype and phagocytic function, Biomaterials 203 (2019) 31–42.
[107] D.K. Patel, S.D. Dutta, J. Hexiu, K. Ganguly, K.-T. Lim, 3D-printable chitosan/silk fibroin/cellulose nanoparticle scaffolds for bone regeneration via M2 macrophage polarization, Carbohydr. Polym. (2022), 119077.
[108] D. Reichel, M. Tripathi, J.M. Perez, Biological effects of nanoparticles on macrophage polarization in the tumor microenvironment, Nanotheranostics 3 (2019) 66.
[109] Y.-J. Huang, K.-C. Hung, H.-S. Hung, S-h Hsu, Modulation of macrophage phenotype by biodegradable polyurethane nanoparticles: possible relation between macrophage polarization and immune response of nanoparticles, ACS Appl. Mater. Interfaces 10 (2018) 19436–19448.
[110] A.-K. Fuchs, T. Syrovets, K.A. Haas, C. Loos, A. Musyanovych, V. Mailänder, et al., Carboxyl-and amino-functionalized polystyrene nanoparticles differentially affect the polarization profile of M1 and M2 macrophage subsets, Biomaterials 85 (2016) 78–87.
[111] J. Wu, J. Zhu, Q. Wu, Y. An, K. Wang, T. Xuan, et al., Mussel-inspired surface immobilization of heparin on magnetic nanoparticles for enhanced wound repair via sustained release of a growth factor and M2 macrophage polarization, ACS Appl. Mater. Interfaces 13 (2021) 2230–2244.
[112] T.-H. Tran, R. Rastogi, J. Shelke, M.M. Amiji, Modulation of macrophage functional polarity towards anti-inflammatory phenotype with plasmid DNA delivery in CD44 targeting hyaluronic acid nanoparticles, Sci. Rep. 5 (2015) 1–15.
[113] W. Zhang, S. Cao, S. Liang, C.H. Tan, B. Luo, X. Xu, et al., Differently charged super-paramagnetic iron oxide nanoparticles preferentially induced M1-like phenotype of macrophages, Front. Bioeng. Biotechnol. 8 (2020) 537.
[114] Y. Yang, L. Guo, Z. Wang, P. Liu, X. Liu, J. Ding, et al., Targeted silver nanoparticles for rheumatoid arthritis therapy via macrophage apoptosis and Re-polarization, Biomaterials 264 (2021), 120390.
[115] L. Kou, H. Huang, Y. Tang, M. Sun, Y. Li, J. Wu, et al., Opsonized nanoparticles target and regulate macrophage polarization for osteoarthritis therapy: a trapping strategy, J. Contr. Release 347 (2022) 237–255.
[116] B. Wei, J. Pan, R. Yuan, B. Shao, Y. Wang, X. Guo, et al., Polarization of tumor-associated macrophages by nanoparticle-loaded Escherichia coli combined with immunogenic cell death for cancer immunotherapy, Nano Lett. 21 (2021) 4231–4240.
[117] M. Azadpour, M.M. Farajollahi, H. Dariushnejad, A.M. Varzi, A. Varezardi, M. Barati, Effects of synthetic silymarin-PLGA nanoparticles on M2 polarization and inflammatory cytokines in LPS-treated murine peritoneal macrophages, Iranian Journal of Basic Medical Sciences 24 (2021) 1446.
[118] X. Zhao, K. Guo, K. Zhang, S. Duan, M. Chen, N. Zhao, et al., Orchestrated yolk–shell nanohybrids regulate macrophage polarization and dendritic cell maturation for oncotherapy with augmented antitumor immunity, Adv. Mater. 34 (2022), 2108263.
[119] X. Bai, D. Chen, Y. Dai, S. Liang, J. Guo, B. Dai, et al., Bone formation recovery with gold nanoparticle-induced M2 macrophage polarization in mice, Nanomed. Nanotechnol. Biol. Med. 38 (2021), 102457.
[120] M. Zhao, J. Li, J. Liu, M. Xu, H. Ji, S. Wu, et al., Charge-switchable nanoparticles enhance Cancer immunotherapy based on mitochondrial dynamic regulation and immunogenic cell death induction, J. Contr. Release 335 (2021) 320–332.
[121] G. Qing, S. Zhao, Y. Xiong, Z. Lv, F. Jiang, Y. Liu, et al., Chiral effect at protein/graphene interface: a bioinspired perspective to understand amyloid formation, J. Am. Chem. Soc. 136 (2014) 10736–10742.
[122] T. Sun, D. Han, K. Rhemann, L. Chi, H. Fuchs, Stereospecific interaction between immune cells and chiral surfaces, J. Am. Chem. Soc. 129 (2007) 1496–1497.
[123] N.S. Kehr, H.-J. Galla, K. Riehemann, H. Fuchs, Self-assembled monolayers of enantiomerically functionalized periodic mesoporous organosilicas and the effect of surface chirality on cell adhesion behaviour, RSC Adv. 5 (2015) 5704–5710.
[124] R.M. Visalakshan, M.N. MacGregor, S. Sasidharan, A. Ghazaryan, A. M. Mierczynska-Vasilev, S. Morsbach, et al., Biomaterial surface hydrophobicity-mediated serum protein adsorption and immune responses, ACS Appl. Mater. Interfaces 11 (2019) 27615–27623.
[125] A. Rich, A.K. Harris, Anomalous preferences of cultured macrophages for hydrophobic and roughened substrata, J. Cell Sci. 50 (1981) 1–7.
[126] K.M. Hotchkiss, G.B. Reddy, S.L. Hyzy, Z. Schwartz, B.D. Boyan, R. Olivares-Navarrete, Titanium surface characteristics, including topography and wettability, alter macrophage activation, Acta Biomater. 31 (2016) 425–434.
[127] L. Lv, Y. Xie, K. Li, T. Hu, X. Lu, Y. Cao, et al., Unveiling the mechanism of surface hydrophilicity-modulated macrophage polarization, Advanced Healthcare Materials 7 (2018), 1800675.
[128] Y.W. Chun, W. Wang, J. Choi, T.-H. Nam, Y.-H. Lee, K.-K. Cho, et al., Control of macrophage responses on hydrophobic and hydrophilic carbon nanostructures, Carbon 49 (2011) 2092–2103.
[129] S. Chen, J.A. Jones, Y. Xu, H.-Y. Low, J.M. Anderson, K.W. Leong, Characterization of topographical effects on macrophage behavior in a foreign body response model, Biomaterials 31 (2010) 3479–3491.
[130] F.Y. McWhorter, T. Wang, P. Nguyen, T. Chung, W.F. Liu, Modulation of macrophage phenotype by cell shape, Proc. Natl. Acad. Sci. USA 110 (2013) 17253–17258.
[131] S.M. Hamlet, S. Ivanovski, Inflammatory Cytokine Response to Titanium Surface Chemistry and Topography. The Immune Response to Implanted Materials and Devices, Springer, 2017, pp. 151–167.
[132] A.K. Refai, M. Textor, D.M. Brunette, J.D. Waterfield, Effect of titanium surface topography on macrophage activation and secretion of proinflammatory cytokines and chemokines, J. Biomed. Mater. Res. Part A: An Official Journal of The Society for Biomaterials 70 (2004) 194–205. The Japanese Society for Biomaterials, and The Australian Society for Biomaterials and the Korean Society for Biomaterials.
[133] K. Wang, W.-D. Hou, X. Wang, C. Han, I. Vuletic, N. Su, et al., Overcoming foreign-body reaction through nanotopography: biocompatibility and immunoisolation properties of a nanofibrous membrane, Biomaterials 102 (2016) 249–258.
[134] A.D. Schoenenberger, H. Tempfer, C. Lehner, J. Egloff, M. Mauracher, A. Bird, et al., Macromechanics and polycaprolactone fiber organization drive macrophage polarization and regulate inflammatory activation of tendon in vitro and in vivo, Biomaterials 249 (2020), 120034.
[135] X. Dong, S. Liu, Y. Yang, S. Gao, W. Li, J. Cao, et al., Aligned microfiber-induced macrophage polarization to guide schwann-cell-enabled peripheral nerve regeneration, Biomaterials 272 (2021), 120767.
[136] B.N. Brown, R. Londono, S. Tottey, L. Zhang, K.A. Kukla, M.T. Wolf, et al., Macrophage phenotype as a predictor of constructive remodeling following the implantation of biologically derived surgical mesh materials, Acta Biomater. 8 (2012) 978–987.
[137] F. Razzi, L. Fratila-Apachitei, N. Fahy, Y.M. Bastiaansen-Jenniskens, I. Apachitei, E. Farrell, et al., Immunomodulation of surface biofunctionalized 3D printed porous titanium implants, Biomed. Mater. 15 (2020), 035017.
[138] M. Friedemann, L. Kalbitzer, S. Franz, S. Moeller, M. Schnabelrauch, J.C. Simon, et al., Instructing human macrophage polarization by stiffness and glycosaminoglycan functionalization in 3D collagen networks, Advanced healthcare materials 6 (2017), 1600967.
[139] D. Li, Y. Li, A. Shrestha, S. Wang, Q. Wu, L. Li, et al., Effects of programmed local delivery from a micro/nano-hierarchical surface on titanium implant on infection clearance and osteogenic induction in an infected bone defect, Advanced healthcare materials 8 (2019), 1900002.
[140] S. Gao, L. Wang, Y. Zhang, L. Li, Y. Zhang, X. Gao, et al., Tanshinone IIA-loaded aligned microfibers facilitate stem cell recruitment and capillary formation by inducing M2 macrophage polarization, Appl. Mater. Today 21 (2020), 100841.
[141] M. Bohner, L. Galea, N. Doebelin, Calcium phosphate bone graft substitutes: failures and hopes, J. Eur. Ceram. Soc. 32 (2012) 2663–2671.
[142] S. Franz, S. Rammelt, D. Scharnweber, J.C. Simon, Immune responses to implants–a review of the implications for the design of immunomodulatory biomaterials, Biomaterials 32 (2011) 6692–6709.
[143] L. Chung, D.R. Maestas Jr., F. Housseau, J.H. Elisseeff, Key players in the immune response to biomaterial scaffolds for regenerative medicine, Adv. Drug Deliv. Rev. 114 (2017) 184–192.
[144] H. Wu, S. Han, B. Wu, X. Du, Z. Sheng, J. Lin, et al., Single-cell mass cytometry reveals in vivo immunological response to surgical biomaterials, Appl. Mater. Today 16 (2019) 169–178.
[145] K. Sadtler, M.T. Wolf, S. Ganguly, C.A. Moad, L. Chung, S. Majumdar, et al., Divergent immune responses to synthetic and biological scaffolds, Biomaterials 192 (2019) 405–415.

[146] B.H. Cha, S.R. Shin, J. Leijten, Y.C. Li, S. Singh, J.C. Liu, et al., Integrin-mediated interactions control macrophage polarization in 3D hydrogels, Advanced healthcare materials 6 (2017), 1700289.
[147] S. Kim, H. Nie, V. Nesin, U. Tran, P. Outeda, C.-X. Bai, et al., The polycystin complex mediates Wnt/Ca2+ signalling, Nat. Cell Biol. 18 (2016) 752–764.
[148] J. Li, W. Liu, D. Kilian, X. Zhang, M. Gelinsky, P.K. Chu, Bioinspired interface design modulates pathogen and immunocyte responses in biomaterial-centered infection combination therapy, Mater. Horiz. 6 (2019) 1271–1282.
[149] W. Liu, J. Li, M. Cheng, Q. Wang, Y. Qian, K.W. Yeung, et al., A surface-engineered polyetheretherketone biomaterial implant with direct and immunoregulatory antibacterial activity against methicillin-resistant Staphylococcus aureus, Biomaterials 208 (2019) 8–20.
[150] M. Shi, Z. Chen, S. Farnaghi, T. Friis, X. Mao, Y. Xiao, et al., Copper-doped mesoporous silica nanospheres, a promising immunomodulatory agent for inducing osteogenesis, Acta Biomater. 30 (2016) 334–344.
[151] A. Sindrilaru, T. Peters, S. Wieschalka, C. Baican, A. Baican, H. Peter, et al., An unrestrained proinflammatory M1 macrophage population induced by iron impairs wound healing in humans and mice, J. Clin. Investig. 121 (2011) 985–997.
[152] C. Pan, L. Chen, R. Wu, H. Shan, Z. Zhou, Y. Lin, et al., Lithium-containing biomaterials inhibit osteoclastogenesis of macrophages in vitro and osteolysis in vivo, J. Mater. Chem. B 6 (2018) 8115–8126.
[153] J. Sugimoto, A.M. Romani, A.M. Valentin-Torres, A.A. Luciano, C.M.R. Kitchen, N. Funderburg, et al., Magnesium decreases inflammatory cytokine production: a novel innate immunomodulatory mechanism, J. Immunol. 188 (2012) 6338–6346.
[154] J. Li, J. Wen, B. Li, W. Li, W. Qiao, J. Shen, et al., Valence state manipulation of cerium oxide nanoparticles on a titanium surface for modulating cell fate and bone formation, Adv. Sci. 5 (2018), 1700678.
[155] L. Liang, D. Song, K. Wu, Z. Ouyang, Q. Huang, G. Lei, et al., Sequential activation of M1 and M2 phenotypes in macrophages by Mg degradation from Ti-Mg alloy for enhanced osteogenesis, Biomater. Res. 26 (2022) 1–19.
[156] J. Wang, H. Zhou, G. Guo, J. Tan, Q. Wang, J. Tang, et al., Enhanced anti-infective efficacy of ZnO nanoreservoirs through a combination of intrinsic anti-biofilm activity and reinforced innate defense, ACS Appl. Mater. Interfaces 9 (2017) 33609–33623.
[157] Z. Chen, W. Zhang, M. Wang, L.J. Backman, J. Chen, Effects of Zinc, Magnesium, and Iron Ions on Bone Tissue Engineering, ACS Biomaterials Science & Engineering, 2022.
[158] W. Liu, N.H. Golshan, X. Deng, D.J. Hickey, K. Zeimer, H. Li, et al., Selenium nanoparticles incorporated into titania nanotubes inhibit bacterial growth and macrophage proliferation, Nanoscale 8 (2016) 15783–15794.
[159] X.-T. He, X. Li, M. Zhang, B.-M. Tian, L.-J. Sun, C.-S. Bi, et al., Role of molybdenum in material immunomodulation and periodontal wound healing: targeting immunometabolism and mitochondrial function for macrophage modulation, Biomaterials 283 (2022), 121439.
[160] H.C. Bygd, K.D. Forsmark, K.M. Bratlie, Altering in vivo macrophage responses with modified polymer properties, Biomaterials 56 (2015) 187–197.
[161] D. Zeng, X. Zhang, X. Wang, Q. Huang, J. Wen, X. Miao, et al., The osteoimmunomodulatory properties of MBG scaffold coated with amino functional groups, Artif. Cell Nanomed. Biotechnol. 46 (2018) 1425–1435.
[162] T.L. Lopez-Silva, D.G. Leach, A. Azares, I.-C. Li, D.G. Woodside, J.D. Hartgerink, Chemical functionality of multidomain peptide hydrogels governs early host immune response, Biomaterials 231 (2020), 119667.
[163] V. Mulens-Arias, J.M. Rojas, S. Pérez-Yagüe, M.P. Morales, D.F. Barber, Polyethylenimine-coated SPIONs trigger macrophage activation through TLR-4 signaling and ROS production and modulate podosome dynamics, Biomaterials 52 (2015) 494–506.
[164] T.D. Zaveri, J.S. Lewis, N.V. Dolgova, M.J. Clare-Salzler, B.G. Keselowsky, Integrin-directed modulation of macrophage responses to biomaterials, Biomaterials 35 (2014) 3504–3515.
[165] L. Schirmer, P. Atallah, C. Werner, U. Freudenberg, StarPEG-heparin hydrogels to protect and sustainably deliver IL-4, Advanced healthcare materials 5 (2016) 3157–3164.
[166] R. Liu, S. Chen, P. Huang, G. Liu, P. Luo, Z. Li, et al., Immunomodulation-based strategy for improving soft tissue and metal implant integration and its implications in the development of metal soft tissue materials, Adv. Funct. Mater. 30 (2020), 1910672.
[167] X.-T. He, X. Li, Y. Xia, Y. Yin, R.-X. Wu, H.-H. Sun, et al., Building capacity for macrophage modulation and stem cell recruitment in high-stiffness hydrogels for complex periodontal regeneration: experimental studies in vitro and in rats, Acta Biomater. 88 (2019) 162–180.
[168] L. Cardilo-Reis, S. Gruber, S.M. Schreier, M. Drechsler, N. Papac-Milicevic, C. Weber, et al., Interleukin-13 protects from atherosclerosis and modulates plaque composition by skewing the macrophage phenotype, EMBO Mol. Med. 4 (2012) 1072–1086.
[169] V. Riabov, F. Salazar, S.S. Htwe, A. Gudima, C. Schmuttermaier, J. Barthes, et al., Generation of anti-inflammatory macrophages for implants and regenerative medicine using self-standing release systems with a phenotype-fixing cytokine cocktail formulation, Acta Biomater. 53 (2017) 389–398.
[170] K.L. Spiller, S. Nassiri, C.E. Witherel, R.R. Anfang, J. Ng, K.R. Nakazawa, et al., Sequential delivery of immunomodulatory cytokines to facilitate the M1-to-M2 transition of macrophages and enhance vascularization of bone scaffolds, Biomaterials 37 (2015) 194–207.
[171] J. Braune, U. Weyer, C. Hobusch, J. Mauer, J.C. Brüning, I. Bechmann, et al., IL-6 regulates M2 polarization and local proliferation of adipose tissue macrophages in obesity, J. Immunol. 198 (2017) 2927–2934.
[172] K. Sadtler, B.W. Allen, K. Estrellas, F. Housseau, D.M. Pardoll, J.H. Elisseeff, The scaffold immune microenvironment: biomaterial-mediated immune polarization in traumatic and nontraumatic applications, Tissue Eng. 23 (2017) 1044–1053.
[173] S.D. Sommerfeld, C. Cherry, R.M. Schwab, L. Chung, D.R. Maestas Jr., P. Laffont, et al., Interleukin-36γ–producing macrophages drive IL-17–mediated fibrosis, Science immunology 4 (2019), eaax4783.
[174] M.B. Ariganello, D.T. Simionescu, R.S. Labow, J.M. Lee, Macrophage differentiation and polarization on a decellularized pericardial biomaterial, Biomaterials 32 (2011) 439–449.
[175] S.-W. Kim, G.-B. Im, G.-J. Jeong, S. Baik, J. Hyun, Y.-J. Kim, et al., Delivery of a spheroids-incorporated human dermal fibroblast sheet increases angiogenesis and M2 polarization for wound healing, Biomaterials 275 (2021), 120954.
[176] S.H. Nam, D. Kim, D. Lee, H.-M. Lee, D.-G. Song, J.W. Jung, et al., Lysyl-tRNA synthetase–expressing colon spheroids induce M2 macrophage polarization to promote metastasis, J. Clin. Investig. 128 (2018) 5034–5055.
[177] Z. Chen, C. Wu, W. Gu, T. Klein, R. Crawford, Y. Xiao, Osteogenic differentiation of bone marrow MSCs by β-tricalcium phosphate stimulating macrophages via BMP2 signalling pathway, Biomaterials 35 (2014) 1507–1518.
[178] F. Wei, Y. Zhou, J. Wang, C. Liu, Y. Xiao, The immunomodulatory role of BMP-2 on macrophages to accelerate osteogenesis, Tissue Eng. 24 (2018) 584–594.
[179] J. Tan, Q.-Y. Zhang, Y.-T. Song, K. Huang, Y.-L. Jiang, J. Chen, et al., Accelerated bone defect regeneration through sequential activation of the M1 and M2 phenotypes of macrophages by a composite BMP-2@ SIS hydrogel: an immunomodulatory perspective, Compos. B Eng. 243 (2022), 110149.
[180] H. Wu, Y. Yin, X. Hu, C. Peng, Y. Liu, Q. Li, et al., Effects of environmental pH on macrophage polarization and osteoimmunomodulation, ACS Biomater. Sci. Eng. 5 (2019) 5548–5557.
[181] W. Liu, M. Yu, F. Chen, L. Wang, C. Ye, Q. Chen, et al., A novel delivery nanobiotechnology: engineered miR-181b exosomes improved osteointegration by regulating macrophage polarization, J. Nanobiotechnol. 19 (2021) 1–18.
[182] N. Linde, W. Lederle, S. Depner, N. Van Rooijen, C.M. Gutschalk, M.M. Mueller, Vascular endothelial growth factor-induced skin carcinogenesis depends on recruitment and alternative activation of macrophages, J. Pathol. 227 (2012) 17–28.
[183] J.E. Engel, E. Williams, M.L. Williams, G.L. Bidwell III, A.R. Chade, Targeted VEGF (vascular endothelial growth factor) therapy induces long-term renal recovery in chronic kidney disease via macrophage polarization, Hypertension 74 (2019) 1113–1123.
[184] C. Baumeier, F. Escher, G. Aleshcheva, H. Pietsch, H.-P. Schultheiss, Plasminogen activator inhibitor-1 reduces cardiac fibrosis and promotes M2 macrophage polarization in inflammatory cardiomyopathy, Basic Res. Cardiol. 116 (2021) 1–9.
[185] C. Cao, D.A. Lawrence, Y. Li, C.A. Von Arnim, J. Herz, E.J. Su, et al., Endocytic receptor LRP together with tPA and PAI-1 coordinates Mac-1-dependent macrophage migration, EMBO J. 25 (2006) 1860–1870.
[186] A. Mantovani, S. Sozzani, M. Locati, P. Allavena, A. Sica, Macrophage polarization: tumor-associated macrophages as a paradigm for polarized M2 mononuclear phagocytes, Trends Immunol. 23 (2002) 549–555.
[187] K.J. Rogers, B. Brunton, L. Mallinger, D. Bohan, K.M. Sevcik, J. Chen, et al., IL-4/IL-13 polarization of macrophages enhances Ebola virus glycoprotein-dependent infection, PLoS Neglected Trop. Dis. 13 (2019), e0007819.
[188] D. Hachim, S.T. LoPresti, C.C. Yates, B.N. Brown, Shifts in macrophage phenotype at the biomaterial interface via IL-4 eluting coatings are associated with improved implant integration, Biomaterials 112 (2017) 95–107.
[189] Y. Degboé, B. Rauwel, M. Baron, J.-F. Boyer, A. Ruyssen-Witrand, A. Constantin, et al., Polarization of rheumatoid macrophages by TNF targeting through an IL-10/STAT3 mechanism, Front. Immunol. 10 (2019) 3.
[190] O.R. Mahon, D.C. Browe, T. Gonzalez-Fernandez, P. Pitacco, I.T. Whelan, S. Von Euw, et al., Nano-particle mediated M2 macrophage polarization enhances bone formation and MSC osteogenesis in an IL-10 dependent manner, Biomaterials 239 (2020), 119833.
[191] R.J. Snyder, J. Lantis, R.S. Kirsner, V. Shah, M. Molyneaux, M.J. Carter, Macrophages: a review of their role in wound healing and their therapeutic use, Wound Repair Regen. 24 (2016) 613–629.
[192] D. Kwon, B.G. Cha, Y. Cho, J. Min, E.-B. Park, S.-J. Kang, et al., Extra-large pore mesoporous silica nanoparticles for directing in vivo M2 macrophage polarization by delivering IL-4, Nano Lett. 17 (2017) 2747–2756.
[193] C. Huang, G. Yang, S. Zhou, E. Luo, J. Pan, C. Bao, et al., Controlled delivery of growth factor by hierarchical nanostructured core–shell nanofibers for the efficient repair of critical-sized rat calvarial defect, ACS Biomater. Sci. Eng. 6 (2020) 5758–5770.
[194] H. Kang, S. Kim, D.S.H. Wong, H.J. Jung, S. Lin, K. Zou, et al., Remote manipulation of ligand nano-oscillations regulates adhesion and polarization of macrophages in vivo, Nano Lett. 17 (2017) 6415–6427.
[195] J. Wosik, W. Chen, K. Qin, R.M. Ghobrial, J.Z. Kubiak, M. Kloc, Magnetic field changes macrophage phenotype, Biophys. J. 114 (2018) 2001–2013.
[196] H. Wang, R.T.T. Morales, X. Cui, J. Huang, W. Qian, J. Tong, et al., A photoresponsive hyaluronan hydrogel nanocomposite for dynamic macrophage immunomodulation, Advanced healthcare materials 8 (2019), 1801234.
[197] S.D. Dutta, T. Park, K. Ganguly, D.K. Patel, J. Bin, M.-C. Kim, et al., Evaluation of the sensing potential of stem cell-secreted proteins via a microchip device under electromagnetic field stimulation, ACS Appl. Bio Mater. 4 (2021) 6853–6864.

[198] J.I. Hoare, A.M. Rajnicek, C.D. McCaig, R.N. Barker, H.M. Wilson, Electric fields are novel determinants of human macrophage functions, J. Leukoc. Biol. 99 (2016) 1141–1151.
[199] F. Klug, H. Prakash, P.E. Huber, T. Seibel, N. Bender, N. Halama, et al., Low-dose irradiation programs macrophage differentiation to an iNOS+/M1 phenotype that orchestrates effective T cell immunotherapy, Cancer Cell 24 (2013) 589–602.
[200] B.D. Ratner, Reducing capsular thickness and enhancing angiogenesis around implant drug release systems, J. Contr. Release 78 (2002) 211–218.
[201] C.J. Wilson, R.E. Clegg, D.I. Leavesley, M.J. Pearcy, Mediation of biomaterial–cell interactions by adsorbed proteins: a review, Tissue Eng. 11 (2005) 1–18.
[202] L.B. Moore, T.R. Kyriakides, Molecular characterization of macrophage-biomaterial interactions, Immune Responses to Biosurfaces: Mechanisms and Therapeutic Interventions (2015) 109–122.
[203] G. Zhou, T. Groth, Host responses to biomaterials and anti-inflammatory design—a brief review, Macromol. Biosci. 18 (2018), 1800112.
[204] D.P. Vasconcelos, A.P. Águas, J.N. Barbosa, The inflammasome in biomaterial-driven immunomodulation, Journal of Tissue Engineering and Regenerative Medicine 16 (2022) 1109–1120.
[205] S. Mukherjee, S. Darzi, K. Paul, J.A. Werkmeister, C.E. Gargett, Mesenchymal stem cell-based bioengineered constructs: foreign body response, cross-talk with macrophages and impact of biomaterial design strategies for pelvic floor disorders, Interface Focus 9 (2019), 20180089.
[206] Y. Chandorkar, B. Basu, The foreign body response demystified, ACS Biomater. Sci. Eng. 5 (2018) 19–44.
[207] D.K. Patel, K. Ganguly, S.D. Dutta, T.V. Patil, K.-T. Lim, Cellulose nanocrystals vs. cellulose nanospheres: a comparative study of cytotoxicity and macrophage polarization potential, Carbohydr. Polym. 303 (2023), 120464.
[208] R. Maitra, C.C. Clement, B. Scharf, G.M. Crisi, S. Chitta, D. Paget, et al., Endosomal damage and TLR2 mediated inflammasome activation by alkane particles in the generation of aseptic osteolysis, Mol. Immunol. 47 (2009) 175–184.
[209] C.L. Bueter, C.K. Lee, J.P. Wang, G.R. Ostroff, C.A. Specht, S.M. Levitz, Spectrum and mechanisms of inflammasome activation by chitosan, J. Immunol. 192 (2014) 5943–5951.
[210] A.F. Malik, R. Hoque, X. Ouyang, A. Ghani, E. Hong, K. Khan, et al., Inflammasome components Asc and caspase-1 mediate biomaterial-induced inflammation and foreign body response, Proc. Natl. Acad. Sci. USA 108 (2011) 20095–20100.
[211] G. Vallés, F. Bensiamar, L. Crespo, M. Arruebo, N. Vilaboa, L. Saldana, Topographical cues regulate the crosstalk between MSCs and macrophages, Biomaterials 37 (2015) 124–133.
[212] N. Kartikasari, M. Yamada, J. Watanabe, W. Tiskratok, X. He, H. Egusa, Titania nanospikes activate macrophage phagocytosis by ligand-independent contact stimulation, Sci. Rep. 12 (2022) 1–18.
[213] A.J. Sawyer, W. Tian, J.K. Saucier-Sawyer, P.J. Rizk, W.M. Saltzman, R. V. Bellamkonda, et al., The effect of inflammatory cell-derived MCP-1 loss on neuronal survival during chronic neuroinflammation, Biomaterials 35 (2014) 6698–6706.
[214] E.A. Skokos, A. Charokopos, K. Khan, J. Wanjala, T.R. Kyriakides, Lack of tnf-α–induced MMP-9 production and abnormal e-cadherin redistribution associated with compromised fusion in MCP-1–null macrophages, Am. J. Pathol. 178 (2011) 2311–2321.
[215] J.E. Mooney, K.M. Summers, M. Gongora, S.M. Grimmond, J.H. Campbell, D. A. Hume, et al., Transcriptional switching in macrophages associated with the peritoneal foreign body response, Immunol. Cell Biol. 92 (2014) 518–526.
[216] J.M. Daley, S.K. Brancato, A.A. Thomay, J.S. Reichner, J.E. Albina, The phenotype of murine wound macrophages, J. Leukoc. Biol. 87 (2010) 59–67.
[217] M.S. Hayden, S. Ghosh, Shared principles in NF-κB signaling, Cell 132 (2008) 344–362.
[218] F. Suska, C. Gretzer, M. Esposito, L. Emanuelsson, A. Wennerberg, P. Tengvall, et al., In vivo cytokine secretion and NF-κB activation around titanium and copper implants, Biomaterials 26 (2005) 519–527.
[219] M. Yu, X. Qi, J.L. Moreno, D.L. Farber, A.D. Keegan, NF-κB signaling participates in both RANKL-and IL-4–induced macrophage fusion: receptor cross-talk leads to alterations in NF-κB pathways, J. Immunol. 187 (2011) 1797–1806.
[220] I.B. Lobov, S. Rao, T.J. Carroll, J.E. Vallance, M. Ito, J.K. Ondr, et al., WNT7b mediates macrophage-induced programmed cell death in patterning of the vasculature, Nature 437 (2005) 417–421.
[221] A. Muley, Y. Odaka, I.P. Lewkowich, S. Vemaraju, T.P. Yamaguchi, C. Shawber, et al., Myeloid Wnt ligands are required for normal development of dermal lymphatic vasculature, PLoS One 12 (2017), e0181549.
[222] K.M. Irvine, A.D. Clouston, V.L. Gadd, G.C. Miller, W.-Y. Wong, M. Melino, et al., Deletion of Wntless in myeloid cells exacerbates liver fibrosis and the ductular reaction in chronic liver injury, Fibrogenesis Tissue Repair 8 (2015) 1–13.
[223] X. He, H. Wang, T. Jin, Y. Xu, L. Mei, J. Yang, TLR4 activation promotes bone marrow MSC proliferation and osteogenic differentiation via Wnt3a and Wnt5a signaling, PLoS One 11 (2016), e0149876.
[224] J.O. Abaricia, A.H. Shah, M. Chaubal, K.M. Hotchkiss, R. Olivares-Navarrete, Wnt signaling modulates macrophage polarization and is regulated by biomaterial surface properties, Biomaterials 243 (2020), 119920.
[225] F. Ginhoux, S. Jung, Monocytes and macrophages: developmental pathways and tissue homeostasis, Nat. Rev. Immunol. 14 (2014) 392–404.
[226] X. Liu, B. Gaihre, S. Park, L. Li, B. Dashtdar, M.D.A. Potes, et al., 3D-printed scaffolds with 2D hetero-nanostructures and immunomodulatory cytokines provide pro-healing microenvironment for enhanced bone regeneration, Bioact. Mater. 27 (2023) 216–230.
[227] T. Wang, J. Bai, M. Lu, C. Huang, D. Geng, G. Chen, et al., Engineering immunomodulatory and osteoinductive implant surfaces via mussel adhesion-mediated ion coordination and molecular clicking, Nat. Commun. 13 (2022) 1–17.
[228] Y. Wang, J. Wang, R. Gao, X. Liu, Z. Feng, C. Zhang, et al., Biomimetic glycopeptide hydrogel coated PCL/nHA scaffold for enhanced cranial bone regeneration via macrophage M2 polarization-induced osteo-immunomodulation, Biomaterials 285 (2022), 121538.
[229] J.A. Jones, D.T. Chang, H. Meyerson, E. Colton, I.K. Kwon, T. Matsuda, et al., Proteomic analysis and quantification of cytokines and chemokines from biomaterial surface-adherent macrophages and foreign body giant cells, J. Biomed. Mater. Res. Part A: An Official Journal of The Society for Biomaterials 83 (2007) 585–596. The Japanese Society for Biomaterials, and The Australian Society for Biomaterials and the Korean Society for Biomaterials.
[230] J. Yun, K. DeFife, E. Colton, S. Stack, A. Azeez, L. Cahalan, et al., Human monocyte/macrophage adhesion and cytokine production on surface-modified poly (tetrafluoroethylene/hexafluoropropylene) polymers with and without protein preadsorption, J. Biomed. Mater. Res. 29 (1995) 257–268.
[231] V. Karageorgiou, D. Kaplan, Porosity of 3D biomaterial scaffolds and osteogenesis, Biomaterials 26 (2005) 5474–5491.
[232] S. Yin, W. Zhang, Z. Zhang, X. Jiang, Recent advances in scaffold design and material for vascularized tissue-engineered bone regeneration, Advanced healthcare materials 8 (2019), 1801433.
[233] M.W. Laschke, Y. Harder, M. Amon, I. Martin, J. Farhadi, A. Ring, et al., Angiogenesis in tissue engineering: breathing life into constructed tissue substitutes, Tissue Eng. 12 (2006) 2093–2104.
[234] Y. Kuboki, Q. Jin, M. Kikuchi, J. Mamood, H. Takita, Geometry of artificial ECM: sizes of pores controlling phenotype expression in BMP-induced osteogenesis and chondrogenesis, Connect. Tissue Res. 43 (2002) 529–534.
[235] D. Li, L. Huifang, J. Zhao, Z. Yang, X. Xie, Z. Wei, et al., Porous lithium-doped hydroxyapatite scaffold seeded with hypoxia-preconditioned bone-marrow mesenchymal stem cells for bone-tissue regeneration, Biomed. Mater. 13 (2018), 055002.
[236] X. Zheng, X. Zhang, Y. Wang, Y. Liu, Y. Pan, Y. Li, et al., Hypoxia-mimicking 3D bioglass-nanoclay scaffolds promote endogenous bone regeneration, Bioact. Mater. 6 (2021) 3485–3495.
[237] E. Quinlan, S. Partap, M.M. Azevedo, G. Jell, M.M. Stevens, F.J. O'Brien, Hypoxia-mimicking bioactive glass/collagen glycosaminoglycan composite scaffolds to enhance angiogenesis and bone repair, Biomaterials 52 (2015) 358–366.
[238] Z. Deng, B. Lin, Z. Jiang, W. Huang, J. Li, X. Zeng, et al., Hypoxia-mimicking cobalt-doped borosilicate bioactive glass scaffolds with enhanced angiogenic and osteogenic capacity for bone regeneration, Int. J. Biol. Sci. 15 (2019) 1113.
[239] M. Touri, F. Moztarzadeh, N.A. Abu Osman, M.M. Dehghan, P. Brouki Milan, S. Farzad-Mohajeri, et al., Oxygen-releasing scaffolds for accelerated bone regeneration, ACS Biomater. Sci. Eng. 6 (2020) 2985–2994.
[240] C. Wu, Y. Zhou, W. Fan, P. Han, J. Chang, J. Yuen, et al., Hypoxia-mimicking mesoporous bioactive glass scaffolds with controllable cobalt ion release for bone tissue engineering, Biomaterials 33 (2012) 2076–2085.
[241] S. Hao, J. Meng, Y. Zhang, J. Liu, X. Nie, F. Wu, et al., Macrophage phenotypic mechanomodulation of enhancing bone regeneration by superparamagnetic scaffold upon magnetization, Biomaterials 140 (2017) 16–25.
[242] Z. Chen, S. Ni, S. Han, R. Crawford, S. Lu, F. Wei, et al., Nanoporous microstructures mediate osteogenesis by modulating the osteo-immune response of macrophages, Nanoscale 9 (2017) 706–718.
[243] L. Lei, Z. Liu, P. Yuan, R. Jin, X. Wang, T. Jiang, et al., Injectable colloidal hydrogel with mesoporous silica nanoparticles for sustained co-release of microRNA-222 and aspirin to achieve innervated bone regeneration in rat mandibular defects, J. Mater. Chem. B 7 (2019) 2722–2735.
[244] H. Liu, F. Chen, Y. Zhang, P. Wu, Z. Yang, S. Zhang, et al., Facile fabrication of biomimetic silicified gelatin scaffolds for angiogenesis and bone regeneration by a bioinspired polymer-induced liquid precursor, Mater. Des. 222 (2022), 111070.
[245] D. Huang, K. Xu, X. Huang, N. Lin, Y. Ye, S. Lin, et al., Remotely temporal scheduled macrophage phenotypic transition enables optimized immunomodulatory bone regeneration, Small (2022), 2203680.
[246] Z.-C. Hu, J.-Q. Lu, T.-W. Zhang, H.-F. Liang, H. Yuan, D.-H. Su, et al., Piezoresistive MXene/Silk fibroin nanocomposite hydrogel for accelerating bone regeneration by Re-establishing electrical microenvironment, Bioact. Mater. 22 (2023) 1–17.
[247] N. Lohmann, L. Schirmer, P. Atallah, E. Wandel, R.A. Ferrer, C. Werner, et al., Glycosaminoglycan-based hydrogels capture inflammatory chemokines and rescue defective wound healing in mice, Sci. Transl. Med. 9 (2017), eaai9044.
[248] L. Li, Y. Qian, C. Jiang, Y. Lv, W. Liu, L. Zhong, et al., The use of hyaluronan to regulate protein adsorption and cell infiltration in nanofibrous scaffolds, Biomaterials 33 (2012) 3428–3445.
[249] C.E. Olingy, C.L. San Emeterio, M.E. Ogle, J.R. Krieger, A.C. Bruce, D.D. Pfau, et al., Non-classical monocytes are biased progenitors of wound healing macrophages during soft tissue injury, Sci. Rep. 7 (2017) 1–16.
[250] J.W. Kim, C. Mahapatra, J.Y. Hong, M.S. Kim, K.W. Leong, H.W. Kim, et al., Functional recovery of contused spinal cord in rat with the injection of optimal-dosed cerium oxide nanoparticles, Adv. Sci. 4 (2017), 1700034.
[251] B.M. Sicari, J.L. Dziki, B.F. Siu, C.J. Medberry, C.L. Dearth, S.F. Badylak, The promotion of a constructive macrophage phenotype by solubilized extracellular matrix, Biomaterials 35 (2014) 8605–8612.
[252] Z. Wang, Y. Cui, J. Wang, X. Yang, Y. Wu, K. Wang, et al., The effect of thick fibers and large pores of electrospun poly (ε-caprolactone) vascular grafts on

macrophage polarization and arterial regeneration, Biomaterials 35 (2014) 5700–5710.
[253] D. Song, Y. Xu, S. Liu, L. Wen, X. Wang, Progress of 3D bioprinting in organ manufacturing, Polymers 13 (2021) 3178.
[254] Z. Gu, J. Fu, H. Lin, Y. He, Development of 3D bioprinting: from printing methods to biomedical applications, Asian J. Pharm. Sci. 15 (2020) 529–557.
[255] A. Atala, Introduction: 3D Printing for Biomaterials, ACS Publications, 2020, pp. 10545–10546.
[256] J. Malda, J. Groll, Building Blocks for Biofabricated Models, Wiley Online Library, 2019, 1900326.
[257] U. Jammalamadaka, K. Tappa, Recent advances in biomaterials for 3D printing and tissue engineering, J. Funct. Biomater. 9 (2018) 22.
[258] F. Salaris, A. Rosa, Construction of 3D in vitro models by bioprinting human pluripotent stem cells: challenges and opportunities, Brain Res. 1723 (2019), 146393.
[259] E. Lepowsky, M. Muradoglu, S. Tasoglu, Towards preserving post-printing cell viability and improving the resolution: past, present, and future of 3D bioprinting theory, Bioprinting 11 (2018), e00034.
[260] K. Hölzl, S. Lin, L. Tytgat, S. Van Vlierberghe, L. Gu, A. Ovsianikov, Bioink properties before, during and after 3D bioprinting, Biofabrication 8 (2016), 032002.
[261] J. Adhikari, A. Roy, A. Das, M. Ghosh, S. Thomas, A. Sinha, et al., Effects of processing parameters of 3D bioprinting on the cellular activity of bioinks, Macromol. Biosci. 21 (2021), 2000179.
[262] A. Blaeser, D.F. Duarte Campos, U. Puster, W. Richtering, M.M. Stevens, H. Fischer, Controlling shear stress in 3D bioprinting is a key factor to balance printing resolution and stem cell integrity, Advanced healthcare materials 5 (2016) 326–333.
[263] H. Xu, J. Casillas, S. Krishnamoorthy, C. Xu, Effects of Irgacure 2959 and lithium phenyl-2, 4, 6-trimethylbenzoylphosphinate on cell viability, physical properties, and microstructure in 3D bioprinting of vascular-like constructs, Biomed. Mater. 15 (2020), 055021.
[264] N.T. Raveendran, C. Vaquette, C. Meinert, D.S. Ipe, S. Ivanovski, Optimization of 3D bioprinting of periodontal ligament cells, Dent. Mater. 35 (2019) 1683–1694.
[265] B. Webb, B.J. Doyle, Parameter optimization for 3D bioprinting of hydrogels, Bioprinting 8 (2017) 8–12.
[266] Z. Wang, H. Kumar, Z. Tian, X. Jin, J.F. Holzman, F. Menard, et al., Visible light photoinitiation of cell-adhesive gelatin methacryloyl hydrogels for stereolithography 3D bioprinting, ACS Appl. Mater. Interfaces 10 (2018) 26859–26869.
[267] A. Erdem, M.A. Darabi, R. Nasiri, S. Sangabathuni, Y.N. Ertas, H. Alem, et al., 3D bioprinting of oxygenated cell-laden gelatin methacryloyl constructs, Advanced healthcare materials 9 (2020), 1901794.
[268] T. Jungst, W. Smolan, K. Schacht, T. Scheibel, Groll Jr., Strategies and molecular design criteria for 3D printable hydrogels, Chem. Rev. 116 (2016) 1496–1539.
[269] C. Yu, J. Schimelman, P. Wang, K.L. Miller, X. Ma, S. You, et al., Photopolymerizable biomaterials and light-based 3D printing strategies for biomedical applications, Chem. Rev. 120 (2020) 10695–10743.
[270] V. Anwari, A. Lai, A. Ursani, K. Rego, B. Karasfi, S. Sajja, et al., 3D printed CT-based abdominal structure mannequin for enabling research, 3D Printing in Medicine 6 (2020) 1–12.
[271] K. Markstedt, A. Mantas, I. Tournier, H. Martínez Ávila, D. Hagg, P. Gatenholm, 3D bioprinting human chondrocytes with nanocellulose–alginate bioink for cartilage tissue engineering applications, Biomacromolecules 16 (2015) 1489–1496.
[272] N. Ashammakhi, S. Ahadian, I. Pountos, S.-K. Hu, N. Tellisi, P. Bandaru, et al., In situ three-dimensional printing for reparative and regenerative therapy, Biomed. Microdevices 21 (2019) 1–6.
[273] F. Agostinacchio, X. Mu, S. Dirè, A. Motta, D.L. Kaplan, In situ 3D printing: opportunities with silk inks, Trends Biotechnol. 39 (2021) 719–730.
[274] Y. Wang, H. Cui, Y. Wang, C. Xu, T.J. Esworthy, S.Y. Hann, et al., 4D printed cardiac construct with aligned myofibers and adjustable curvature for myocardial regeneration, ACS Appl. Mater. Interfaces 13 (2021) 12746–12758.
[275] G. Constante, I. Apsite, H. Alkhamis, M. Dulle, M. Schwarzer, A. Caspari, et al., 4D biofabrication using a combination of 3D printing and melt-electrowriting of shape-morphing polymers, ACS Appl. Mater. Interfaces 13 (2021) 12767–12776.
[276] A. Kirillova, R. Maxson, G. Stoychev, C.T. Gomillion, L. Ionov, 4D biofabrication using shape-morphing hydrogels, Adv. Mater. 29 (2017), 1703443.
[277] R. Dimitriou, E. Jones, D. McGonagle, P.V. Giannoudis, Bone regeneration: current concepts and future directions, BMC Med. 9 (2011) 1–10.
[278] G. Fernandez de Grado, L. Keller, Y. Idoux-Gillet, Q. Wagner, A.-M. Musset, N. Benkirane-Jessel, et al., Bone substitutes: a review of their characteristics, clinical use, and perspectives for large bone defects management, J. Tissue Eng. 9 (2018), 2041731418776819.
[279] D. Smrke, P. Rožman, M. Veselko, B. Gubina, Treatment of Bone Defects—Allogenic Platelet Gel and Autologous Bone Technique. Regenerative Medicine and Tissue Engineering, IntechOpen, 2013.
[280] C.W. Schlickewei, H. Kleinertz, D.M. Thiesen, K. Mader, M. Priemel, K.-H. Frosch, et al., Current and future concepts for the treatment of impaired fracture healing, Int. J. Mol. Sci. 20 (2019) 5805.
[281] M. Kang, W. Lee, K. Oh, J. Han, K. Song, B. Cha, et al., The short-term changes of bone mineral metabolism following bone marrow transplantation, Bone 26 (2000) 275–279.
[282] S.L. Teitelbaum, Stem cells and osteoporosis therapy, Cell Stem Cell 7 (2010) 553–554.
[283] J. Phetfong, T. Sanvoranart, K. Nartprayut, N. Nimsanor, K. Seenprachawong, V. Prachayasittikul, et al., Osteoporosis: the current status of mesenchymal stem cell-based therapy, Cell. Mol. Biol. Lett. 21 (2016) 1–20.
[284] C. Robin, F. Hémery, C. Dindorf, J. Thillard, L. Cabanne, R. Redjoul, et al., Economic burden of preemptive treatment of CMV infection after allogeneic stem cell transplantation: a retrospective study of 208 consecutive patients, BMC Infect. Dis. 17 (2017) 1–8.
[285] B.J. Webb, R. Harrington, J. Schwartz, J. Kammerer, J. Spalding, E. Lee, et al., The clinical and economic impact of cytomegalovirus infection in recipients of hematopoietic stem cell transplantation, Transpl. Infect. Dis. 20 (2018), e12961.
[286] A. Sanghani-Kerai, D. McCreary, H. Lancashire, L. Osagie, M. Coathup, G. Blunn, Stem cell interventions for bone healing: fractures and osteoporosis, Curr. Stem Cell Res. Ther. 13 (2018) 369–377.
[287] C. Wang, W. Huang, Y. Zhou, L. He, Z. He, Z. Chen, et al., 3D Printing of Bone Tissue Engineering Scaffolds, Bioact. Mater, 2020.
[288] D. Stanco, P. Urbán, S. Tirendi, G. Ciardelli, J. Barrero, 3D bioprinting for orthopaedic applications: current advances, challenges and regulatory considerations, Bioprinting 20 (2020), e00103.
[289] Y. Zhang, T. Lei, C. Tang, Y. Chen, Y. Liao, W. Ju, et al., 3D printing of chemical-empowered tendon stem/progenitor cells for functional tissue repair, Biomaterials 271 (2021), 120722.
[290] M. Seidenstuecker, L. Kerr, A. Bernstein, H.O. Mayr, N.P. Suedkamp, R. Gadow, et al., 3D powder printed bioglass and β-tricalcium phosphate bone scaffolds, Materials 11 (2017) 13.
[291] L. Chen, C. Deng, J. Li, Q. Yao, J. Chang, L. Wang, et al., 3D printing of a lithium-calcium-silicate crystal bioscaffold with dual bioactivities for osteochondral interface reconstruction, Biomaterials 196 (2019) 138–150.
[292] H.N. Chia, B.M. Wu, Recent advances in 3D printing of biomaterials, J. Biol. Eng. 9 (2015) 1–14.
[293] S. Waheed, J.M. Cabot, N.P. Macdonald, T. Lewis, R.M. Guijt, B. Paull, et al., 3D printed microfluidic devices: enablers and barriers, Lab Chip 16 (2016) 1993–2013.
[294] M. Asadollahi, E. Gerashi, M. Zohrevand, M. Zarei, S.S. Sayedain, R. Alizadeh, et al., Improving mechanical properties and biocompatibility of 3D printed PLA by the addition of PEG and titanium particles, using a novel incorporation method, Bioprinting 27 (2022), e00228.
[295] L. Joharji, R.B. Mishra, F. Alam, S. Tytov, F. Al-Modaf, N. El-Atab, 4D printing: a detailed review of materials, techniques, and applications, Microelectron. Eng. (2022), 111874.
[296] P. Kijartorn, J. Wongpairojpanich, F. Thammarakcharoen, J. Suwanprateeb, B. Buranawat, Clinical evaluation of 3D printed nano-porous hydroxyapatite bone graft for alveolar ridge preservation: a randomized controlled trial, J. Dent. Sci. 17 (2022) 194–203.
[297] L.P. Hatt, K. Thompson, J.A. Helms, M.J. Stoddart, A.R. Armiento, Clinically relevant preclinical animal models for testing novel cranio-maxillofacial bone 3D-printed biomaterials, Clin. Transl. Med. 12 (2022), e690.
[298] M. Mirkhalaf, Y. Men, R. Wang, Y. No, H. Zreiqat, Personalized 3D printed bone scaffolds: a review, Acta Biomater. (2022).
[299] M. Anderson, N. Dubey, K. Bogie, C. Cao, J. Li, J. Lerchbacker, et al., Three-dimensional printing of clinical scale and personalized calcium phosphate scaffolds for alveolar bone reconstruction, Dent. Mater. 38 (2022) 529–539.
[300] B.I. Oladapo, S. Zahedi, A. Adeoye, 3D printing of bone scaffolds with hybrid biomaterials, Compos. B Eng. 158 (2019) 428–436.
[301] J.A. Inzana, D. Olvera, S.M. Fuller, J.P. Kelly, O.A. Graeve, E.M. Schwarz, et al., 3D printing of composite calcium phosphate and collagen scaffolds for bone regeneration, Biomaterials 35 (2014) 4026–4034.
[302] A.A. El-Rashidy, J.A. Roether, L. Harhaus, U. Kneser, A.R. Boccaccini, Regenerating bone with bioactive glass scaffolds: a review of in vivo studies in bone defect models, Acta Biomater. 62 (2017) 1–28.
[303] S. Stucker, J. Chen, F.E. Watt, A.P. Kusumbe, Bone angiogenesis and vascular niche remodeling in stress, aging, and diseases, Front. Cell Dev. Biol. 8 (2020), 602269.
[304] M.G. Burger, A. Grosso, P.S. Briquez, G.M. Born, A. Lunger, F. Schrenk, et al., Robust coupling of angiogenesis and osteogenesis by VEGF-decorated matrices for bone regeneration, Acta Biomater. 149 (2022) 111–125.
[305] X. Sun, Z. Ma, X. Zhao, W. Jin, C. Zhang, J. Ma, et al., Three-dimensional bioprinting of multicell-laden scaffolds containing bone morphogenic protein-4 for promoting M2 macrophage polarization and accelerating bone defect repair in diabetes mellitus, Bioact. Mater. 6 (2021) 757–769.
[306] L. Zhou, J. You, Z. Wang, Y. Gu, D. Chen, B. Lin, et al., 3D printing monetite-coated Ti-6Al-4V surface with osteoimmunomodulatory function to enhance osteogenesis, Biomaterials Advances 134 (2022), 112562.
[307] Y. Niu, Z. Wang, Y. Shi, L. Dong, C. Wang, Modulating macrophage activities to promote endogenous bone regeneration: biological mechanisms and engineering approaches, Bioact. Mater. 6 (2021) 244–261.
[308] J.C. Moses, T. Saha, B.B. Mandal, Chondroprotective and osteogenic effects of silk-based bioinks in developing 3D bioprinted osteochondral interface, Bioprinting 17 (2020), e00067.
[309] B. Zhang, M. Zhang, Y. Sun, M. Li, F. Han, C. Wu, Haversian bone-mimicking bioceramic scaffolds enhancing MSC-macrophage osteo-imunomodulation, Prog. Nat. Sci.: Mater. Int. 31 (2021) 883–890.
[310] Y. Zhang, M. Huo, Y. Wang, L. Xiao, J. Wu, Y. Ma, et al., A tailored bioactive 3D porous poly (lactic-acid)-exosome scaffold with osteo-immunomodulatory and osteogenic differentiation properties, J. Biol. Eng. 16 (2022) 1–14.
[311] M. Wang, H. Li, Y. Yang, K. Yuan, F. Zhou, H. Liu, et al., A 3D-bioprinted scaffold with doxycycline-controlled BMP2-expressing cells for inducing bone

regeneration and inhibiting bacterial infection, Bioact. Mater. 6 (2021) 1318–1329.
[312] X. Ji, X. Yuan, L. Ma, B. Bi, H. Zhu, Z. Lei, et al., Mesenchymal stem cell-loaded thermosensitive hydroxypropyl chitin hydrogel combined with a three-dimensional-printed poly (ε-caprolactone)/nano-hydroxyapatite scaffold to repair bone defects via osteogenesis, angiogenesis and immunomodulation, Theranostics 10 (2020) 725.
[313] X. Liu, W. Chen, B. Shao, X. Zhang, Y. Wang, S. Zhang, et al., Mussel patterned with 4D biodegrading elastomer durably recruits regenerative macrophages to promote regeneration of craniofacial bone, Biomaterials 276 (2021), 120998.
[314] M. Wang, W. Li, Z. Luo, G. Tang, X. Mu, X. Kuang, et al., A multifunctional micropore-forming bioink with enhanced anti-bacterial and anti-inflammatory properties, Biofabrication 14 (2022), 024105.
[315] B. Zhang, F. Han, Y. Wang, Y. Sun, M. Zhang, X. Yu, et al., Cells-micropatterning biomaterials for immune activation and bone regeneration, Adv. Sci. (2022), 2200670.
[316] H. Xue, Z. Zhang, Z. Lin, J. Su, A.C. Panayi, Y. Xiong, et al., Enhanced tissue regeneration through immunomodulation of angiogenesis and osteogenesis with a multifaceted nanohybrid modified bioactive scaffold, Bioact. Mater. (2022).
[317] L. Yang, I. Ullah, K. Yu, W. Zhang, J. Zhou, T. Sun, et al., Bioactive Sr2+/Fe3+ co-substituted hydroxyapatite in cryogenically 3D printed porous scaffolds for bone tissue engineering, Biofabrication 13 (2021), 035007.
[318] N. Quintal-Bojórquez, M.R. Segura-Campos, Bioactive peptides as therapeutic adjuvants for cancer, Nutr. Cancer 73 (2021) 1309–1321.
[319] L. Wang, H. Zhang, L. Sun, W. Gao, Y. Xiong, A. Ma, et al., Manipulation of macrophage polarization by peptide-coated gold nanoparticles and its protective effects on acute lung injury, J. Nanobiotechnol. 18 (2020) 1–16.
[320] D.F. Williams, Biocompatibility pathways and mechanisms for bioactive materials: the bioactivity zone, Bioact. Mater. 10 (2022) 306–322.
[321] L.D. Jones, P. Pangloli, H.B. Krishnan, V.P. Dia, BG-4, a novel bioactive peptide from Momordica charantia, inhibits lipopolysaccharide-induced inflammation in THP-1 human macrophages, Phytomedicine 42 (2018) 226–232.
[322] Y. Sun, B. Zhang, D. Zhai, C. Wu, Three-dimensional printing of bioceramic-induced macrophage exosomes: immunomodulation and osteogenesis/angiogenesis, NPG Asia Mater. 13 (2021) 1–16.
[323] T.R. Kyriakides, H.-J. Kim, C. Zheng, L. Harkins, W. Tao, E. Deschenes, Foreign body response to synthetic polymer biomaterials and the role of adaptive immunity, Biomed. Mater. 17 (2022), 022007.
[324] P.T. Coburn, X. Li, J. Li, Y. Kishimoto, N.Y. Li-Jessen, Progress in vocal fold regenerative biomaterials: an immunological perspective, Advanced NanoBiomed Research 2 (2022), 2100119.
[325] G. Liu, X. Zhou, L. Zhang, Y. Zou, J. Xue, R. Xia, et al., Cell-free immunomodulatory biomaterials mediated in situ periodontal multi-tissue regeneration and their immunopathophysiological processes, Materials Today Bio 16 (2022), 100432.
[326] J. Li, C. Wu, P.K. Chu, M. Gelinsky, 3D printing of hydrogels: rational design strategies and emerging biomedical applications, Mater. Sci. Eng. R Rep. 140 (2020), 100543.
[327] X. Han, A. Alu, H. Liu, Y. Shi, X. Wei, L. Cai, et al., Biomaterial-assisted biotherapy: a brief review of biomaterials used in drug delivery, vaccine development, gene therapy, and stem cell therapy, Bioact. Mater. (2022).
[328] X. Xu, T. Wan, H. Xin, D. Li, H. Pan, J. Wu, et al., Delivery of CRISPR/Cas9 for therapeutic genome editing, J. Gene Med. 21 (2019), e3107.
[329] L. Duan, K. Ouyang, X. Xu, L. Xu, C. Wen, X. Zhou, et al., Nanoparticle delivery of CRISPR/Cas9 for genome editing, Front. Genet. 12 (2021), 673286.
[330] T. Wei, Q. Cheng, L. Farbiak, D.G. Anderson, R. Langer, D.J. Siegwart, Delivery of tissue-targeted scalpels: opportunities and challenges for in vivo CRISPR/Cas-based genome editing, ACS Nano 14 (2020) 9243–9262.
[331] Y.-L. Luo, C.-F. Xu, H.-J. Li, Z.-T. Cao, J. Liu, J.-L. Wang, et al., Macrophage-specific in vivo gene editing using cationic lipid-assisted polymeric nanoparticles, ACS Nano 12 (2018) 994–1005.
[332] C. Xu, Z. Lu, Y. Luo, Y. Liu, Z. Cao, S. Shen, et al., Targeting of NLRP3 inflammasome with gene editing for the amelioration of inflammatory diseases, Nat. Commun. 9 (2018) 4092.
[333] X. Wan, Z. Liu, L. Li, Manipulation of stem cells fates: the master and multifaceted roles of biophysical cues of biomaterials, Adv. Funct. Mater. 31 (2021), 2010626.
[334] J.J. Vaca-González, J.M. Guevara, M.A. Moncayo, H. Castro-Abril, Y. Hata, D. A. Garzón-Alvarado, Biophysical stimuli: a review of electrical and mechanical stimulation in hyaline cartilage, Cartilage 10 (2019) 157–172.
[335] B. Bakhshandeh, N. Ranjbar, A. Abbasi, E. Amiri, A. Abedi, M.R. Mehrabi, et al., Recent progress in the manipulation of biochemical and biophysical cues for engineering functional tissues, Bioengineering & Translational Medicine (2022), e10383.
[336] Z. Wang, M. Li, B. Wang, Y. Xu, J. Li, S. Zhang, et al., Biomimetic niche of vascular intima with biophysical orientation and biochemical stimulation for rapid endothelialization and long-term patency, Chem. Eng. J. 451 (2023), 138805.
[337] S.D. Dutta, K. Ganguly, A. Randhawa, T. Patil, D.K. Patel, K.-T. Lim, Electrically stimulated 3D bioprinting of gelatin-polypyrrole hydrogel with dynamic semi-IPN network induces osteogenesis via collective signaling and immunopolarization, Biomaterials (2023), 121999.
[338] R. Luo, Y. Liang, J. Yang, H. Feng, Y. Chen, X. Jiang, et al., Reshaping the endogenous electric field to boost wound repair via electrogenerative dressing, Adv. Mater. (2023), 2208395.
[339] K. Ganguly, H. Jin, S.D. Dutta, D.K. Patel, T.V. Patil, K.-T. Lim, Magnetic field-assisted aligned patterning in an alginate-silk fibroin/nanocellulose composite for guided wound healing, Carbohydr. Polym. 287 (2022), 119321.
[340] K. Ganguly, S.D. Dutta, A. Randhawa, D.K. Patel, T.V. Patil, K.T. Lim, Transcriptomic changes towards osteogenic differentiation of mesenchymal stem cells on 3D printed GelMA/CNC hydrogel under pulsatile pressure environment, Advanced Healthcare Materials (2023), 2202163.
[341] F. Zanotti, M. Trentini, I. Zanolla, E. Tiengo, C. Mantarro, L. Dalla Paola, et al., Playing with biophysics: how a symphony of different electromagnetic fields acts to reduce the inflammation in diabetic derived cells, Int. J. Mol. Sci. 24 (2023) 1754.
[342] B. Guo, P.X. Ma, Conducting polymers for tissue engineering, Biomacromolecules 19 (2018) 1764–1782.
[343] N.K. Guimard, N. Gomez, C.E. Schmidt, Conducting polymers in biomedical engineering, Prog. Polym. Sci. 32 (2007) 876–921.
[344] S. Li, C. Wei, Y. Lv, Preparation and application of magnetic responsive materials in bone tissue engineering, Curr. Stem Cell Res. Ther. 15 (2020) 428–440.
[345] T. Hourani, A. Perez-Gonzalez, K. Khoshmanesh, R. Luwor, A.A. Achuthan, S. Baratchi, et al., Label-free macrophage phenotype classification using machine learning methods, Sci. Rep. 13 (2023) 5202.
[346] V.S. Viswanathan, P. Toro, G. Corredor, S. Mukhopadhyay, A. Madabhushi, The state of the art for artificial intelligence in lung digital pathology, J. Pathol. 257 (2022) 413–429.
[347] P. Jabbari, N. Rezaei, Artificial intelligence and immunotherapy, Expet Rev. Clin. Immunol. 15 (2019) 689–691.
[348] J. Xue, S.V. Schmidt, J. Sander, A. Draffehn, W. Krebs, I. Quester, et al., Transcriptome-based network analysis reveals a spectrum model of human macrophage activation, Immunity 40 (2014) 274–288.
[349] K. Sawa-Wejksza, A. Dudek, M. Lemieszek, K. Kaławaj, M. Kandefer-Szerszeń, Colon cancer–derived conditioned medium induces differentiation of THP-1 monocytes into a mixed population of M1/M2 cells, Tumor Biol. 40 (2018), 1010428318797880.
[350] H.M. Rostam, P.M. Reynolds, M.R. Alexander, N. Gadegaard, A. M. Ghaemmaghami, Image based machine learning for identification of macrophage subsets, Sci. Rep. 7 (2017) 1–11.
[351] N. Pavillon, A.J. Hobro, S. Akira, N.I. Smith, Noninvasive detection of macrophage activation with single-cell resolution through machine learning, Proc. Natl. Acad. Sci. USA 115 (2018) E2676–E2685.
[352] V.J. Jameson, T. Luke, Y. Yan, A. Hind, M. Evrard, K. Man, et al., Unlocking autofluorescence in the era of full spectrum analysis: implications for immunophenotype discovery projects, Cytometry 101 (2022) 922–941.